4-6-2012

Laser-induced Multi-energy Processing in Diamond Growth

Zhiqiang Xie

University of Nebraska-Lincoln, zhqxie@gmail.com

Report Documentation Page

Public reporting burden for the collection of information is estimated to average 1 hour per response, including the time for reviewing instructions, searching existing data sources, gathering and maintaining the data needed, and completing and reviewing the collection of information. Send comments regarding this burden estimate or any other aspect of this collection of information, including suggestions for reducing this burden, to Washington Headquarters Services, Directorate for Information Operations and Reports, 1215 Jefferson Davis Highway, Suite 1204, Arlington VA 22202-4302. Respondents should be aware that notwithstanding any other provision of law, no person shall be subject to a penalty for failing to comply with a collection of information if it does not display a currently valid OMB control number.

1. REPORT DATE **2012**	2. REPORT TYPE	3. DATES COVERED **00-00-2012 to 00-00-2012**

4. TITLE AND SUBTITLE **Laser-induced Multi-energy Processing In Diamond Growth**	5a. CONTRACT NUMBER
	5b. GRANT NUMBER
	5c. PROGRAM ELEMENT NUMBER
6. AUTHOR(S)	5d. PROJECT NUMBER
	5e. TASK NUMBER
	5f. WORK UNIT NUMBER
7. PERFORMING ORGANIZATION NAME(S) AND ADDRESS(ES) **University of Nebraska,Lincoln,NE,68588**	8. PERFORMING ORGANIZATION REPORT NUMBER
9. SPONSORING/MONITORING AGENCY NAME(S) AND ADDRESS(ES)	10. SPONSOR/MONITOR'S ACRONYM(S)
	11. SPONSOR/MONITOR'S REPORT NUMBER(S)

12. DISTRIBUTION/AVAILABILITY STATEMENT
Approved for public release; distribution unlimited

13. SUPPLEMENTARY NOTES

14. ABSTRACT

Laser-induced multi-energy processing (MEP) introduces resonant vibrational excitations of precursor molecules to conventional chemical vapor deposition methods for material synthesis. In this study, efforts were extended to explore the capability of resonant vibrational excitations for promotion of energy efficiency in chemical reactions for enhancement of diamond deposition, and for control of chemical reactions. The research project mainly focused on resonant vibrational excitations of precursor molecules using lasers in combustion flame deposition of diamond, which led to: 1) promotion of chemical reactions; 2) enhancement of diamond growth with higher growth rate and better crystallizations; 3) steering of chemical reactions which lead to preferential growth of {100}-oriented diamond films and crystals; and 4) mode-selective excitations of precursor molecules toward bond-selective control of chemical reactions.

15. SUBJECT TERMS

16. SECURITY CLASSIFICATION OF:			17. LIMITATION OF ABSTRACT	18. NUMBER OF PAGES	19a. NAME OF RESPONSIBLE PERSON
a. REPORT **unclassified**	b. ABSTRACT **unclassified**	c. THIS PAGE **unclassified**	**Same as Report (SAR)**	**167**	

LASER-INDUCED MULTI-ENERGY PROCESSING IN DIAMOND GROWTH

by

Zhiqiang Xie

A DISSERTATION

Presented to the Faculty of

The Graduate College at the University of Nebraska

In Partial Fulfillment of Requirements

For the Degree of Doctor of Philosophy

Major: Engineering (Electrical Engineering)

Under the Supervision of Professor Yongfeng Lu

Lincoln, Nebraska

May, 2012

LASER-INDUCED MULTI-ENERGY PROCESSING IN DIAMOND GROWTH

Zhiqiang Xie, Ph.D.

University of Nebraska, 2012

Adviser: Yongfeng Lu

Laser-induced multi-energy processing (MEP) introduces resonant vibrational excitations of precursor molecules to conventional chemical vapor deposition methods for material synthesis. In this study, efforts were extended to explore the capability of resonant vibrational excitations for promotion of energy efficiency in chemical reactions, for enhancement of diamond deposition, and for control of chemical reactions. The research project mainly focused on resonant vibrational excitations of precursor molecules using lasers in combustion flame deposition of diamond, which led to: 1) promotion of chemical reactions; 2) enhancement of diamond growth with higher growth rate and better crystallizations; 3) steering of chemical reactions which lead to preferential growth of {100}-oriented diamond films and crystals; and 4) mode-selective excitations of precursor molecules toward bond-selective control of chemical reactions.

Diamond films and crystals were deposited in open air by combustion flame deposition through resonant vibrational excitations of precursor molecules, including ethylene (C_2H_4) and propylene (C_3H_6). A kilowatt wavelength-tunable CO_2 laser with spectral range from 9.2 to 10.9 μm was tuned to match vibrational modes of the precursor

molecules. Resonant vibrational excitations of these molecules were achieved with high energy efficiency as compared with excitations using a common CO_2 laser (fixed wavelength at $10.591\,\mu m$). With resonant vibrational excitations, the diamond growth rate was increased; diamond quality was promoted; diamond crystals with lengths up to 5 mm were deposited in open air; preferential growth of {100}-oriented diamond films and single crystals was achieved; mode-selective excitations of precursor molecules were investigated toward control of chemical reactions.

Optical emission spectroscopy (OES), mass spectrometry (MS), and molecular dynamic simulations were conducted to obtain an in-depth understanding of the resonant vibrational excitations. Species concentrations in flames without and with laser excitations under different wavelengths were investigated both experimentally and theoretically. Detection of C_2, CH, and OH radicals, as well as C_xH_y species and their oxides (C_xH_yO) (x=1, 2; y=0~5) using OES and MS, together with reaction pathway simulations, were used to explain the effect of vibrational excitations of precursor molecules on chemical reactions and on diamond depositions.

ACKNOWLEDGEMENTS

Huifu Luo; Misters Xiangnan He, Wei Xiong, Masoud Mahjouri-Samani, Yang Gao, Matt Mitchell, Xu Ji, Lijia Jiang, Xi Huang, Mengmeng Wang, Thomas Guillemet, Lianbo Guo, Changmao Li, Misses Lisha Fan, Lei Liu, Min Qian, and many other friends.

I feel greatly indebted to my family, including my parents, Mr. Xiantuan Xie, Ms. Zhenying Li, my wife, Ms. Jinjing Wang and my daughter, Katherine Junyi Xie. They have been supporting and will support me without any reservation in all respects of life. Without their supports it would have been very hard for me to get through the Ph.D. studies.

TABLE OF CONTENTS

LIST OF FIGURES

LIST OF TABLES

CHAPTER 1

Introduction

1.1 Motivation

1.2 Dissertation Outline

1.1 Motivation

Chemical reactions hinge on energy distribution among internal and translational energies of reagents [1, 2]. Conventionally, chemical reactions in methods for chemical vapor deposition (CVD) of materials are driven by collisions among molecules, atoms, ions and electrons [3]. The indiscriminate nature of collisions makes energy efficiency of the conventional thermal-driven methods very low. Another disadvantage caused by the indiscriminateness is that it is almost impossible to control bond breakings and hence directions of the chemical reactions in CVD of materials. Chemical reactions in CVD processes involve bond breaking and bond rearrangement, which directly result from vibrational excitations of molecules or molecular ions [3]. It is hence believed that vibrational excitations of molecules or molecular ions are critical for chemical reactions in CVD processes for materials synthesis [1-4]. Multi-energy processing (MEP) is hence proposed to 1) increase efficiency of energy coupling, 2) promote growth rate and quality of materials, and 3) achieve steering and control of chemicals reactions in CVD processes for materials synthesis. In this dissertation, MEP refers to driving of chemical reactions through a combination of thermal method (translational energy) and vibrational excitations using lasers. Because frequencies of molecular vibrations are in the infrared (IR) range, IR lasers are ideal energy sources to achieve resonant excitations of molecular vibrations. Another advantage of IR lasers is that their narrow bandwidth prepares a single vibrational eigenstate, which makes control of reaction pathways feasible [2].

Due to its extreme properties, diamond has found widespread applications not only for conventional applications but also as a supreme semiconductor for microelectronics with wide band-gap, high carrier mobility, high breakdown fields, high workable temperature, and negative electron affinity [5-9]. The ability to be operated in harsh and extreme environments also renders diamond an appealing material [9-14]. Although various methods have been developed to synthesize diamonds, high cost, extreme environment, low growth rate, and inferior quality limit production and subsequent applications. In this dissertation, a novel synthetic strategy is developed to grow diamond films and crystals in open air using laser-induced MEP through laser resonant vibrational excitations and defy the traditional difficulties in diamond growth.

In this dissertation, efforts are extended to explore the capability of vibrational excitations in promotion of energy efficiency in chemical reactions, enhancement of diamond deposition, and control of chemical reactions in CVD of diamond. The research project mainly focused on resonant vibrational excitations of precursor molecules using lasers in combustion flame deposition of diamond, which lead to: 1) promotion of efficiency of chemical reactions; 2) enhancement of diamond growth with higher growth rate and better crystallizations; 3) steering of chemical reactions which lead to preferential growth of {100}-oriented diamond films and crystals; and 4) mode-selective control of chemical reactions through selective excitations of precursor vibrational modes.

1.2 Dissertation Outline

This dissertation focuses on applying laser resonant vibrational excitations of precursor molecules for multi-energy processing (MEP) in deposition of diamond films and crystals. The whole dissertation will be divided into eight chapters. Chapter 1 introduces the motivation and outline of this dissertation. Chapter 2 reviews backgrounds of MEP, laser-assisted materials synthesis, and diamond growth. In chapter 3, resonant vibrational excitations of ethylene (C_2H_4) molecules for combustion flame deposition of diamond films are introduced. Comparison between excitations by a common CO_2 laser (10.591 µm) and a wavelength-tunable CO_2 laser (10.532 µm) which matches the CH_2 wagging mode of ethylene was conducted, which demonstrated the advantages of resonant excitations with matching wavelengths. In chapter 4, efforts were extended to fast growth of diamond crystals in open air with resonant vibrational excitations of ethylene molecules. Diamond crystals of high quality were deposited with high growth rate. Excitations of ethylene molecules with different laser powers were discussed in chapter 5. Detailed investigations were conducted on: 1) efficiency of energy absorption, 2) concentrations of free radicals, and 3) morphology and quality of diamond films under laser excitations with different laser powers. In chapter 6, a novel method for synthesis of {100}-oriented diamond films and crystals is described. The ethylene molecules were excited to a higher vibrational level with higher rotational energy with the CO_2 laser tuned to 10.22 µm. Chemical reactions were steered, resulting to increase of

concentration of oxide species, which favored preferential growth of the {100}-oriented diamond. Single-crystal diamonds with high crystal quality were grown in open air using this method. In chapter 7, mode-selective excitations of propylene (C_3H_6) molecules were studied toward bond-selective control of chemical reactions through vibrational excitations of different vibrational modes of a precursor molecule. This approach is called active intervention, in which the phases of reagent motions are controlled during the course of the reaction, which may preferentially lead reagents to one of many different reaction routes. Concentrations of species for diamond growth were steered by excitations of different vibrational mode of the propylene molecules, and diamond growth differed accordingly. This approach is believed to be a significant step toward bond-selective control of chemical reactions. Chapter 8 concludes this work with important results and suggested future research directions.

References

[1]. Crim F. F., "Making Energy Count", Science **317,** 1707 (2007).

[2]. Killelea, D. R., Campbell, V. L. Shuman, N. S., and Utz, A. L., "Bond-selective control of a heterogeneously catalyzed reaction", Science **319,** 790 (2008).

[3]. Asmussen, J. and Reinhard, D. K. Diamond Films Handbook. Marcel Dekker, Inc., New York, p. 645, (2002).

[4]. Zare, R. N., "Laser Control of Chemical Reactions", Science **279,** 1875 (1998).

[5]. Nazare, M. H. and Neves, A. J., Properties, growth and applications of diamond. INSPEC, the Institution of Electrical Engineers: London, (2001).

[6]. Davis, R. F., Diamond films and coatings - Development, Properties, and Applications. Noyes Publications: Park Ridge, New Jersey, (1993).

[7]. Marinkovic, S. N., Chemistry and Physics of Carbon **29,** 71 (2004).

[8]. Railkar, T. A., Kang, W. P., Windischmann, H., Malshe, A. P., Naseem, H. A., Davidson, J. L., and Brown, W. D., "A critical review of chemical vapor-deposited (CVD) diamond for electronicapplications", Critical Reviews in Solid State and Materials Sciences **25,** 163 (2000).

[9]. Hauert, R., "An overview on the tribological behavior of dimond-like carbon in in technical and medical applications", Tribology International **37,** 991 (2004).

[10]. Aleksov, A., Denisenko, A., Kunze, M., Vescan, A., Bergmaier, A., Dollinger, G., Ebert, W., and Kohn, E., "Diamond diodes and transistors", Semiconductor Science and Technology **18,** S59 (2003).

[11]. Gurbuz, Y., Esame, O., Tekin, I., Kang, W. P., and Davidson, J. L., "Diamond semiconductor technology for RF device applications", Solid-State Electronics **49,** 1055 (2005).

[12].   Kohn, E., Ebert, W., Adamschik, M., Schmid, P., and Denisenko, A., "Diamond-based MEMS devices", New Diamond and Frontier Carbon Technology **11,** 81 (2001).

[13].   Auciello, O., Birrell, J., Carlisle, J. A., Gerbi, J. E., Xiao, X. C., Peng, B., and Espinosa, H. D., "Materials science and fabrication processes for a new MEMS technoloey based on ultrananocrystalline diamond thin films", Journal of Physics-Condensed Matter **16,** R539 (2004).

[14].   Kohn, E., Adamschik, M., Schmid, P., Denisenko, A., Aleksov, A., and Ebert, W., "Prospects of diamond devices", Journal of Physics D-Applied Physics **34,** R77 (2001).

CHAPTER 2

Background and Reviews

2.1 Introduction to laser-induced multi-energy processing

2.2 Introduction to laser-assisted material synthesis

2.3 Introduction to diamond growth

2.3.1 High-Pressure High-Temperature (HPHT) method

2.3.2 Shock Wave (SW) process

2.3.3 Chemical Vapor Deposition (CVD)

2.1 Introduction to multi-energy processing

In a CVD process for material synthesis, gases comprise molecules, atoms, ions and electrons (in terms of plasmas and combustion flames). In addition to translation in three coordinate directions possessed by particles, molecules and molecular ions also store energy in rotations, vibrations, and electrical excitations, as schematically illustrated in Fig. 2.1 [1]. Chemical reactions in CVD processes involve bond breaking and rearrangement, which directly result from vibrational excitations of molecules or molecular ions [2]. It is hence believed that vibrational excitations of molecules or molecular ions are critical for chemical reactions in CVD processes for materials synthesis [2, 3]. However, in most conventional CVD methods, energy is transferred to the reactions through translation energy. The translation energy added to the reaction processes by heating eventually transits to other forms of energy (rotation and vibration) through collisions. Usually, equilibrium of energy between translation and rotation energies requires tens of collisions. In contrast, collisions required for vibration energy to equilibrate with translation and rotation energy is much more (usually in the order of thousands of collisions ore more). Because vibration excitation is necessary to drive endothermic reactions, it can be seen that simple thermal heating is inefficient in driving vapor phase chemical reactions [1]. Also, because of the indiscriminateness of the thermal collisions, it is almost impossible to control bond breakings and directions of chemical reactions in CVD of materials [2].

Molecular translation   Molecular rotation

Molecular vibration   Electronic excitation
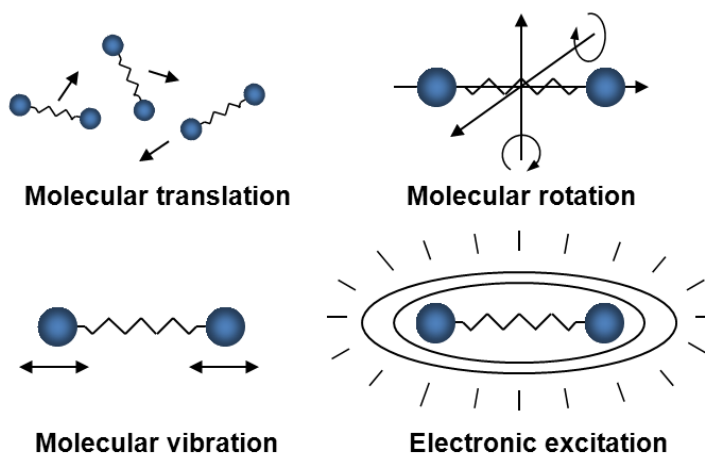
Figure 2.1 Schematics of different forms of energy storage for a diatomic molecule [1].

Here we introduce a new approach called multi-energy processing (MEP) in order to 1) promote chemical reactions, 2) increase growth rate and quality of materials, and 3) achieve steering and control of chemicals reactions in CVD processes for material synthesis. In this study, MEP refers to driving of chemical reactions using multiple energy forms, including translational energy (through heating) and vibrational energy (through laser resonant excitations). Because frequencies of molecular vibrations are in the infrared (IR) range, IR lasers are ideal energy sources to achieve resonant excitations of molecular vibrations [4]. Another advantage of IR lasers is that their narrow bandwidth prepares a single vibrational eigenstate, which makes control of reaction pathways feasible [3]. One approach to laser control is active intervention, in which the phases of reagent motions are controlled during the course of the reaction. This active intervention may preferentially lead reagents to one of many different reaction routes [4]. In this study, we introduced active intervention to combustion flame deposition of diamond and

achieved mode-selective reactions toward control of the chemical reactions.

Oxyacetylene (C_2H_2/O_2) combustion flame is the first and most common method for flame deposition of diamond [5-8]. An acetylene molecule has seven normal modes of vibrations. But these modes are either IR inactive or have very low IR activity, which means acetylene molecule has weak IR absorption and hence this molecule is not a suitable candidate for vibrational (IR) excitations. Ethylene (C_2H_4) has also been applied as precursor molecules in combustion flame deposition of diamond [9]. A C_2H_4 molecule has twelve normal modes of vibrations, one of which, called CH_2 wagging mode (v_7, 949.3 cm^{-1}, or 10.534 μm) as schematically illustrated in Fig. 2.2, has strong IR activity. Furthermore, this mode is in the range of a wavelength-tunable CO_2 laser (9.2~10.9 μm) and matches one wavelength (10.532 μm) of the laser. In this dissertation, we added ethylene molecules to the oxyacetylene flame to form a $C_2H_4/C_2H_2/O_2$ flame for diamond deposition. We used the wavelength-tunable CO_2 laser to resonantly excite the CH_2 wagging mode of the C_2H_4 molecules in the combustion flame, and achieved MEP in diamond deposition. Detailed studies are described in Chapters 3 through 6. Propylene (C_3H_6) is another precursor that has been applied for combustion flame deposition of diamond [10]. A C_3H_6 molecule has twenty-one modes of vibrations, four of which locate in the wavelength range of the wavelength-tunable CO_2 laser and are IR active. These vibrational modes, as schematically illustrated in Fig. 2.3, are (a) CH_3 rocking mode (out-of-plane wagging, v_{17}, 1044.7 cm^{-1}, or 9.572 μm), (b) a combination of C=C-C bending and C=CH_2 twisting modes (963 cm^{-1}, or 10.384 μm), (c) CH_3 symmetric

wagging mode (v_{12}, 934.5 cm^{-1}, or 10.7 μm), and (d) C-C stretching mode (v_{13}, 919 cm^{-1}, or 10.881 μm) [11, 12]. Each of these modes can be resonantly excited by the CO_2 laser tuned to a matching wavelength, respectively. The variety of suitable modes provides feasibility of mode-selective excitations toward mode-selective control of chemical reactions in diamond deposition. Detailed studies are described in Chapter 7.
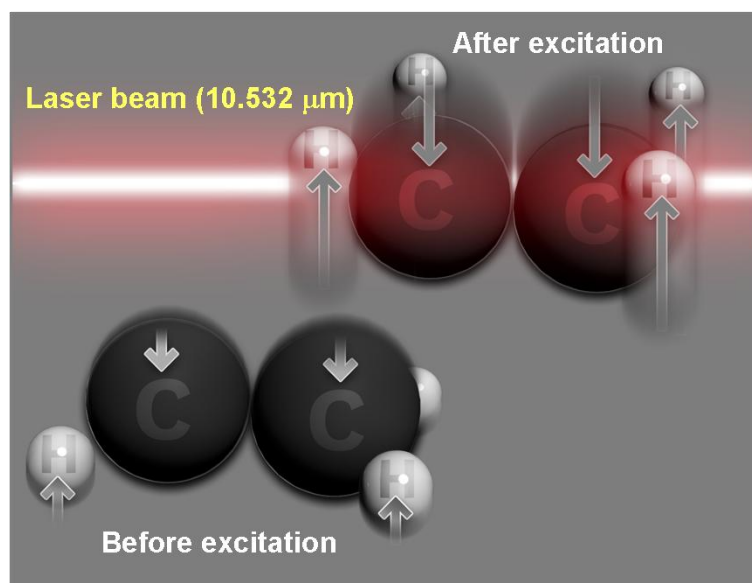
Figure 2.2 Schematic of the CH_2 wagging mode of a C_2H_4 molecule. When exposed into a CO_2 laser beam at a wavelength of 10.532 μm, the vibrational mode is resonantly excited.
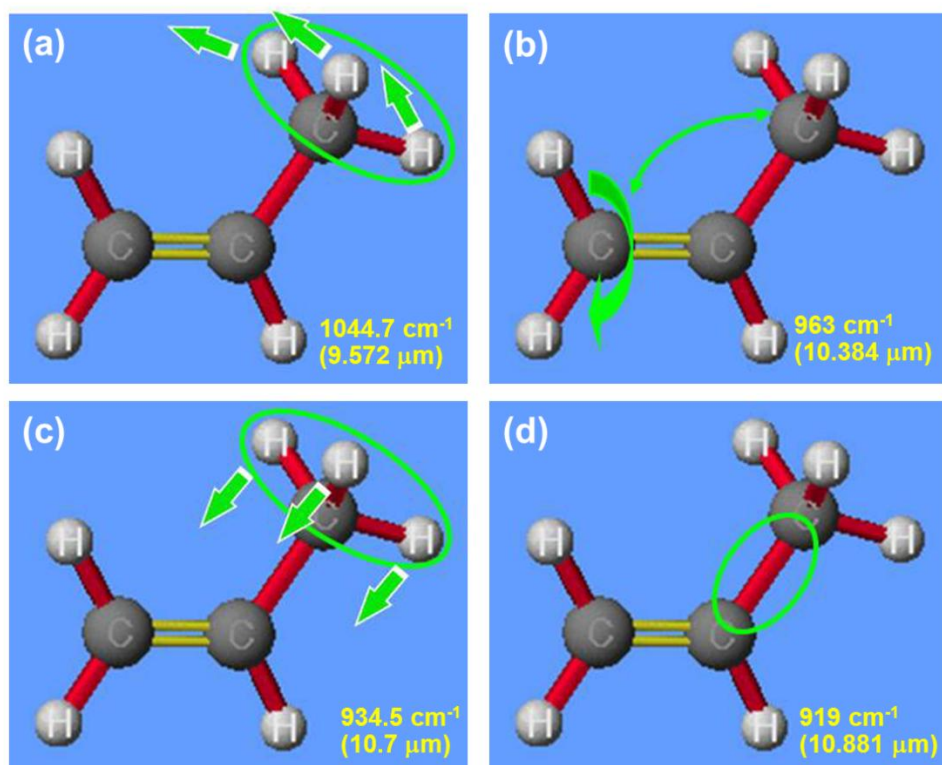
Figure 2.3 Schematic of four modes of vibrations of a C_3H_6 molecule: (a) CH_3 rocking mode (out-of-plane wagging, ν_{17}, 1044.7 cm^{-1}, or 9.572 µm), (b) a combination of C=C-C bending and C=CH$_2$ twisting modes (963 cm^{-1}, or 10.384 µm), (c) CH_3 symmetric wagging mode (ν_{12}, 934.5 cm^{-1}, or 10.7 µm), and (d) C-C stretching mode (ν_{13}, 919 cm^{-1}, or 10.881 µm).

2.2 Introduction to laser-assisted materials synthesis

Laser light can induce chemical reactions either homogenously within the gas or liquid phase or heterogeneously at gas-solid [13] and liquid-solid [14, 15] interfaces. In general, laser chemical processing involves photothermal and photolytic processes. In a photothermal process, multiple photons in visible infrared (Vis-IR) range must be absorbed to elevate molecules to higher vibrational levels until an atom is ionized or a molecule is dissociated. In a photolytic process, by absorption of visible ultraviolet (UV-Vis) photons, molecules can be electronically dissociated in a single step.

Since the 1960s, laser material processing has become an expanding field and has been well established in a wide variety of industrial applications. Some of the established areas include laser welding, soldering, drilling, and cutting in laser mechanical technology [16, 17], laser hardening, rapid solidification, glazing, cladding, and powder metallurgy in laser metals technology [16, 17], and laser recrystallization, doping, and annealing in semiconductor technologies [18, 19]. Laser chemical processing is one of the active areas in laser material processing that can efficiently assist etching and thin film deposition via chemical channels. Through laser-assisted chemical vapor deposition (LCVD), a variety of materials, such as metals (from metal halides, alkyls, and carbonyls), semiconductors (amorphous and crystalline germanium (Ge), silicon (Si), and compound semiconductors), insulators (oxides and nitrides), and heterostructures can be deposited [20]. Table 2.1 lists some typical LCVD processes with specific lasers and

wavelengths and gas precursors.

Table 2.1 Laser chemical vapor deposition or vapor phase epitaxy of various materials

Deposited Materials	Carrier Gases	Substrates	Laser/Wavelength (nm)	References
Au	$Au(CH_3)_2$	Si	Ar^+/515	Baum and Jones 1985 [21]
W	WF_6/SiH_4	GaAs	KrF/248	Turney *et al.* 1992; Tabbal *et al.* 1997 [22, 23]
a-Si	SiH_4	Glass	XeCl/308	Lee *et al.* 2006 [24]
a-SiC:H	$C_3H_{10}Si$	Quartz	CO_2/10.6 μm	Jensen and Chiu 2006 [25]
SiO_2	SiH_4/N_2O	Si	Tunable CO_2/10.6 10.28, 9.6, 9.28 μm	Tsai *et al.* 2001 [26]
GaAs	$Ga(CH_3)_3$/AsH_3	GaAs	Ar^+/488-514	Boutros *et al.* 1996 [27]
Diamond	CH_4/H_2	Si	CO_2/10.6 μm	Molian and Waschek 1993 [28]
Diamond-like carbon (DLC)	C_6H_6	W	KrF/248	Shi *et al.* 2005 [29]
a-CN$_x$ (x<1.3)	C_2H_2/N_2O/NH_3	SiO_2, Al_2O_3, Ti/Al_2O_3	CO_2/10.6 μm, KrF/248, ArF/193	Alexandrescu *et al.* 1997 [30]

LCVD opens up new possibilities in materials synthesis by enabling new reaction pathways and altered kinetics. In particular, at parallel incidence to the substrate surface, lasers permit pure gas-phase excitation without substrate heating. This is one of the main advantages over conventional CVD. Intense efforts have been made in the LCVD of high-quality thin films at lower substrate temperature [20]. A great deal of successful synthesis of compound semiconductor films with lower substrate temperatures have been reported, including gallium arsenide (GaAs) [31], gallium phosphide (GaP) [32], indium

phosphide (InP) [33], cadmium telluride (CdTe) [34], and mercury telluride (HgTe) [35].

The surface morphology of films was significantly improved compared with those grown

by standard CVD. With lower substrate temperatures, interdiffusion of elements at

interfaces between films as well as thermal defects were significantly reduced.

2.3 Introduction to diamond growth

Diamond has a wide range of extreme properties [36-40], which make it not only a promising material for conventional applications but also as a supreme semiconductor for microelectronics with wide band-gap, high carrier mobility, high breakdown fields, high workable temperature, and negative electron affinity. The ability to be operated in harsh and extreme environments also renders diamond an appealing material [40-45].
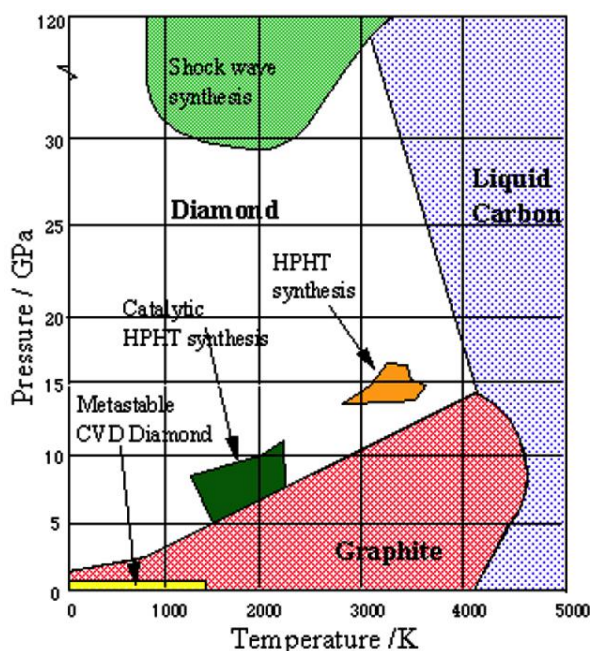
Figure 2.4 The carbon phase diagram [48], showing that at low temperatures and pressures graphite is the stable form of carbon. Diamond is only stable at sufficiently high temperatures and pressures.

Since the first diamond synthetic method was reported in 1955 [46], several strategies have been developed [36, 37, 47]. The synthesizing methods can be divided into two major groups: high-pressure and low-pressure routes. According to the carbon

phase diagram as shown in Fig. 2.4 [48], diamond is a stable phase of carbon at high pressure with respect to graphite, in which all carbon atoms are sp^3 hybridized and tetrahedrally bonded to form a cubic lattice (diamond lattice) of great rigidity and strength with a bond length of 1.54 Å. Therefore, it would be reasonable to find the high-pressure routes used for diamond synthesis. On the other hand, low-pressure routes come from completely different concepts. Using the chemical vapor deposition (CVD) method as an example [37-39], growth is conceptually realized by adding one carbon atom at a time to the initial template. Then the tetrahedrally bonded diamond is formed. Brief reviews of each synthetic method are provided below.

2.3.1 High-Pressure High-Temperature (HPHT) method

The HPHT techniques were deduced according to the carbon phase diagram (Fig. 2.4) [48]. Diamond is less stable than graphite at room temperature and atmospheric pressure [47]. Although graphite is more stable, diamond can exist in a metastable phase due to a significant kinetic barrier. Therefore, the transformation from diamond to graphite under mild conditions is extremely slow, unless the temperature is increased [47], as the thermodynamic stability of diamond decreases at high temperatures. The first reproducible HPHT diamond synthesis was reported to operate in a high-pressure (>75,000 atm) and high-temperature (1200 ~ 2000 °C) environment [46, 47]:

$$C_{graphite} \xrightarrow[\substack{\text{Metal catalysts/}\\\text{solvents}}]{\text{HPHT}} C_{diamond}$$

(1)
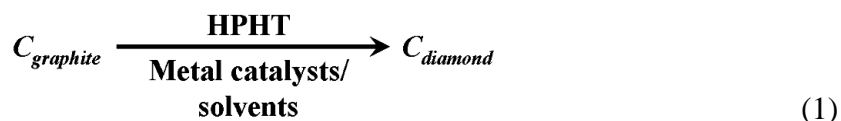
The metal catalysts used in the reaction reduce the activating energy for the reaction and act as good solvents for nondiamond carbons but poor solvents for diamond [46-50]. In the HPHT process, diamond is crystallized from metal-solvated carbon at a pressure of 50-100 kBar and a temperature of 1,500-2,000 °C. In 1970, the first successful synthesis of large gem-quality diamond crystals was achieved [51-53]. The HPHT method has been commercialized for more than 40 years. Yet, synthesized diamond crystals are generally small in size unless catalyst and diamond seeds are applied. Substantial energy requirements and costs limit the production of high-quality diamond. Meanwhile, the low growth rate of the HPHT-produced diamond cannot satisfy the rapidly advancing demands for more complex diamond bulks and films, structures, and devices.

2.3.2 Shock Wave (SW) process

The principles for the SW process are similar to those of the HPHT method, except that the high pressures and temperatures are generated by instant explosions [54-56]. In an extremely short time, an explosion generates an instantaneous pressure exceeding five million pounds per square inch (psi) at a temperature of 1,000 °C. During this process, graphite melts immediately and forms diamond. The SW diamond is a

mixture of diamond (cubic) and lonsdaleite (hexagonal) forms of carbon, in which the latter is called "hexagonal diamond". The shortcomings of the SW process include low purity in the carbon mixture synthesized, lack of shape and crystal controls, and small crystal sizes [37].

2.3.3 Chemical Vapor Deposition (CVD)

First introduced in 1962 [57] and rapidly developed since the 1980s [58, 59], CVD is a gas-phase chemical reaction process involving activation of an appropriate gaseous mixture via chemical reactions, which occurs in the vicinity of a substrate upon which diamond may deposit. All CVD methods for diamond synthesis require activated gas-phase carbon-containing precursor molecules. The activation process can be realized by several techniques, including hot filament (HF), microwave or radio frequency (RF) plasma, direct charge (DC) arc jet, thermal heating, and combustion flame [37, 39, 58-62]. Laser-assisted and optical pumping techniques are also studied [63, 64] but not widely used due to limitations in laser wavelengths and powers. CVD diamond could be realized in several gas mixtures, including a hydrocarbon/H_2 system, C/H/O system, C/H/halogen system, and fullerene/argon system [39, 47, 61]. The reaction mechanisms differ significantly from each other. No unique mechanism or growth model is capable of explaining all reaction systems. A typical phase diagram of the precursor elements in CVD methods is represented in the C-H-O diagram for CVD of diamond shown in Fig.

2.5 [65]. Only a narrow band for the ratio of C, H, and O is suitable for diamond synthesis.
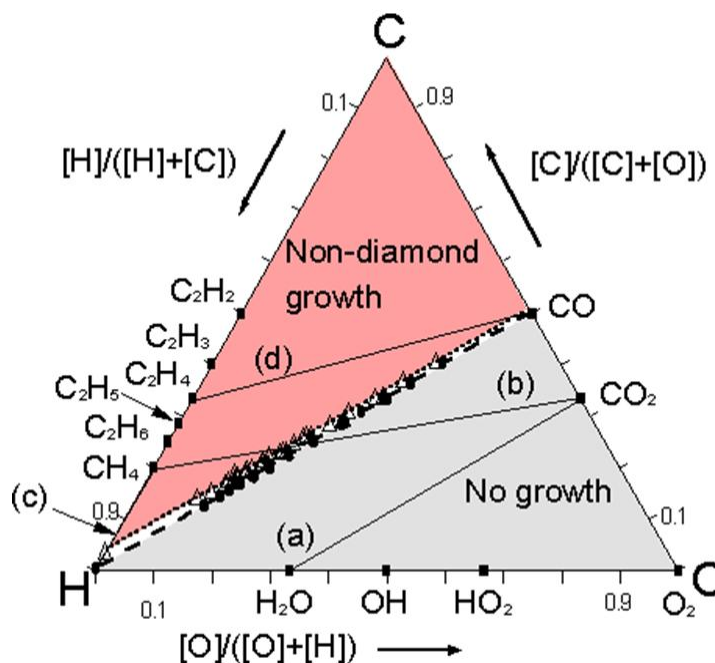
Figure 2.5 C-H-O diagram for chemical vapor deposition of diamond [65].

Although CVD methods differ significantly, they share some common characteristics [37]:   1) a gas phase must be activated and contain carbon species, 2) a sufficient concentration of species that etch graphite or suppresses gaseous graphite precursors must be present (in most cases, atomic hydrogen plays this role, while other species like atomic oxygen and halogen can exert similar functions), 3) the substrates must be pretreated to support the nucleation and growth of diamond, and 4) a driving force to transport the carbon-bearing species from the gas phase to the substrate surface should be introduced.

In summary, the three key steps involved in CVD methods are activation of carbon sources, transport and diffusion of radicals, and nucleation and growth. Although many efforts have been made to improve these key processes, CVD methods generally produce polycrystalline diamond films with morphologies sensitive to the growth environment. Growth rates for each method vary considerably with regard to diamond quality. High-quality diamond films are steadily produced by microwave plasma-enhanced CVD (MPCVD) with a growth rate up to 150 μm/hr [8]. HF-CVD also obtains high-quality diamond films (except for contamination from hot filaments), but the process has a much slower growth (0.1 to 10 μm per hour) [37, 38, 64]. Combustion methods can deposit diamond films in open atmosphere with simpler equipment and much lower cost but with poor process control and inferior diamond films [38, 65-68]. However, the high cost and low growth rate of MPCVD cannot cater for more applications.

CVD methods allow coating diamond on nondiamond substrates, as well as self-standing diamond plates, which substantially expands the diamond applications [37-39, 69-72]. In addition to the inherent shortcomings associated with individual CVD methods [38] (e.g., low growth rate and filament contamination in HF-CVD, poor quality and process control in combustion-CVD, high heat fluxes and small deposition areas in DC-CVD, high heat fluxes in RF-CVD, and microwave leakage and poor morphology control in MPCVD), there are still several common challenges associated with CVD

technologies [36-39, 61]. For example, there is a need to increase growth rate without compromising diamond film quality in a cost effective manner and to overcome the low energy efficiency. In addition, it is critical to improve our understanding of the mechanisms for heteroepitaxial growth of diamond upon nondiamond substrates for sizeable flawless diamond crystals.

References

[1]. Asmussen, J. and Reinhard D. K. Diamond Films Handbook Ch. 4, Marcel Dekker, New York, NY (2002).

[2]. Crim, F. F., "Making Energy Count", Science **317,** 1707 (2007).

[3]. Killelea, D. R., Campbell, V. L. Shuman, N. S. and Utz, A. L., "Bond-selective control of a heterogeneously catalyzed reaction", Science **319,** 790 (2008).

[4]. Zare, R. N., "Laser Control of Chemical Reactions", Science **279,** 1875 (1998).

[5]. Hirose, H. and Komaki, K. European Patent Application, EP324538 (1988).

[6]. Kim, J. S. and Cappelli, M. A., "A model of diamond growth in low pressure premixed flames", Journal of Applied Physics **72,** 5461 (1992).

[7]. Murayama, M., Kojima, S., Uchida, K., "Uniform deposition of diamond films using a flat flame stabilized in the stagnation‑point flow", Journal of Applied Physics **69,** 7924 (1991).

[8]. Ravi, K. V., "Combustion synthesis: is it the most flexible of the diamond synthesis processes?", Diamond and Related Materials **4,** 243 (1995).

[9]. Kim, J. S. and Cappelli, M. A., "Diamond film growth in low pressure premixed ethylene‑oxygen flames", Applied Physics Letters **65,** 2786 (1994).

[10]. Shin, H. S. and Goodwin, D. G., "Diamond growth in premixed propylene‑oxygen flames", Applied Physics Letters **66,** 2909 (1995).

[11]. Chao, J. and Zwolinski, B. J., "Ideal gas thermodynamic properties of ethylene and propylene", Journal of Physical Chemistry Ref. Data **4,** 251 (1975).

[12]. Lord, R. C. and Venkateswarlu, P., "The Infrared Spectra of Propylene and Propylene-d$_6$", Journal of Optical Society of America **43,** 1079 (1953).

[13]. Cheng, Y. H., Qiao, X. L., Chen, J. G., Wu, Y. P., Xie, C. S., Muo, S. B., Sun, Y. B., and Tay, B. K., "Synthesis of carbon nitride films by direct current plasma assisted pulsed laser deposition", Applied Physics a-Material **74**, 225 (2002).

[14]. Wang, J. B., Liu, Q. X., and Yang, G. W., "Nano-crystalline dia-mond prepared by laser ablation solid target in liquid", Chemical Journal of Chinese Universities **19**, 1719 (1998).

[15]. Yang, G. W., and Wang, J. B., "Carbon nitride nanocrystals having cubic structure using pulsed laser induced liquid-solid interfacial reaction", Applied Physics a-Materials **71**, 343 (2000).

[16]. Bass, M., Laser Materials Processing, Amsterdam, North-Holland (1983).

[17]. Steen, W. M., "Laser material processing—an overview", Journal of Optics A-Pure Applied Optics **5**, S3 (2003).

[18]. Markevich, M. I., Podol'tsev, A. S., Piskunov, F. A., and Chao, C., "Pulsed-laser annealing of GaAs in a multilayer semiconductor structure", Inorganic Materials **35**, 224 (1999).

[19]. Hatanaka, Y., Niraula, M., Nakamura, A., and Aoki, T., "Excimer laser doping techniques for II±VI semiconductors", Applied Surface Science **175**, 462 (2001).

[20]. Bauerle, D., Laser Processing and Chemistry, 3rd Ed. Springer-Verlag Berlin, (2000).

[21]. Baum, T. H. and Jones, C. R., "Laser chemical vapor deposition of gold", Applied Physics Letters **47,** 538 (1985).

[22]. Turney, W., Hung, Y. M., Starcevich, S. G., Cardinahl, P. S., Grassian, V. H., and Singmaster, K. A., "Pulsed laser-assisted chemical vapor deposition of W, Mo, and V thin films", Chemistry of Materials **4,** 1192 (1992).

[23]. Tabbal, M., Meunier, M., Izquierdo, R., Beau, B., and Yelon, A., "Laser-chemical vapor deposition of W Schottky contacts on GaAs using WF_6 and SiH_4", Journal of Applied Physics **81,** 6607 (1997).

[24]. Lee, S. H., Hong, W. S., Kim, J. M., Lim, H. C., Park, K. B., Cho, C. L., Lee, K. E., Kim, D. Y., Jung, J. S., Kwon, J. Y., and Noguchi, T., "Liquid Phase Epitaxy Growth of m-Plane GaN Substrate Using the Na Flux Method", Japanese Journal of Applied Physics **45,** L227 (2006).

[25]. Jensen, C. J., and Chiu, W. K. S., "Open-Air Laser-Induced Chemical Vapor ... Coatings", Surface Coating Technology **201,** 2822 (2006).

[26]. Tsai, H. S., Chiu, H. C., Chang, S. H., Cheng, C. C., Lee, C. T., and Liu, H. P., "CO_2-Laser-Assisted Plasma-Enhanced Chemical Vapor Deposition of Silicon Dioxide Thin Film", Japanese Journal of Applied Physics **40,** 3093 (2001).

[27]. Boutros, K. S., Roberts, J. C., and Bedair, S. M., "Direct writing of GaAs optical waveguides by laser‑assisted chemical vapor deposition", Applied Physics Letters **68,** 2041 (1996).

[28]. Molian, P. A. and Waschek, A., "Laser physico-chemical vapour deposition of cubic boron nitride thin films", Journal of Materials Science **28,** 1733 (1993).

[29]. Shi, J., Lu, Y. F., Chen, X. Y., Cherukuri, R. S., Mendu, K. K., Wang, H., and Batta, N., "Phase-graded deposition of diamond-like carbon on nanotips by near-field induced chemical vapor deposition", Applied Physics Letters **86,** 131918 (2005).

[30]. Alexandrescu, R., Cireasa, R., Pugna, G., Crunteanu, A., Petcu, S., Morjan, I., Mihailescu, I. N., and Andrei, A., "CN_x thin films obtained by laser induced CVD in different gas-substrate systems", Applied Surface Science **110,** 544 (1997).

[31]. Aoyagi. Y., "Beam assisted atomic layer controlled epitaxy and etching of GaAs", Materials Research Society Symposium Processing **222,** 121 (1991).

[32]. Sudarsan, U., Cody, N. W., Dosluoglu, T., and Solanki, R., "Excimer laser assisted selective epitaxy of GaP", Applied Physics A **50,** 325 (1990).

[33]. Donnelly, V. M., Brasen, D., Appelbaum, A., and Geva, M., "Excimer laser induced deposition of InP", Journal of Vacuum Science and Technology A **4,** 716 (1986).

[34]. Irvine, S. J. C., Hill, H., Brown, G. T., Barnett, S. J., Hails, J. E., Dosser, O. D., and Mullin, J. B., "Selected area epitaxy in II–VI compounds by laser-induced photo-metalorganic vapor phase epitaxy", Journal of Vacuum Science and Technology B **7,** 1191 (1989).

[35]. Fujita, Y., Fujii, S. and Iuchi, T., "Ultraviolet spectra of II–VI organometallic compounds and their application to in situ measurements of the photolysis in a

metalorganic chemical vapor deposition reactor", Journal of Vacuum Science and Technology A **7,** 276 (1989).

[36]. Nazare, M. H. and Neves, A. J., Properties, growth and applications of diamond. INSPEC, the Institution of Electrical Engineers: London, (2001).

[37]. Davis, R. F., Diamond films and coatings - Development, Properties, and Applications. Noyes Publications: Park Ridge, New Jersey, (1993).

[38]. Marinkovic, S. N., Diamond synthesized at low pressure. In Chemistry and Physics of Carbon, **29,** 71 (2004).

[39]. Railkar, T. A., Kang, W. P., Windischmann, H., Malshe, A. P., Naseem, H. A., Davidson, J. L., and Brown, W. D., "A Critical Review of Chemical Vapor-Deposited (CVD) Diamond for Electronic Applications", Critical Reviews in Solid State and Materials Sciences **25,** 163 (2000).

[40]. Hauert, R., "An overview on the tribological behavior of diamond-like carbon in technical and medical applications", Tribology International **37,** 991 (2004).

[41]. Aleksov, A., Denisenko, A., Kunze, M., Vescan, A., Bergmaier, A., Dollinger, G., Ebert, W., and Kohn, E., "Diamond diodes and transistors", Semiconductor Science and Technology **18,** S59 (2003).

[42]. Gurbuz, Y., Esame, O., Tekin, I., Kang, W. P., and Davidson, J. L., "Diamond semiconductor technology for RF device applications", Solid-State Electronics **49,** 1055 (2005).

[43]. Kohn, E., Ebert, W., Adamschik, M., Schmid, P., and Denisenko, A.,

"Diamond-based MEMS devices", New Diamond and Frontier Carbon Technology **11,** 81 (2001).

[44]. Auciello, O., Birrell, J., Carlisle, J. A., Gerbi, J. E., Xiao, X. C., Peng, B., and Espinosa, H. D., "Materials science and fabrication processes for a new MEMS technoloey based on ultrananocrystalline diamond thin films", Journal of Physics-Condensed Matter **16,** R539 (2004).

[45]. Kohn, E., Adamschik, M., Schmid, P., Denisenko, A., Aleksov, A., and Ebert, W., "Prospects of diamond devices", Journal of Physics D-Applied Physics **34,** R77 (2001).

[46]. Bundy, F. P., Hall, H. T., Strong, H. M., and Wentorf, R. H., "Man-made diamonds", Nature **176,** 51 (1955).

[47]. Ferro, S., "Synthesis of diamond", Journal of Materials Chemistry **12,** 2843 (2002).

[48]. Bundy, F. P., "The P, T Phase and Reaction Diagram for Elemental Carbon", Journal of Geophysical Research **85,** 6930 (1980).

[49]. Litvin, Y. A., Inorganic Materials **4,** 144 (1968).

[50]. Bovenkerk, H. P., Bundy, F. P., Hall, H. T., Strong, H. M., and Wentorf, R. H. J., "The Preparation of Diamond", Nature **184,** 1094 (1959).

[51]. Sumiya H., and Toda N., "Growth of high-quality large diamond crystals under high pressure and high temperature", Diamond and Related Materials **5,** 1359, (1996).

[52]. Wentorf, R. H. J., "Diamond growth rates", Journal of Physical Chemistry **75,** 1833

(1971).

[53]. Strong, H. M. and Chrenko, R. M., "Diamond growth rates and physical properties of laboratory-made diamond", Journal of Physical Chemistry **75,** 1838 (1971).

[54]. Trueb, L. C., "Microstructural Study of Diamonds Synthesized under Conditions of High Temperature and Moderate Explosive Shock Pressure", Journal of Applied Physics **42,** 503 (1971).

[55]. Cowan, G. R., Dunnington, B. W., and Hottzman, A. H., US Patent No. 3,401,019 (1968).

[56]. DeCarli, P. S. and Jamieson, J. C., "Formation of Diamond by Explosive Shock", Science **133,** 1821 (1961).

[57]. Eversole, W. G., Synthesis of diamond. U.S. Patent 3030188, 1962.

[58]. Kamo, M., Sato, S. Y., Matsumoto, S., and Setaka, N., "Diamond synthesis from gas phase in microwave plasma", Journal of Crystal Growth **62,** 642 (1983).

[59]. Matsumoto, S., Sato, S. Y., Kamo, M., and Setaka, N., "Vapor Deposition of Diamond Particles from Methane", Japanese Journal of Applied Physics Part 1-Regular Papers Short Notes & Review Papers **21,** L183 (1982).

[60]. Lee, S. T., Lin, Z. D., and Jiang, X., "CVD diamond films: nucleation and growth", Materials Science & Engineering R-Reports **25,** 123 (1999).

[61]. Celii, F. G. and Butler, J. E., "Diamond Chemical Vapor-Deposition", Annual Review of Physical Chemistry **42,** 643 (1991).

[62]. Yarbrough, W. A., and Messier, R., "Current Issues and Problems in the Chemical Vapor-Deposition of Diamond", Science 247, 688 (1990).

[63]. Buerki, P. R. and Leutwyler, S., "Homogeneous Nucleation of Diamond Powder by CO_2-Laser-Driven Gas-Phase Reactions", Surface & Coatings Technology **47,** 22 (1991).

[64]. Buerki, P. R. and Leutwyler, S., "Synthesis of Submicron Diamond Powders by CO_2-Laser Pyrolysis of C_2H_4", Journal of Applied Physics **69,** 3739 (1991).

[65]. Petherbridge, J. R., May, P. W., and Ashfold, M. N. R., "Modeling of the gas-phase chemistry in C–H–O gas mixtures for diamond chemical vapor deposition", Journal of Applied Physics **89,** 5219 (2001).

[66]. Yan, C. S., Vohra, Y. K., Mao, H. K., and Hemley, R. J., "Very high growth rate chemical vapor deposition of single-crystal diamond", Proceedings of the National Academy of Sciences **99,** 12523 (2002).

[67]. Buckley, R. G., Moustakas, T. D., Ye, L., and Varon, J., "Characterization of filament-assisted chemical vapor deposition diamond films using Raman spectroscopy", Journal of Applied Physics **66,** 3595 (1989).

[68]. Howard, W., Huang, D., Yuan, J., Frenklach, M., Spear, K. E., Koba, R., and Phelps, A. W., "Synthesis of Diamond Powder in Acetylene Oxygen Plasma", Journal of Applied Physics **68,** 1247 (1990).

[69]. Huang, S. M., Lu, Y. F., and Sun, Z., "Conversion of diamond clusters from a polymer by Nd : YAG pulsed laser (532 nm) irradiation", Applied Surface Science **151,** 244 (1999).

[70]. Wu, K. H., Wang, E. G., Cao, Z. X., Wang, Z. L., and Jiang, X., "Microstructure and its effect on field electron emission of grain-size-controlled nanocrystalline diamond films", Journal of Applied Physics **88,** 2967 (2000).

[71]. Zhu, W., Kochanski, G., Jin, S., Seibles, L., Jacobson, D. C., McCormack, M., and White, A. E., "Electron Field-Emission From Ion-Implanted Diamond", Applied Physics Letters **67,** 1157 (1995).

[72]. Zhu, W., Kochanski, G. P., and Jin, S., "Low-field electron emission from undoped nanostructured diamond", Science **282,** 1471 (1998).

CHAPTER 3

Laser Resonant Excitation of Ethylene Molecules to Enhance Deposition of Diamond Films

3.1 Introduction

3.2 Absorption of laser energy by flames

3.3 Promotion of chemical reactions

3.4 Enhancement of diamond deposition

3.1 Introduction

Currently, diamond synthesis by chemical vapor deposition (CVD) including

thermal-assisted (hot filament) CVD [1], microwave plasma-assisted CVD [2-5], plasma

torch CVD [6], and combustion flame CVD [7-9] has been widely investigated.

Combustion synthesis of diamond using an oxyacetylene combustion flame was firstly

demonstrated by Hirose and Kondo in 1988 [10]. It has been argued that combustion

synthesis of diamond is the most flexible of the CVD alternatives because of its scalable

nature, minimum utility requirement, and significantly reduced capital costs relative to

plasma-aided process [11]. Laser-assisted CVD was regarded as a promising way due to

its unique means of fast heating [12, 13] and selective optical pumping of the reactive

species [14-16]. In addition, a number of substrate pretreatment methods, such as

scratching and seeding [17, 18], have been studied to enhance the diamond nucleation.

Lasers are also ideal energy sources for vibrational resonant excitations. Laser-assisted

chemical reaction control was investigated during the past years [19]. CO_2 laser is a

typical energy source widely used in laser chemistry due to its high energy efficiency and

high output power. However, common commercial CO_2 lasers only produce a fixed

wavelength of 10.591 μm, which cannot match the wavelengths required for effective

vibrational resonant excitations. Excitation of C_2H_4 molecules through the broadening of

the absorption band using a common CO_2 laser at 10.591 μm was investigated in our

previous study [20]. In this dissertation, efforts are focused on resonant vibrational

excitations using a wavelength-tunable CO_2 laser with a high power output up to 1000 W. The CO_2 laser wavelength can be precisely tuned to match the CH_2-wagging mode of C_2H_4 molecules to achieve the optimal resonant excitation to significantly improve the diamond deposition in the CVD processes using the $C_2H_4/C_2H_2/O_2$ gas mixture.

In this study, resonant vibrational excitation of C_2H_4 molecules by perfect wavelength match using a tunable CO_2 laser in $C_2H_4/C_2H_2/O_2$ combustion CVD of diamond films was investigated in open air. Instead of the commonly used 10.591 μm, the CO_2 laser wavelength was tuned to 10.532 μm to match the vibrational frequency of the CH_2-wagging mode (v_7, 949.3 cm^{-1}) in C_2H_4 molecules. Although both C_2H_2 and O_2 yield an ideal element ratio in combustion CVD of diamond, there is no wavelength-matching laser which has required wavelengths to resonantly excite the C_2H_2 or O_2 molecules. Therefore, C_2H_4, another precursor for diamond growth [21, 22], was added into the combustion flame to couple laser energy into the chemical reactions through resonant excitations. Laser pyrolysis and decomposition of C_2H_4 molecules through vibrational excitations have been studied and used to produce diamond powders [23]. However, vibrational resonant excitation of precursor molecules using a tunable CO_2 laser has rarely been reported to date. Through the perfect wavelength matching, high-efficient energy coupling into the CVD reactions, and significant enhancement of diamond growth using the tunable CO_2 laser resonant excitation were investigated. Multi-energy processing was achieved by introducing the resonant vibrational excitation of precursor molecules to the thermal-driven CVD method.

Figure 3.1 shows the experimental setup for the CO_2 laser-assisted combustion flame CVD of diamond. A commercial oxygen–acetylene torch with a 1.5 mm orifice tip was used to generate the flame. The fuel was a mixture of C_2H_4 and C_2H_2 with a gas flow ratio of 1:1, which was then mixed with O_2 with a volume ratio of 1.03 [$(C_2H_4+C_2H_2)/O_2$]. A wavelength-tunable CO_2 laser (PRC, spectrum range from 9.2 to 10.9 μm) was used in the synthesis process to achieve resonant excitation of the C_2H_4 precursor molecules. The CH_2 wagging mode (v_7, 949.3 cm^{-1}) of the ethylene molecules corresponds to a wavelength of 10.534 μm, which has a close match with the CO_2 laser line at 10.532 μm. Laser energy was coupled into the reactions through resonant excitation of the C_2H_4 molecules. Tungsten carbide (WC) plates (BS-6S, Basic Carbide Corp., containing 6% cobalt) with a dimension of $12.7 \times 12.7 \times 1.6$ mm^3 were used as substrates. The surface roughness of the WC substrates was 400 nm. The substrate was placed on a water cooling box mounted on a motorized X-Y-Z stage. The CO_2 laser, tuned to 10.532 μm with a power of 800 W, was directed in parallel with the substrate surface but perpendicularly to the flame axis. The laser beam was focused using a ZnSe convex lens (focal length = 254 mm) to 2 mm in diameter, which was the same as the average diameter of the inner flame. The original length of the flame was around 6 mm, which shrunk to about 3 mm when the 10.532-μm laser beam was introduced into the flame right underneath the nozzle. The distance between the inner flame tip and the diamond growth site was maintained at about 0.5 mm, by the program-controlled X-Y-Z stage. The temperature of the growth site was monitored by a pyrometer (Omega Engineering, Inc., OS3752). The temperature

was maintained at 760 - 780 ℃ by adjusting the flow rate of the water-cooling box.

Diamond samples were also prepared with 10.532-μm laser irradiation and without laser

irradiation, but under the same condition of gas flow ratio and deposition temperature.
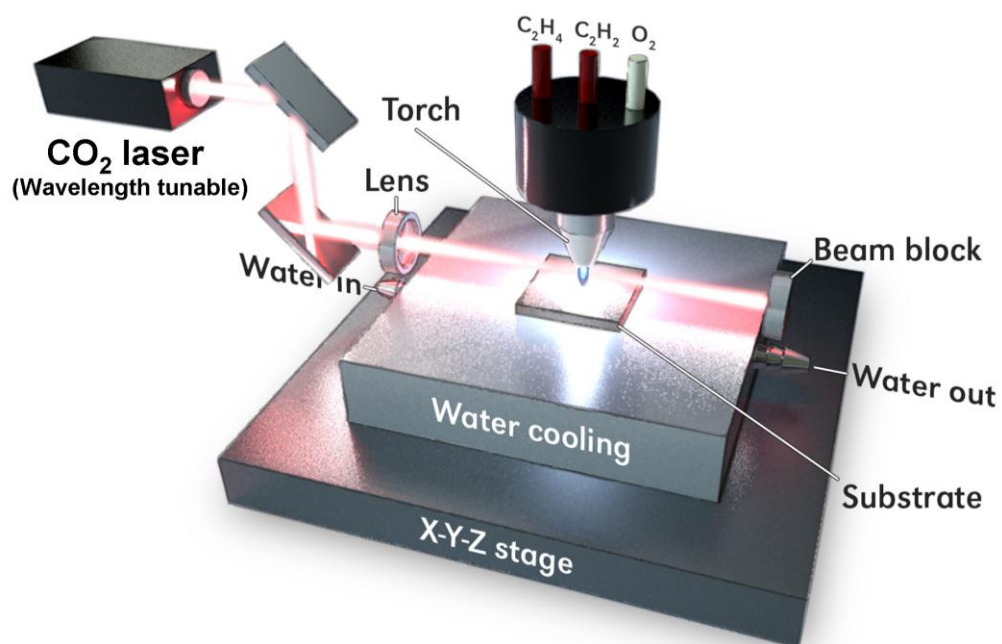
Figure 3.1 Schematic experimental setup of laser-assisted combustion flame CVD for diamond deposition.

3.2 Absorption of laser energy by flames

Figure 3.2 shows the optical images of the $C_2H_4/C_2H_2/O_2$ flames under irradiations of the tunable CO_2 laser with 10.591 and 10.532 μm, respectively. The length of the inner flame was about 6 mm without laser irradiation, as shown in Fig. 3.2(a). When a CO_2 laser beam of 10.591 μm irradiated the flame, the inner flame became brighter and shorter as shown in Fig. 3.2(b). At a laser power of 800 W, the length of the inner flame was shortened to 4.8 mm with a 20% increase in the diameter. Figure 3.2(c) shows the optical images of the flame under laser irradiations at the wavelength of 10.532 μm, which matches the CH_2-wagging vibration mode of C_2H_4. At this wavelength, the length of the flame inner cone was reduced to about 3 mm with an 80% increase in the diameter when the laser power was 800 W. The shorter inner flame is due to the enhanced reactions in the flame induced by the laser resonant excitation. A power meter was used to monitor the absorption of the laser powers by comparing the measured powers with and without the flame absorption. When the laser power was around 800 W, 3.4% of the incident laser power was absorbed by the flame at 10.591 μm, whereas 14.7% of the incident laser power was absorbed for at 10.532 μm under the same experimental condition.
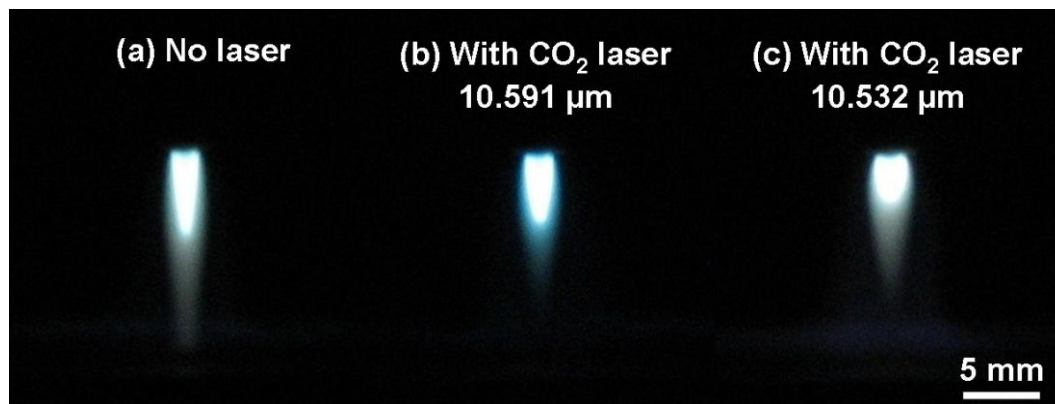
Figure 3.2 Images of flames (a) without laser, (b) with CO$_2$ laser irradiation at 10.591 μm, 800 W, and (c) with CO$_2$ laser irradiation at 10.532 μm, 800 W.

A power meter was used to monitor the absorption of the laser powers by comparing the measured powers before and after the flame absorption. Laser power absorption spectra of the precursors were then measured within a spectral range from 9.2 to 10.9 μm. By irradiating the laser beam through the C$_2$H$_4$/C$_2$H$_2$/O$_2$ flame used for the laser-assisted growth of diamond crystals, an obvious absorption peak was observed at 10.532 μm, as shown in Fig. 3.3. The absorption peak at 10.532 μm by the C$_2$H$_4$/C$_2$H$_2$/O$_2$ flame was ascribed to the resonant excitation of the CH$_2$ wagging mode (v_7, 949.3 cm^{-1}) of the C$_2$H$_4$ molecules, as illustrated in the inset of Fig. 3.3. At the ground state, the C$_2$H$_4$ molecule vibrates like a butterfly. By absorbing laser energy at 10.532 μm, the CH$_2$ wagging mode vibration is resonantly excited. It has been reported that at higher temperature, the peak position of the Q branch of molecular vibrations has red shifts. But the shift is in magnitudes of 10^{-3} μm, which is relatively small as compared with the differences between two laser emitting lines [24]. This explains why the absorption peak

of the CO_2 laser is still at 10.532 μm at the high flame temperature.
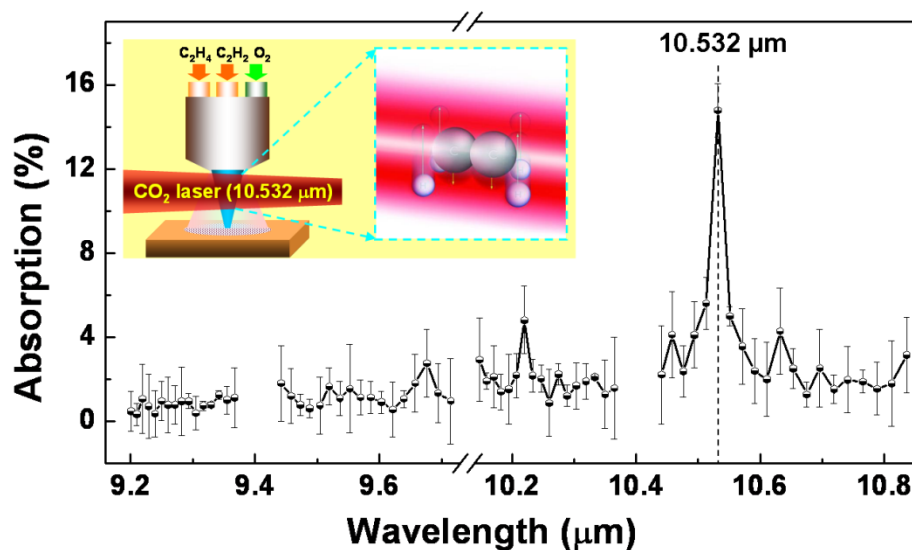
Figure 3.3 Absorption of CO_2 laser power by the C_2H_4/C_2H_2/O_2 flame used for the laser-assisted growth of diamond crystals as a function of laser wavelength. Inset is a schematic of the CH_2 wagging mode excitation of an ethylene molecule by the 10.532 μm CO_2 laser.

Without the C_2H_4 gas, C_2H_2/O_2 (1:1) flame had neither laser absorption nor visible change in the flame. The CH_2 wagging vibrational mode of C_2H_4 molecule shows a vibrational wavenumber at 949.3 cm^{-1}. For most common commercial CO_2 lasers, the wavelength is 10.591 μm (equivalent to a wavenumber of 944.2 cm^{-1}), which is close to the infrared absorption band corresponding to the CH_2 wagging vibration mode of the C_2H_4. The rotational partition function spreads the C_2H_4 population over a much wider range under current experimental conditions. Therefore, the CO_2 laser energy can almost be resonantly absorbed by the C_2H_4 molecules through this vibrational mode due to the

broadening of the absorption band. The efficiency of the resonant absorption under this wavelength is relatively low. The absorption coefficient of gaseous C_2H_4 is about 1.77 atm/cm at room temperature with laser wavelength at 10.591 μm. However, when the CO_2 laser wavelength was tuned to 10.532 μm (equivalent to a wavenumber of 949.5 cm^{-1}), the absorption coefficient of gaseous C_2H_4 increased to about 29 atm/cm at room temperature [20]. Although the environment condition in pure C_2H_4 gas at room temperature is different from that in a flame, the difference between the absorption coefficients can indicate the high efficiency of the resonant absorption of the laser energy when the CO_2 laser wavelength is tuned to 10.532 μm. The experimental results supported a high efficiency of vibrational resonant excitation at wavelength of 10.532 μm, as shown in Fig. 3.3.

3.3 Promotion of chemical reactions

Optical emission spectroscopy (OES) was used to study the effects of the resonant vibrational excitations to chemical reactions in diamond CVD. OES spectra of the flames during the film depositions were collected in a direction perpendicular to the flame axis. The setup for OES study is schematically illustrated in Fig. 3.4. The optical emission of the flame was introduced into a spectrometer (Andor Shamrock SR-303i-A) coupled with an ICCD (Andor iStar DH-712) through two lenses and an optical fiber which were all made of UV-grade quartz. All the spectra were taken at a point of 0.3 mm above the tip of the inner flame to compare the deposition conditions. The dimension ratio of the image and the flame was 1:1. The optical fiber, with a diameter of 50 μm, was precisely positioned in the projected image of the inner flame. A background spectrum taken before the collections of the emission spectra was subtracted in all results.
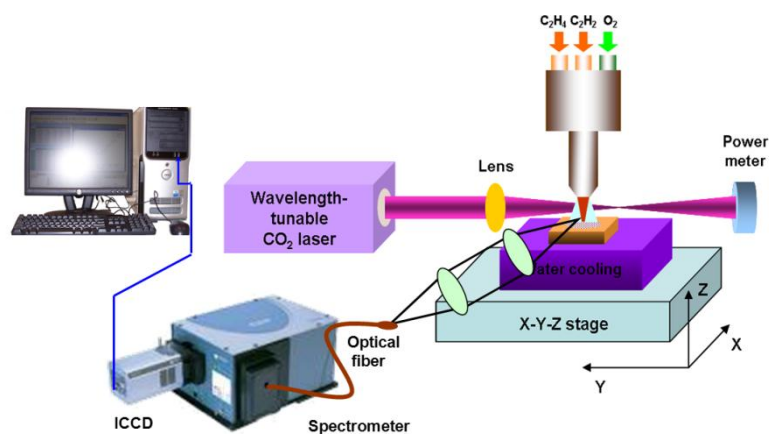
Figure 3.4 Schematic diagram of the experimental setup for laser resonant excitation and OES study.

It was demonstrated that by enhancing the reactions in the flame, laser resonant excitation of the C-H bond vibration in C_2H_4 molecules results in the increased concentrations of several chemical species [9]. According to the optical emission spectra obtained from the flame with and without laser irradiation shown in Fig. 3.5, obvious increases in concentrations of OH, CH and C_2 species were observed in the laser-irradiated flame. It is suggested that OH radicals play a critical role in combustion synthesis of diamond by etching the surface-bond hydrogen and stabilizing the sp^3 hybridized surface carbon bonds [25, 26]. The CH radical is also believed to be helpful in diamond growth [27]. Both increments explain why both growth rate and crystal quality were improved in the laser-assisted combustion synthesis of diamond. The C_2 radical, however, has a two-sided effect on the diamond growth. On the unhydrided surface, the insertion of C_2 into a C=C bond produces a carbene, leading to the formation of the secondary nucleation. On the monohydride surface, however, the addition of a C_2 to a hydrogen-terminated diamond (110) surface is energetically very favorable, making the growth of the existing crystal proceeds readily [28, 29]. Whether the increase in the C_2 concentration induced by laser excitation has a negative or positive impact needs more detailed studies.
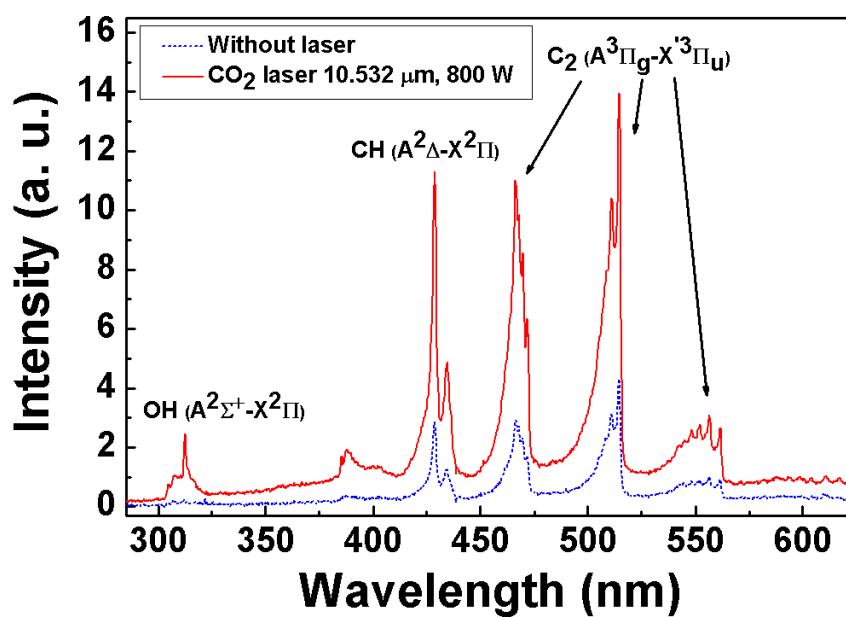
Figure 3.5 Optical emission spectra of the flame before (dashed curve) and after (solid curve) CO₂ laser irradiation at a wavelength of 10.532 μm and a power of 800 W.

3.4 Enhancement of diamond deposition

Diamond films were deposited using the flames with the vibrational excitations of the C_2H_4 molecules. Both laser wavelengths of 10.591 and 10.532 μm were used for the excitations. The temperature of the WC substrates was kept at 780 ℃ during all depositions. Figure 3.6 shows the scanning electron microscope (SEM) images of the deposited films deposited for 30 min without laser excitation (a), with 800 W laser excitations at 10.591 μm (b), and with 800 W laser excitations at 10.532 μm (c). It is observed that most of the diamond grains are around 3~4 μm in the case without the laser excitation as shown in Fig. 3.6(a). The grain sizes in Fig. 3.6(b) increase to around 5~6 μm. In Fig. 3.6(c), most of the grain sizes are about 8~10 μm which was deposited with the 10.532-μm laser excitation of 800 W. The grain sizes of the deposited films showed a significant increase with laser irradiation. When the 10.532-μm laser with power of 800 W was applied, the grain size of the film was three to four times larger than the film without laser excitation and almost twice of the film deposited with laser excitation at 800 W, 10.591 μm. The increase in grain size indicates the accelerated nucleation and higher growth rate with the laser excitation at a wavelength matching the vibrational mode.
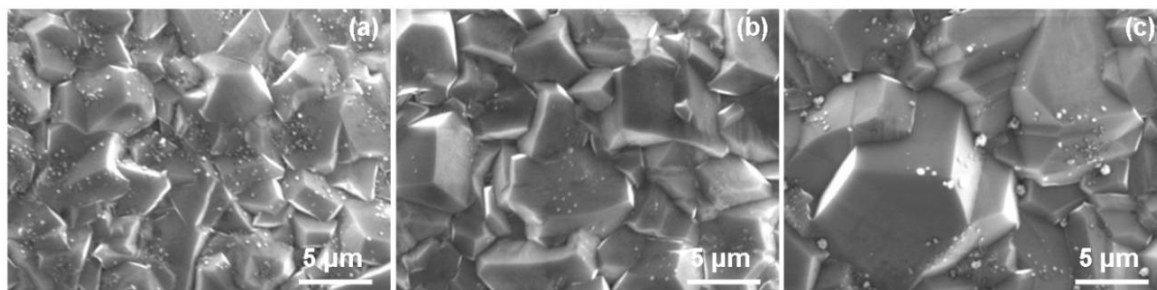
Figure 3.6 SEM images of diamond films deposited for 30 min (a) without laser, (b) with CO$_2$ laser irradiation at 10.591 μm, 800 W and (c) with CO$_2$ laser irradiation at 10.532 μm, 800 W.

Figure 3.7 shows the thickness profiles of the deposited films. Without laser excitation, the film thickness is about 8 μm. When the C$_2$H$_4$ molecules were excited at 10.591 μm, the film thicknesses increased to 12 μm with the irradiation powers of 800 W. Using the common CO$_2$ laser wavelength, the growth rate increased by 50% with 800-W excitation. In our previous study, the film thickness was also increased by 50% with a laser excitation of 600 W at this wavelength using different gas ratio [20]. The highest curve in Fig. 3.7 shows the profile of the film with perfect matching excitations at 10.532 μm. The film thickness is about 21 μm with 800-W excitation. Compared with the curve of the sample without laser irradiation, the growth rate was increased by 160% with 800-W laser irradiation at 10.532 μm.
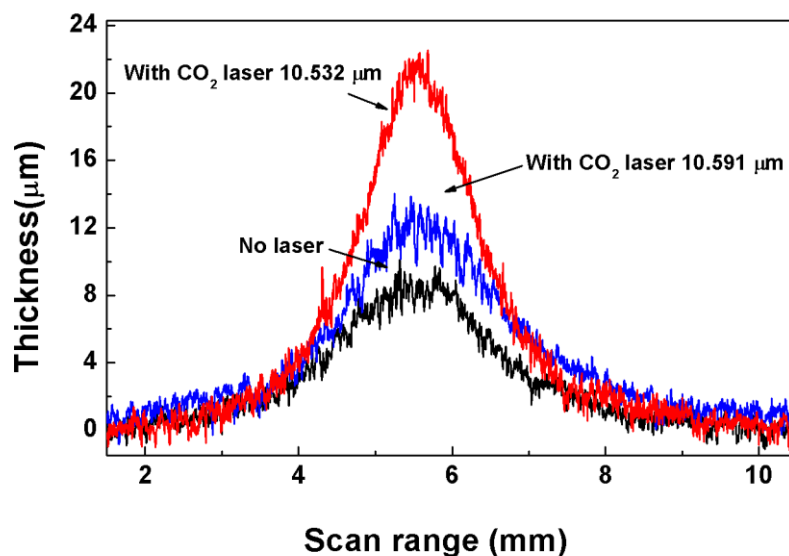
Figure 3.7 Thicknesses of diamond films deposited for 30 min without laser, with CO$_2$ laser irradiation at 10.591 μm, 800 W, and with CO$_2$ laser irradiation at 10.532 μm, 800 W.

To compare the quality of the diamond films deposited with different laser wavelengths and powers, the diamond films were characterized by Raman spectroscopy. The Raman spectra of the deposited diamond films in the wavenumber region from 1100 to 1700 cm^{-1} are shown in Fig. 3.8. The bottom curve in Fig. 3.8 corresponds to the diamond film deposited without laser excitation (black). A peak at 1334 cm^{-1} is the characteristic of diamond. The shift from the original diamond peak at 1332 cm^{-1} is related to stresses in the films [30]. A broad band centered at 1500 cm^{-1} (G band) in the bottom curve is due to graphite-like carbon mixed with amorphous carbon. There is a step from 1340 to 1400 cm^{-1} on the right side of the diamond peak, indicating that the diamond peak is overlapping with a weak D band reflecting disordered carbon in the films. Raman spectra of the diamond films deposited using the 10.591 μm excitation with

laser powers of 800 W is shown in the middle curve (blue). It is clear that the D band

decreased in the case of laser irradiation with 10.591. When the laser wavelength was

tuned to 10.532 μm for perfect wavelength matching with the C_2H_4 vibration mode, the

diamond peak in the top curve shows an obvious increase with 800-W laser excitation

(red). The diamond peak in the case of laser irradiation with 10.532 is sharper and

stronger than the others with weak G band. Therefore, vibrational excitation of C_2H_4

molecules using the CO_2 laser at 10.532 μm not only increased   diamond growth rate,

but also improved diamond crystallinity. These results indicate the high quality of the

diamond films and fast growth rate with 10.532 μm CO_2 laser excitation.
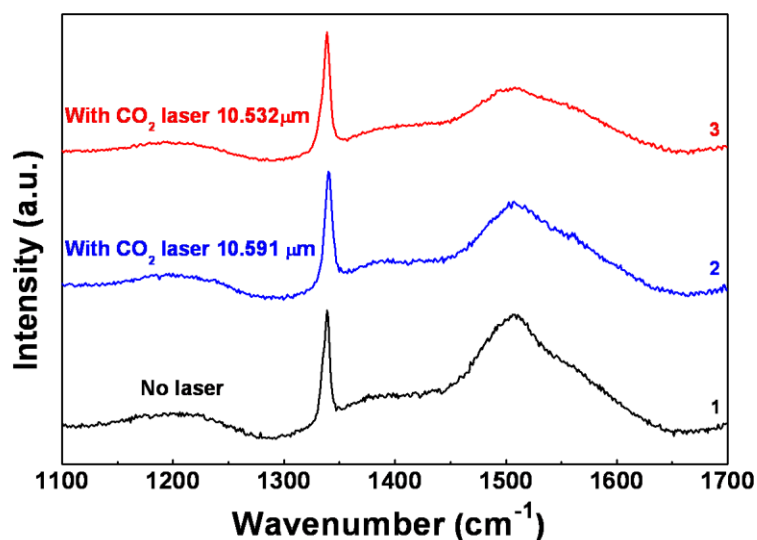
Figure 3.8 Raman spectra of diamond films deposited for 30 min without laser, with

CO_2 laser irradiation at 10.591 μm, 800 W, and with CO_2 laser irradiation at 10.532

μm, 800 W.

In this study, MEP was achieved in diamond CVD by introducing vibrational excitations into the thermal-driven CVD process. Vibrational resonant excitation of the C_2H_4 precursor molecules was studied using a wavelength-tunable CO_2 laser. The CVD processes were accelerated due to the stronger laser energy coupling with the C_2H_4 molecules. Compared with the common CO_2 laser at 10.591 μm, the laser wavelength of 10.532 μm is much more effective to excite the C_2H_4 molecules through the CH_2-wagging vibration mode. The diamond films deposited with the tunable laser excitation have larger grain size, better crystallinity, and faster growth rate than those without laser excitation. Under laser irradiation of at 10.532 μm, 800 W, the diamond grain size and film thickness increased by 200~300% and 160%, respectively. Besides the increases in grain size and film thickness, the crystallization of diamond structure was also enhanced in the films. This study suggests the possibility of laser-induced MEP through resonant vibrational excitations of precursor molecules in materials synthesis.

References

[1]   Haubner, R. and Lux, B., "Diamond growth by hot-filament CVD: State of the art", Diamond and Related Materials **2,** 1277 (1993).

[2]   McCauley, T. S. and Vohra, Y. K., "Homoepitaxial diamond film deposition on a brilliant cut diamond anvil", Applied Physics Letters **66,** 1486 (1995).

[3]   Mokuno, Y., Chayahara, A., Soda, Y., Horinoa, Y., and Fujimori, N., "Synthesizing single-crystal diamond by repetition of high rate homoepitaxial growth by microwave plasma CVD," Diamond and Related Materials **14,** 1743 (2005).

[4]   Asmussen, J., Grotjohn, T. A., Schuelke, T., Becker, M. F., Yaran, M. K., King, D. J., Wicklein, S., and Reinhard, D. K., "Multiple substrate microwave plasma-assisted chemical vapor deposition single crystal diamond synthesis", Applied Physics Letters **93,** 031502 (2008).

[5]   Zou, Y. S., Yang, Y., Chong, Y. M., Ye, Q., He, B., Yao, Z. Q., Zhang, W. J., Lee, S. T., Cai, Y., and Chu, H. S., "Chemical vapor deposition of diamond films on patterned GaN substrates via a thin silicon nitride protective layer", Crystal Growth & Design **8,** 1770 (2008).

[6]   Eguchi, K., Yata, S., and Yoshida, T., "Uniform and large-area deposition of diamond by cyclic thermal plasma chemical vapor deposition," Applied Physics Letters **64,** 58 (1994).

[7]   Grigoryev, E. V., Savenko, V. N., Sheglov, D. V., Matveev, A. V., Cherepanov, V. A., and Zolkin, A. S., "Synthesis of diamond crystals from oxygen-acetylene flames on

a metal substrate at low temperature", Carbon **36,** 581 (1998).

[8]   Donnet, J. B., Oulanti, H., Le Huu, T., and Schmitt, M., "Synthesis of large single crystal diamond using combustion-flame method", Carbon **44,** 374 (2006).

[9]   Shin, H. S. and Goodwin D. G., "Diamond growth in premixed propylene-oxygen flames", Applied Physics Letters **66,** 2909 (1995).

[10] Hirose, H. and Komaki, K., European Patent Application EP324538 (1988).

[11] Ravi, K. V., "Combustion synthesis: is it the most flexible of the diamond synthesis processes?", Diamond and Related Materials **4,** 243 (1995).

[12] Gaze, J., Obata, T., Oyanagi, N., Izawa, H., Ikuhara, Y., Kusunoki, M., and Zhou, W., "The synthesis of diamond particles by a filament assisted CO_2 laser induced CVD", Nuclear Instruments and Methods in Physics Research Section B: Beam Interactions with Materials and Atoms **121,** 427 (1997).

[13] Tóth, Z., Mechler, Á., and Heszler, P., "Local laser-assisted chemical vapor deposition of diamond", Applied Surface Science **168**, 5-8 (2000).

[14] Rich, J. W. and Bergman, R. C., "C_2 and CN formation by optical pumping of CO/Ar and Co/N_2/Ar mixtures at room temperature", Chemical Physics **44,** 53 (1979).

[15] Bergman, R. C., Homicz, G. F., Rich, J. W., and Wolk, G. L., "^{13}C and ^{18}O isotope enrichment by vibrational energy exchange pumping of CO", Journal of Chemical Physics **78,** 1281 (1983).

[16] Deleon, R. L. and Rich, J. W. "Vibrational energy exchange rates in carbon

monoxide", Chemical Physics **107,** 283 (1986).

[17] Snail, K. A., Vardiman, R. G., Estrera, J. P., Glesener, J. W., Merzbacher, C., Craigie, C. J., Marks, C. M., Glosser, R., and Freitas, J. A., "Diamond growth in turbulent oxygen-acetylene flames", Journal of Applied Physics **74,** 7561 (1993).

[18] Oakes, D. B., Butler, J. E., Snail, K. A., Carrington, W. A., and Hanssen, L. M., "Diamond synthesis in oxygen-acetylene flames: Inhomogeneities and the effects of hydrogen addition", Journal of Applied Physics **69,** 2602 (1991).

[19] Zare, R. N., "Laser Control of Chemical Reactions", Science **279,** 1875 (1998).

[20] Ling, H., Sun, J., Han, Y. X., Gebre, T., Xie, Z. Q., Zhao, M., and Lu, Y. F. "Laser-induced resonant excitation of ethylene molecules in $C_2H_4/C_2H_2/O_2$ reactions to enhance diamond deposition", Journal of Applied Physics **105,** 014901 (2009).

[21] Kim, J. S. and Cappelli, M. A., "Diamond film growth in low pressure premixed ethylene-oxygen flames", Applied Physics Letters **65,** 2786 (1994).

[22] Kim, J. S. and Cappelli, M. A., "Temperature measurements in low-pressure, diamond-forming, premixed flames", Journal of Applied Physics **84,** 4595 (1998).

[23] Buerki, P. R. and Leutwyler, S. "Homogeneous nucleation of diamond powder by CO_2-laser-driven gas-phase reactions", Journal of Applied Physics **69,** 3739 (1991).

[24] Myers, D. J., Shigeiwa, Motoyuki, Fayer, M. D., and Silbey, Robert. "Non-exponential relaxation of a single quantum vibrational excitation of a large molecule in collision free gas phase at elevated temperature", Chemical Physics

Letters **312,** 399 (1999).

[25] Komaki, K., Yanagisawa, M., Yamamoto, I. and Hirose, Y. "Synthesis of Diamond in Combustion Flame under Low Pressures", Japanese Journal of Applied Physics **32,** 1814 (1993).

[26] Miller, J. A. and Melius, C. F. "Kinetic and thermodynamic issues in the formation of aromatic compounds in flames of aliphatic fuels", Combustion Flame **91,** 21 (1992).

[27] Yalamanchi, R. S. and Harshavardhan, K. S. "Diamond growth in combustion flames", Journal of Applied Physics **68,** 5941 (1990).

[28] Gruen, D. M., Redfern, P. C., Horner, D. A., Zapol, P. and Curtiss. L. A. "Theoretical studies on nanocrystalline diamond: Nucleation by dicarbon and electronic structure of planar defects", Journal of Physical Chemistry B **103,** 5459 (1999).

[29] Redfern, P. C., Horner, D. A., Curtiss, L. A. and Gruen, D. M. "Theoretical studies of growth of diamond (110) from dicarbon", Journal of Physical Chemistry **100,** 11654 (1996).

[30] Asmussen, J. and Reinhard, D. K. Diamond Films Handbook, Marcel Dekker, Inc., New York, (2002).

CHAPTER 4

Fast Growth of Diamond Crystals in Open Air through Laser-induced MEP

4.1 Introduction

4.2 Growth of diamond crystals

4.3 Characterization of diamond crystals

4.3.1 Morphology study using SEM

4.3.2 Crystallinity study using Raman spectroscopy and X-ray diffraction

4.4 Conclusions

4.1 Introduction

Study on laser-induced MEP in diamond deposition through resonant vibrational excitation of precursor molecules (ethylene) was extended to synthesis of diamond crystals in this chapter. Since the first report of commercially successful synthetic diamond in 1955 using the high-pressure high-temperature technique [1], remarkable advancements have been made in the synthesis of diamond crystals. Currently, diamond synthesis at low pressure by chemical vapor deposition (CVD) including thermal-assisted (hot filament) CVD, microwave plasma-assisted CVD, plasma torch CVD, and combustion CVD has been widely investigated [2-10]. Combustion synthesis of diamond using an oxyacetylene combustion flame was firstly demonstrated by Hirose and Kondo in 1988 [11]. It has been argued that combustion synthesis of diamond is the most flexible of the CVD alternatives because of its scalable nature, minimum utility requirement, and significantly reduced capital costs relative to plasma-aided process [12].

Another important advantage of this method is the high growth rate of diamond films up to about 60 μm/hr [13], which is surpassed only by the plasma torch CVD [14]. Large individual crystals that approach 1 mm in diameter have been obtained using the combustion CVD method [15, 16]. The drawback of this method is that the deposited material often contains significant amount of nondiamond carbons [17]. Quality of large diamond crystals prepared using this technique was degraded by the growth of spherillites consisting of poorly faceted polycrystalline aggregates and even graphite [18],

which hinders the further increase of the size of diamond crystals prepared using the combustion CVD method.

In this study, combustion synthesis was assisted with bond-selective resonant laser energy coupling. A laser-assisted combustion synthesis process was developed for growing high-quality diamond crystals with high growth rates in open air. Same with the previous chapter, C_2H_4 was introduced into the oxyacetylene combustion flame in order to couple the laser energy into the combustion reaction through the resonant excitation of the ethylene molecules. Diamond crystals with an average length of 5 mm and a diameter of 1 mm were obtained on silicon substrates. The effects of the vibrational energy-coupling approach through laser-induced resonant excitation of precursor molecules are investigated.

4.2 Growth of diamond crystals

The experimental setup is similar to Fig. 3.1 for the CO_2 laser-assisted fast growth of diamond crystals in open air. A commercial oxygen–acetylene torch with a 1.5 mm orifice tip was used to generate the flame. The fuel was a mixture of C_2H_4 and C_2H_2 with a gas flow ratio of 1:1, which was then mixed with O_2 with a volume ratio of 1.03 $[(C_2H_4+C_2H_2)/O_2]$. A wavelength-tunable CO_2 laser (PRC, spectrum range from 9.2 to 10.9 μm) was used in the synthesis process to achieve resonant excitation of the C_2H_4 precursor molecules. Since there is no obvious vibrational mode within the laser spectrum range for the acetylene molecules, C_2H_4 was added into the precursor mixture to couple the laser energy into the diamond growth process [19]. The CH_2 wagging mode (v_7, 949.3 cm^{-1}) of the C_2H_4 molecules corresponds to a wavelength of 10.534 μm, which has a close match with the CO_2 laser line at 10.532 μm. Laser energy was then coupled into the reactions through resonant excitation of the C_2H_4 molecules. Silicon (100) wafers with a dimension of $10\times10\times0.6$ mm^3 were used as substrates. The silicon substrates were pre-seeded with 100,000-grit diamond powders (Ebersole Lapidary) with an average size of 0.25 μm. The substrate was placed on a water cooling box mounted on a motorized X-Y-Z stage. The CO_2 laser, tuned to 10.532 μm with a power of 800 W, was directed in parallel with the substrate surface but perpendicularly to the flame axis. The laser beam was focused using a ZnSe convex lens (focal length = 254 mm) to 2 mm in diameter, which was around the same as the average diameter of the inner flame. The original

length of the flame was around 6 mm, which shrunk to about 3.6 mm when the laser beam was introduced into the flame right underneath the nozzle. The distance between the inner flame tip and the diamond growth site was maintained at about 0.5 mm, by the program-controlled X-Y-Z stage. The temperature of the growth site was monitored by a pyrometer (Omega Engineering, Inc., OS3752). The temperature was maintained at 760 - 780 ℃ by adjusting the flow rate of the water-cooling box. To understand the effects of laser-induced energy coupling, diamond samples were also prepared without laser irradiation, but under the same deposition condition including the same gas flow ratio and deposition temperature.

In chapter 3, tungsten carbide plates were used as substrates for deposition of diamond films. Here we used silicon as substrates for diamond large/thick films and crystals. Silicon substrates were used because the tungsten carbide substrates contain cobalt, which decreases adhesion of the deposited films to the substrate and causes a transformation of sp^3-bonded diamond to sp^2-bonded graphite [21, 22].

4.3 Characterization of the diamond crystals

Surface morphologies and dimensions of the grown diamond crystals were characterized by a scanning electron microscope (SEM; XL-30, Philips Electronics). Diamond qualities were evaluated both by Raman spectroscopy (inVia H 18415, Renishaw) and X-ray diffraction (XRD; AXS D8, Bruker). The exciting source of the Raman system is an argon-ion laser with a wavelength of 488 nm and a power of 100 mW, which was operated in the multichannel mode with the beam focused to a spot diameter of approximately 5 μm. Prior to and after the Raman characterization of the diamond samples, the Raman system was calibrated using a single crystal silicon (100) wafer.

4.3.1 Morphology study using SEM

Diamond crystals were grown using a continuous one-step approach. In the initial 1 hour of the diamond deposition, a diamond film was deposited on the silicon substrate with a preferential growth within the central area of the film. This was similar to the previous work of diamond film deposition on tungsten carbide. As the film thickness increased, diamond grains under the inner flame tip exhibited a much higher growth rate and yielded diamond crystals. The diamond crystal shown grown for 5 hours in Fig. 4.1(a) (side view) and Fig. 4.1(e) (top view) illustrates how the crystal started to grow on the diamond film. The diamond crystal reached 0.6 mm long and 0.6 mm in diameter. When

the growth time increased to 15 hour, the diamond crystal grew to a length of around 2 mm and a diameter of 0.8 mm, as shown in Fig. 4.1(b) (side view) and Fig. 4.1(f) (top view). Since the primary growth area was always maintained at the top of the diamond crystal, it is easy to understand that the vertical growth rate was much higher than the horizontal growth rate, leading to the formation of a pillar-like shape. A diamond pillar of 5 mm long and 1 mm in diameter grown for 36 hours is shown in Fig. 2(c) (side view) and Fig. 4.1(g) (top view). The average growth rate for the 36-hour grown crystal was 5 mm / 36 hr which equals to 139 μm/hr. This is more than twice that of the conventional combustion CVD mentioned in the above paragraphs.

It has been reported that for the longer-time deposition, the crystal surface temperature plays a critical role in the uniform growth of diamond [16]. Such a phenomenon was also observed in this work. In the growth longer than 36 hours, the temperature of the diamond surface became higher than 850 ℃ when the diamond grew higher than 5 mm. The higher temperature led to the increase of secondary crystallization, which degraded the uniformity of the diamond crystals. It is believed that the surface temperature could be maintained constant by decreasing the total gas flow and introducing the multi-step deposition method [16].
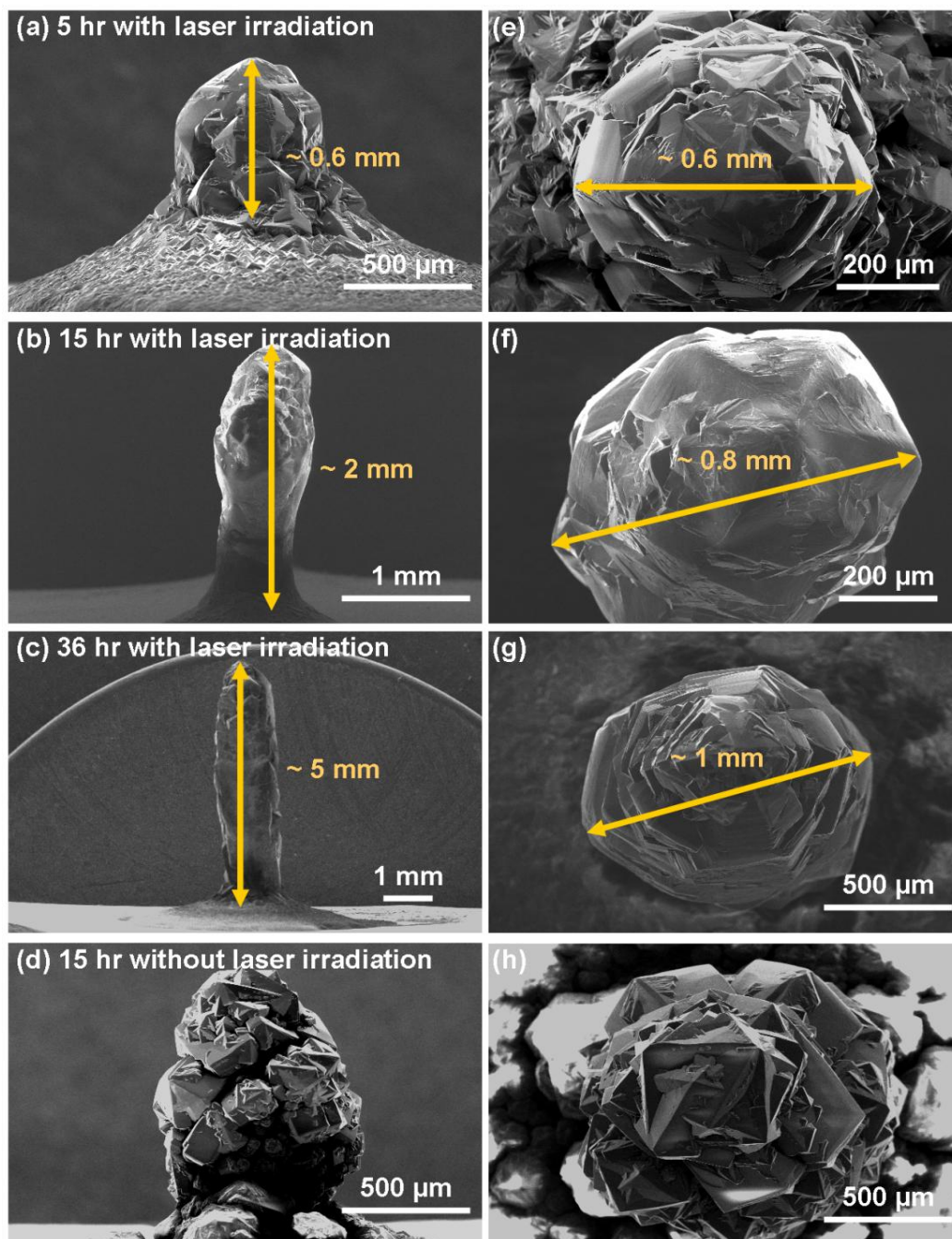
Figure 4.1 SEM images of diamond crystals grown with CO_2 laser excitation at 10.532 μm for (a) 5, (b) 15, and (c) 36 hours, respectively; and (d) diamond grown without laser irradiation for 15 hours. Figures (e), (f), (g), and (h) are the top-views of the samples in (a), (b), (c), and (d), respectively.

Compared with diamond particles obtained in the 15-hour growth without laser irradiation as shown in Fig. 4.1(d) (side view) and Fig. 4.1 (h) (top view), laser-assisted combustion synthesis yielded diamond crystals with better uniformity and larger size. The diamond particles grown without laser irradiation were more like a pile up of polycrystalline diamond grains and graphitized carbons. This observation coincides with the results reported by Snail *et al* [23].

4.3.2 Crystallinity study using Raman spectroscopy and X-ray diffraction

Figure 4.2 shows the Raman spectra of the four diamond samples shown in Fig. 4.1. Intense and sharp Raman peaks at 1332 cm^{-1} were observed in all of the four samples. Diamond crystals obtained from the laser-assisted combustion synthesis only show the 1332 cm^{-1} Raman peak (Figs. 4.2(a)-(c)) with narrow FWHM values of 4.5 - 4.7 cm^{-1}. No other signals were observed in the Raman spectra of these three samples. Both strong Raman peak and narrow FWHM value indicate the high quality of the diamond crystals grown with resonant laser energy coupling. The diamond sample obtained without laser energy coupling shows a Raman peak at 1332 cm^{-1} (Fig. 4.2(d)) but with a much wider FWHM of 9.2 cm^{-1}. A broad band from 1100 to 1600 cm^{-1} was observed in Fig. 4.2(d), indicating the existence of nondiamond carbon species, such as sp^2 hybridized carbon.
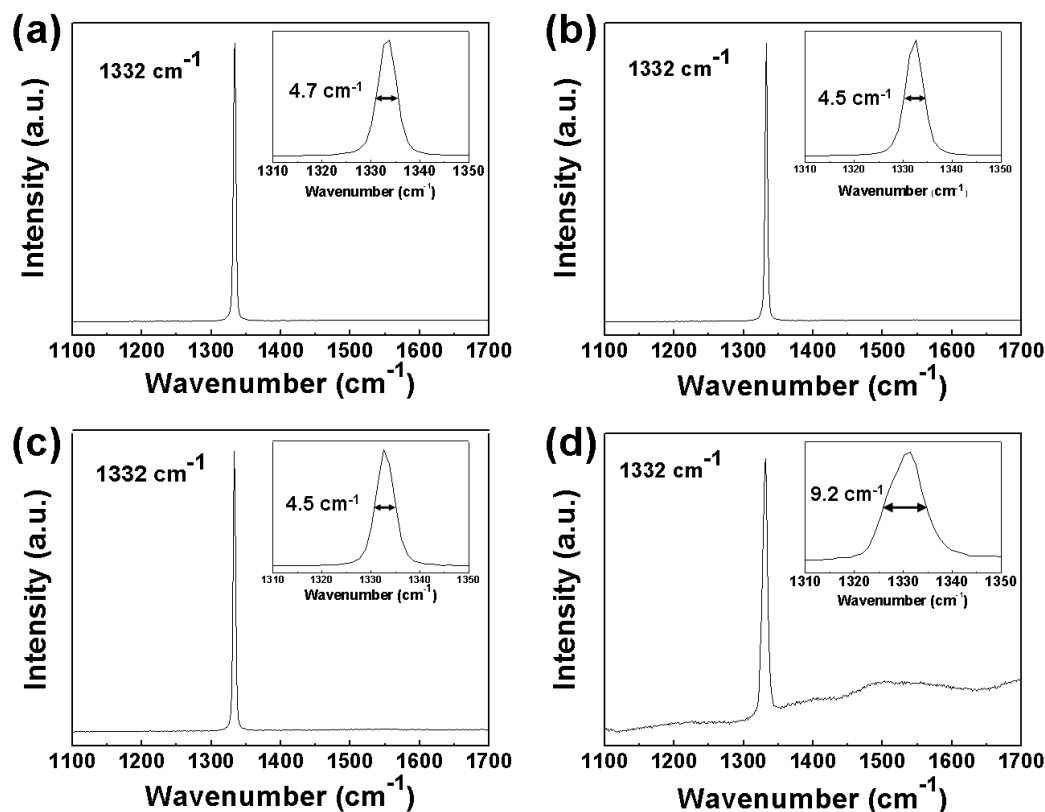
Figure 4.2 Raman spectra of the diamond crystals grown with CO$_2$ laser excitation at 10.532 μm for (a) 5, (b) 15, and (c) 36 hours, respectively; and (d) diamond grown without laser for 15 hours. Insets are the expanded Raman peaks of each spectrum, showing the full width at half maximum.

Figure 4.3 shows the XRD spectra of the four samples. Discrete peaks from the (111), (022), and (311) diamond facets were observed from all of the four samples. The signals are in good agreement with the data from the ASTW 6-675 table for natural diamond, indicating the formation of diamonds. However, a 2θ signal at 26° is observed from sample (d), as shown in Fig. 4.3(d). This signal is ascribed to the (002) plane of graphite, clearly indicating the existence of the graphite phase.
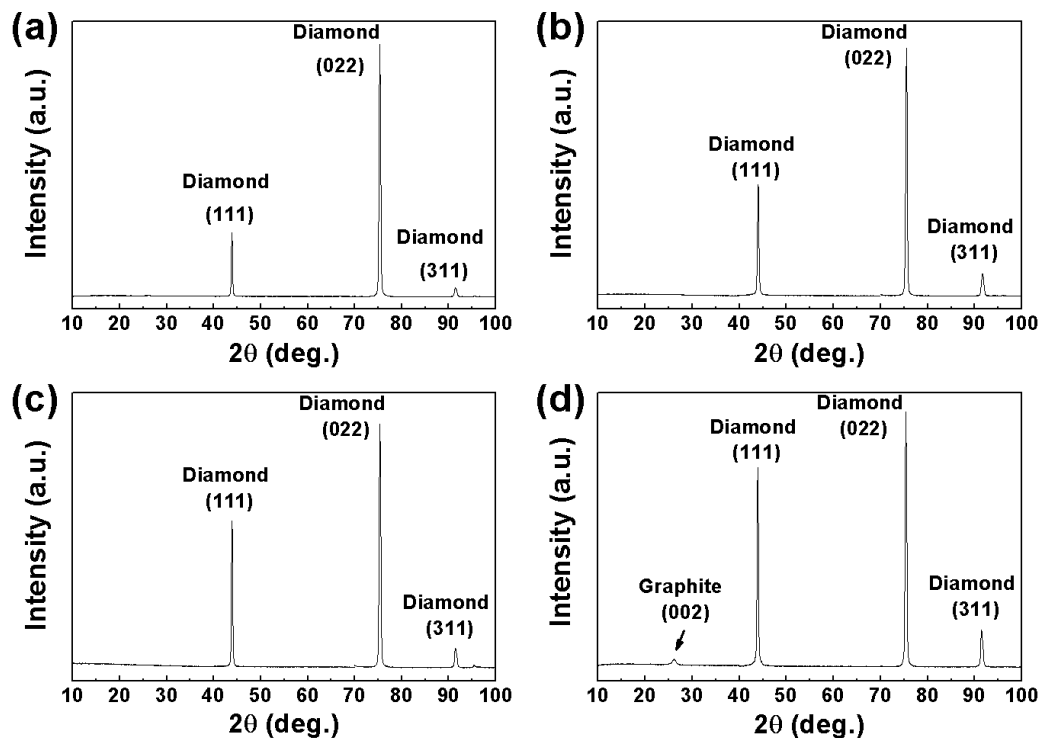
Figure 4.3 X-ray diffraction spectra of the diamond crystals grown with laser excitation at 10.532 μm for (a) 5, (b) 15, and (c) 36 hours, respectively; and (d) diamond grown without laser irradiation for 15 hours.

Both Raman spectroscopy and XRD demonstrate the high quality of the diamond crystals grown with the 10.532 μm CO_2 laser excitation. In the meanwhile, the 15-hr grown sample without laser irradiation exhibits poor diamond crystallization with the extensive existence of non-diamond carbon structures. Both of them indicate the advantage of the laser-induced resonant excitation.

4.4 Conclusions

A laser-assisted MEP process was developed for fast growth of diamond crystals in open air through resonant vibrational excitation of C_2H_4 molecules. High-quality diamond crystals up to 5 mm in length and 1 mm in diameter were obtained. A high diamond growth rate up to 139 μm/hr was achieved on a silicon substrate. The laser-induced vibrational excitation enhances the chemical reactions and increases the active radicals in the flame, which result in fast growth of high-quality diamond crystals. Crystallinity of the diamond crystals were studied using Raman spectroscopy and XRD, both of which indicate high quality of the diamond crystals.

References

[1]. Bundy, F. P., Hall, H. T., Strong, H. M., and Wentorf Jr, R. H., "Manmade diamond", Nature **176,** 51 (1955).

[2]. Haubner, R. and Lux, B. "Diamond growth by hot-filament CVD: State of the art", Diamond and Related Materials **2,** 1277 (1993).

[3]. McCauley, T. S., and Vohra, Y. K., "Homoepitaxial diamond film deposition on a brilliant cut diamond anvil", Applied Physics Letters 66, 1486 (1995).

[4]. Mokuno, Y., Chayahara, A., Soda, Y., HorinoHaH, Y., and Fujimori, N. H. "Synthesizing single-crystal diamond by repetition of high rate homoepitaxial growth by microwave plasma CVD", Diamond and Related Materials 14, 1743 (2005).

[5]. Asmussen, J., Grotjohn, T. A., Schuelke, T., Becker, M. F., Yaran, M. K., King, D. J., Wicklein, S., and Reinhard, D. K., "Multiple substrate microwave plasma-assisted chemical vapor deposition single crystal diamond synthesis", Applied Physics Letters **93,** 031502 (2008).

[6]. Zou Y. S., Yang Y., Chong Y. M., Ye Q., He B., Yao Z. Q., Zhang W. J., Lee S. T., Cai Y., and Chu H. S. "Chemical Vapor Deposition of Diamond Films on Patterned GaN Substrates via a Thin Silicon Nitride Protective Layer", Crystal Growth & Design **8,** 1770 (2008).

[7]. Terranova M. L., Manno D., Rossi M., Serra A., Filippo E., Orlanducci S., and Tamburri E., "Self-Assembly of n-Diamond Nanocrystals Into Supercrystals",

Crystal Growth & Design 9, 1245 (2009).

[8]. Eguchi, K., Yata, S., and Yoshida, T., "Uniform and large‑area deposition of diamond by cyclic thermal plasma chemical vapor deposition", Applied Physics Letters 64, 58 (1994).

[9]. Donnet, J. B., Oulanti, H., Le Huu T., and Schmitt, M., "Synthesis of large single crystal diamond using combustion-flame method", Carbon 44, 374 (2006).

[10]. Grigoryev, E. V., Savenko, V. N., Sheglov, D. V., Matveev, A. V., Cherepanov, V. A., and Zolkin, A. S., "Synthesis of diamond crystals from oxygen-acetylene flames on a metal substrate at low temperature", Carbon 36, 581 (1998).

[11]. Hirose, H. and Komaki, K. Eur. Pat. Appl. EP324538 (1988).

[12]. Ravi, K. V., "Combustion synthesis: is it the most flexible of the diamond synthesis processes?", Diamond and Related Materials **4,** 243 (1995).

[13]. Alers, P., Hanni, W., and Hintermann, H. E., "A comparative study of laminar and turbulent oxygen-acetylene flames for diamond deposition", Diamond and Related Materials **2,** 393 (1992).

[14]. Ohtake, N. and Yoshikawa, M., "Diamond Film Preparation by Arc Discharge Plasma Jet Chemical Vapor Deposition in the Methane Atmosphere", Journal of the Electrochemical Society **137,** 717 (1990).

[15]. Abe, T., Suemitsu, M., Miyamoto, N., and Sato, N., "Formation of 250-μm-diameter diamond crystals by combustion flame method: Effects of preformation of molybdenum oxide on the substrate", Journal of Applied Physics **73,** 971 (1993).

[16]. Wang, X. H., Zhu, W., Vonwindheim, J., and Glass, J. T., "Combustion growth of large diamond crystals", Journal of Crystal Growth **129,** 45 (1993).

[17]. Hanssen, L. M., Snail, K. A., Carrington, W. A., Butler, J. E., Kellogg, S., and Oakes, D. B., "A model of diamond growth in low pressure premixed flames", Thin Solid Films **196,** 271 (1991).

[18]. Cappelli, M. A. and Paul, P. H., "Characterization of the diamond growth process using optical emission spectroscopy", Journal of Applied Physics **67,** 2596 (1990).

[19]. Ling, H., Xie, Z. Q., Gao, Y., Gebre, T., Shen, X. K., and Lu, Y. F., "Enhanced chemical vapor deposition of diamond by wavelength-matched vibrational excitations of ethylene molecules using tunable CO_2 laser irradiation", Journal of Applied Physics **105,** 064901 (2009).

[20]. Ling, H., Sun, J., Han, Y. X., Gebre, T., Xie, Z. Q., and Zhao, M., "Laser-induced resonant excitation of ethylene molecules in $C_2H_4/C_2H_2/O_2$ reactions to enhance diamond deposition", Journal of Applied Physics**105,** 014901 (2009).

[21]. Han, Y. X., Ling, H., and Lu, Y. F., "KrF excimer laser-assisted combustion-flame deposition of diamond films", Journal of Applied Physics **100,** 124911 (2006).

[22]. Donnet, J. B., Paulmier, D., Oulanti, H., and Le Huu, T., "Diffusion of cobalt in diamond films synthesized by combustion flame method", Carbon **42,** 2215 (2004).

[23]. Snail, K. A. and Hanssen, L. M., "High temperature, high rate homoepitaxial growth of diamond in an atmospheric pressure flame", Journal of Crystal Growth **112,** 651-659 (1991).

[24]. Komaki, K., Yanagisawa, M., Yamamoto, I., and Hirose, Y., "Synthesis of Diamond in Combustion Flame under Low Pressures", Japanese Journal of Applied Physics **32,** 1814 (1993).

[25]. Miller, J. A. and Melius, C. F., "Kinetic and thermodynamic issues in the formation of aromatic compounds in flames of aliphatic fuels", Combustion and Flame 91, 21 (1992).

[26]. Yalamanchi, R. S. and Harshavardhan, K. S., "Diamond growth in combustion flames", Journal of Applied Physics **68,** 5941 (1990).

[27]. Gruen, D. M., Redfern, P. C., Horner, D. A., Zapol, P., and Curtiss. L. A., "Theoretical Studies on Nanocrystalline Diamond: Nucleation by Dicarbon and Electronic Structure of Planar Defects", Journal of Physical Chemistry B **103,** 5459 (1999).

[28]. Redfern, P. C., Horner, D. A., Curtiss, L. A., and Gruen, D. M., "Theoretical Studies of Growth of Diamond (110) from Dicarbon", Journal of Physical Chemistry **100,** 11654 (1996).

CHAPTER 5

Excitation of Ethylene Molecules at Different Laser Power Densities

5.1 Introduction

5.2 Experiments, results, and discussion

5.2.1 Absorption of laser power by the flame

5.2.2 Promotion of chemical reactions at different laser power densities

5.2.3 Deposition and characterization of diamond films

5.3 Conclusions

5.1 Introduction

Laser-induced MEP has been achieved in diamond deposition by introducing resonant vibrational excitations of precursor molecules (ethylene) using a wavelength-tunable CO_2 laser. By coupling laser energy into the chemical reactions for diamond growth through vibrational excitation of ethylene molecules, diamond growth rate as well as diamond crystal quality were promoted. High-quality diamond crystals as large as 5 mm in length were grown in open air with a high growth rate. More detailed studies on laser resonant excitations in diamond synthesis are required to obtain a better understanding of the effect of vibrational excitations on chemical reaction and on diamond deposition. Excitation of ethylene molecules at different laser power densities is described in this chapter.

The wavelength of the CO_2 laser was tuned to 10.532 μm in order to match the CH_2 wagging vibrational mode of ethylene. By adjusting the incident laser power density from 0 to 2.7×10^4 W/cm^2, the effect of laser energy coupling on diamond surface morphology, diamond quality, as well as energy coupling efficiency, were studied. At certain incident laser power densities, uniform {100}-textured diamond particles were obtained in the deposited diamond films.

5.2 Experiments, results, and discussion

5.2.1 Absorption of laser energy by the flame.

The experimental setup is similar to that shown in Fig. 3.1. The combustion flame was produced by a gas mixture of C_2H_4, C_2H_2, and O_2 with flow rates of 0.62, 0.62, and 1.20 standard liters per minute (SLPM), respectively. A wavelength-tunable CO_2 laser was tuned to 10.532 μm to match the CH_2 wagging mode of the C_2H_4 molecules. The laser power was tuned from 0 to 800 W to study the effect of different laser power densities in diamond growth. A power meter was placed in the laser path next to the combustion flame. The absorbed laser power was obtained by subtracting the transmitted laser power from the incident laser power. The absorbed laser power was divided by the original output to calculate the laser energy absorption rate.

Optical images of the $C_2H_4/C_2H_2/O_2$ flames without and with laser irradiations at different laser powers shown in Fig. 5.1 indicate that the inner flame is shortened by laser irradiation and the length keeps decreasing as the laser power density increases. The flame shrank from 6 to 3.5 mm in length and was broadened by 70% in width when laser power density was increased to 2.7×10^4 W/cm^2. The shortened inner cone is the result of the accelerated reactions in the flame induced by the laser resonant excitation. Variation of flame brightness also indicates the promotion of chemical reactions in the flames. With an increased laser power, the brightness of the flame was also increased, indicating

promoted chemical reactions and higher concentrations of reacting species.
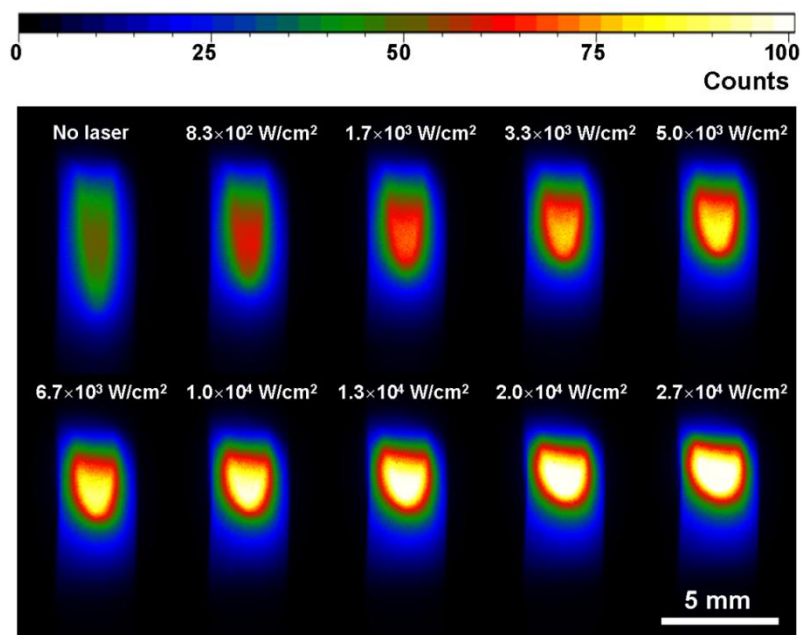
Figure 5.1 Optical images of flames without laser excitation and with laser excitations at different laser power densities.

Figure 5.2 shows the absorbed laser powers (left, solid squares) and the absorption coefficients (right, solid triangles) with respect to the incident laser powers. It is observed that the absorbed laser power increased from ~4.5 to ~72.0 W when the incident laser power density increased from 8.3×10^2 to 2.7×10^4 W/cm^2. On the contrary, the absorption coefficient decreased with the increase in the incident laser power density. It is suggested that with the increase of incident laser power density, absorption of laser power approached its saturation limit due to anharmonic shift between higher-lying vibrational states and therewith decrease in absorption cross-section with increasing laser energy power density [1, 2]. In this study, however, the saturation was not observed due to the limited maximum laser power density.
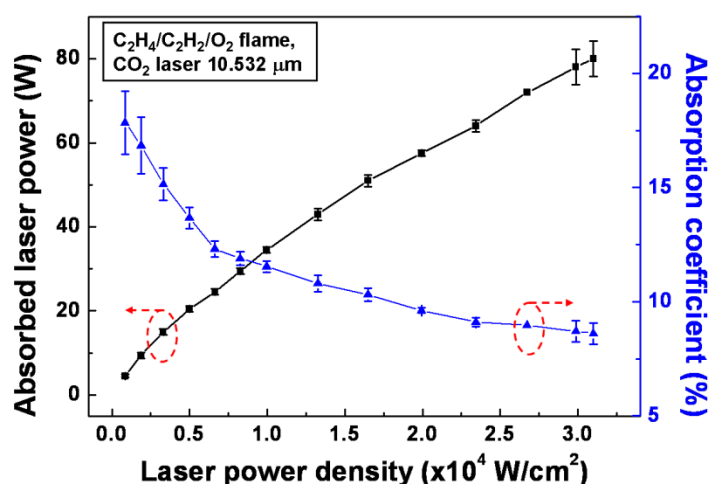
Figure 5.2 Absorbed laser powers (left, solid squares) and absorption coefficient (right, solid triangles) with respect to incident laser power densities.

5.2.2 Promotion of chemical reactions at different laser power densities

Optical emission spectroscopy (OES) was used to study the effects of the resonant laser excitations on diamond growth. OES spectra of the flames during diamond film deposition were collected in a direction perpendicular to the flame axis. The setup for the OES study was similar to that described in previous chapters. The optical emission of a flame was introduced into a spectrometer (Shamrock SR-303i-A, Andor Technology) coupled with an ICCD camera (iStar DH-712, Andor Technology) through a plano-convex lens made of UV-grade quartz. All the spectra were taken with a vertical collecting length of 0.5 mm along the inner flame centered at the tip of the inner flame, and with a horizontal slit width of 30 μm centered at the tip apex of the inner flame. The flame images taken were proportional to the real flames in size. A background spectrum

captured before collecting the emission spectra was subtracted in all the spectra.

It was demonstrated that by accelerating the reactions in the flame, laser resonant excitation of the C-H bond vibration in C_2H_4 molecules results in the increased concentrations of several relevant intermediate species. According to the OES spectra obtained from the flames without and with laser irradiations at different laser powers shown in Fig. 5.3, obvious increases in emission intensities hence concentrations of OH, CH and C_2 species were observed in the laser-irradiated flames. The emission intensities of these species kept increasing as laser power increased. It is suggested that OH radicals play a critical role in combustion synthesis of diamond by etching the surface-bond hydrogen and stabilizing the sp^3 hybridized surface carbon bonds [3, 4]. The CH radicals are also believed to be helpful in diamond growth [5]. Both increments of OH and CH radicals explain the increases in growth rate and crystal quality in the laser-assisted combustion synthesis of diamond. The C_2 radical has a more important effect on the diamond growth [6, 7]. On an unhydrided surface, the insertion of C_2 into a C=C dimer bond produces a carbene, leading to secondary nucleation and fast diamond growth. On the monohydride surface, the addition of a C_2 into C-H bonds of a hydrogen-terminated diamond {100} and especially {110} surface is energetically favorable, making the growth directly proceed from the existing crystal surface at a slow rate [6, 7]. Under our experimental condition where hydrogen is relatively abundant, at medium laser power densities smaller than 1.0×10^4 W/cm^2, the surfaces of diamond crystallites should be almost completely covered by hydrogen atoms and the surfaces are monohydrided, thus

the growth can readily proceed from the parent crystallites and the {100} orientation will dominate, considering the fact that those with higher Miller indices essentially resemble {100} surface [6]. However, when the laser power density increases to above 1.0×10^4 W/cm^2, the C_2 concentration increases to a critically high value, and the small portion of unhydrided surfaces could also increase to a critical value. Under such conditions, diamond growth through secondary nucleation becomes dominant, thus jeopardizing the crystal orientations [6, 7]. At the same time, the crystal grain boundaries (consisting of π-bonded carbon atoms) also increase in proportion and contribute to the slight broadening of the Raman peak at 1332 cm^{-1} for laser power above this point. More detailed studies are required to understand whether the increase in the C_2 concentration induced by laser excitation has a decisive impact, as well as its roles playing in the determination of preferred crystal orientation.
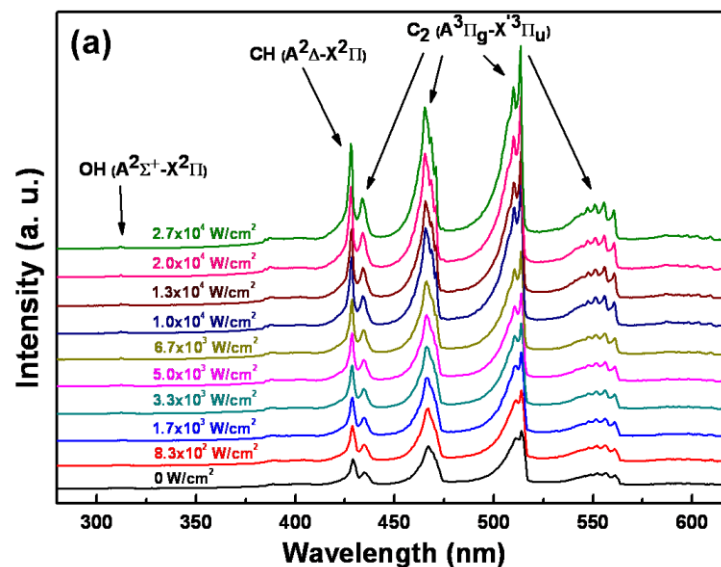
Figure 5.3 Optical emission spectra of flames without laser excitation and with laser excitations at different laser power densities.

5.2.3 Deposition and characterization of diamond films

Tungsten carbide (WC) plates (BS-6S, 6 wt. % Co, Basic Carbide Corp.) with a dimension of 12.7×12.7×1.6 mm^3 were used as substrates. The surface roughness of the WC substrates was 400 nm. The experimental parameters are similar to those described in Chapter 3. Laser power densities were calculated by dividing the incident laser powers with the area of the beam cross-section at the flame (~3×10^{-2} cm^2). The original length of the flame was ~6 mm, which shrank obviously when the 10.532-μm laser beam irradiated the flame. The distance between the tip of the inner flame and the diamond growth site was maintained at about 0.5 mm by the programmable motorized XYZ stage. The local temperature of the growth site was monitored by a pyrometer (OS3752, Omega Engineering, Inc.), and maintained at ~770 ℃ by adjusting the flow rate of the cooling water. The growth time was 1 hour for all the samples.

Morphologies and grain sizes of the deposited diamond films are shown in Fig. 5.4. Diamond films deposited without laser excitations and with low power densities less than 1.7×10^3 W/cm^2 have randomly-oriented grains with small sizes. However, {100}-oriented facets began to dominate in the center areas of the deposited diamond films when the laser power density increased to 3.3×10^3 W/cm^2. The preferential growth of {100} facets became more dominant when the laser power increased. The size and uniformity of the {100} facets reached its maximum at an incident power density of

1.0×10^4 W/cm^2. The orientations of the diamond facets became more randomly distributed with further increased laser power density, as indicated in Figs. 5.4i and 5.4j. The SEM images indicate that the laser resonant excitation of C_2H_4 molecules plays an important role in modifying the morphology of diamond films. Within a certain range of incident laser power densities, uniformly distributed diamond {100} facets can be obtained. The SEM images also show that the grain sizes of the diamond crystals increased with increasing laser power. This trend was further supported by measuring diamond film thicknesses, as shown in Fig. 5.5 (left, solid squares).
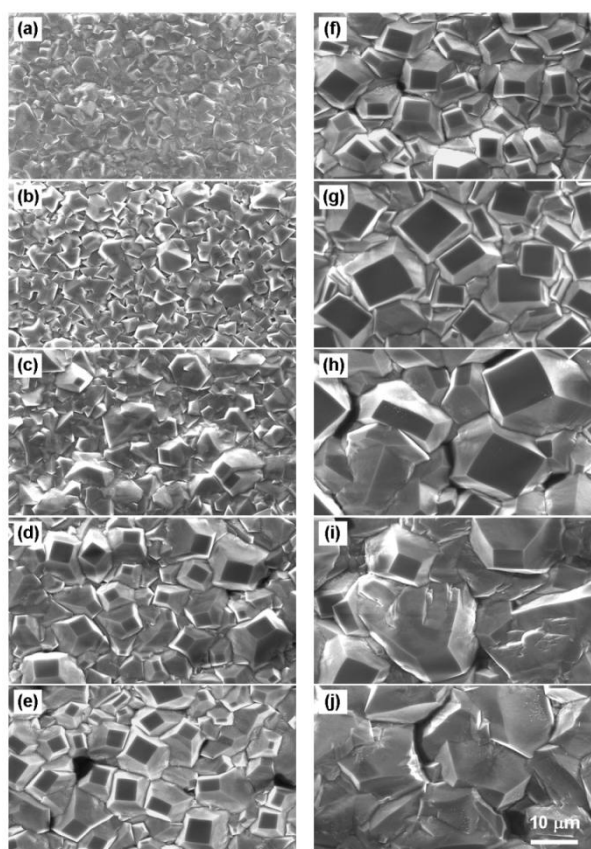
Figure 5.4 SEM images of diamond films deposited (a) without laser excitation and with CO$_2$ laser excitations at power density of (b) 8.3×10^2, (c) 1.7×10^3, (d) 3.3×10^3, (e) 5.0×10^3, (f) 6.7×10^3, (g) 1.0×10^4, (h) 1.3×10^4, (i) 2.0×10^4, and (j) 2.7×10^4 W/cm^2.
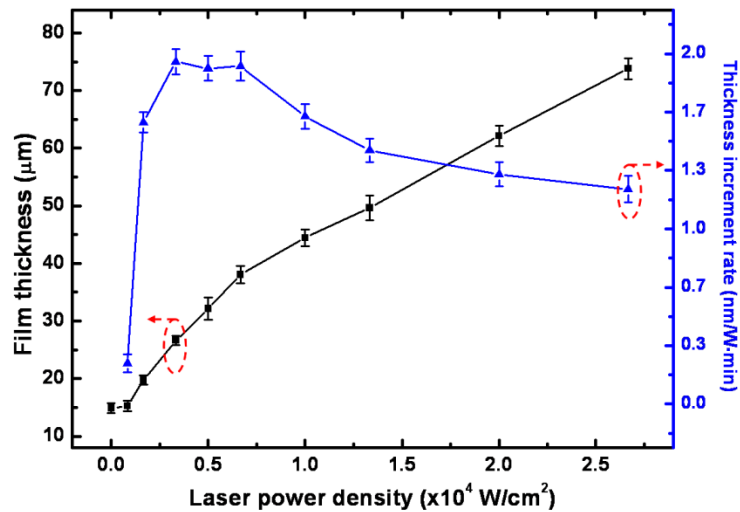
Figure 5.5 Thickness of diamond films (left, solid squares) and thickness increment rate (right, solid triangles) with respect to different laser power densities.

The film thickness was ~14.9 μm without laser excitation, which increased to ~73.8 μm when the laser power density was increased to 2.7×10^4 W/cm^2. Table 5.1 shows the relationship between the film thickness and the incident laser power, where the thickness increment was calculated by subtracting the thickness of the diamond film deposited without laser from those deposited with laser excitations at different laser powers. By dividing these increments with the deposition time and then with the incident laser powers respectively, the thickness increment rate was obtained, as shown in Fig. 5.5 (right, solid triangles). It is observed that the increment rate increased in the beginning, reached its maximum at $3.3 \times 10^3 \sim 6.7 \times 10^3$ W/cm^2, and then slightly decreased, which suggests the strongest laser energy coupling in a power density range of $3.3 \times 10^3 \sim 6.7 \times 10^3$ W/cm^2. In our previous work, the increment rate for the 15-min deposited diamond films were 1.80, 1.50, and 1.10×10^{-3} μm/W min for incident laser powers of

100, 400, and 800 W, respectively. These results are very close to those of the 60-min deposited diamond films (1.95, 1.45, and 1.23×10^{-3} μm/W min for 100, 400, and 800 W, respectively). Therefore, it is believed that the increment is uniform throughout the deposition lasting one full hour.

Table 5.1 Relationship between increment of film thickness and the incident laser power.

Incident power (W)	25	50	100	150	200	300	400	600	800
Thickness increment (μm)	0.35	4.83	11.73	16.25	24.15	29.55	34.75	47.25	58.90
Thickness increment rate (X10^{-3} μm/W·min)	0.23	1.62	1.95	1.80	2.02	1.65	1.45	1.32	1.23

Figure 5.6 shows the Raman spectra for the diamond films deposited without laser excitation and with laser excitations at different incident laser power densities. Sharp diamond peaks around 1332 cm^{-1} and broad amorphous carbon bands around 1500 cm^{-1} were observed in all samples. The sample deposited without laser excitation exhibits a strong band of amorphous carbon and a relatively weak diamond peak. When the laser excitation was used, the band of amorphous carbon was suppressed and the diamond peak became stronger. This trend continued until the laser power density was increased to 5.0×10^{3} W/cm^{2}. As shown in Figs. 5a and 5b, Raman spectra of the diamond samples deposited under laser excitations with laser power densities higher than 5.0×10^{3} W/cm^{2} showed similar relative height of diamond peaks and amorphous carbon bands.
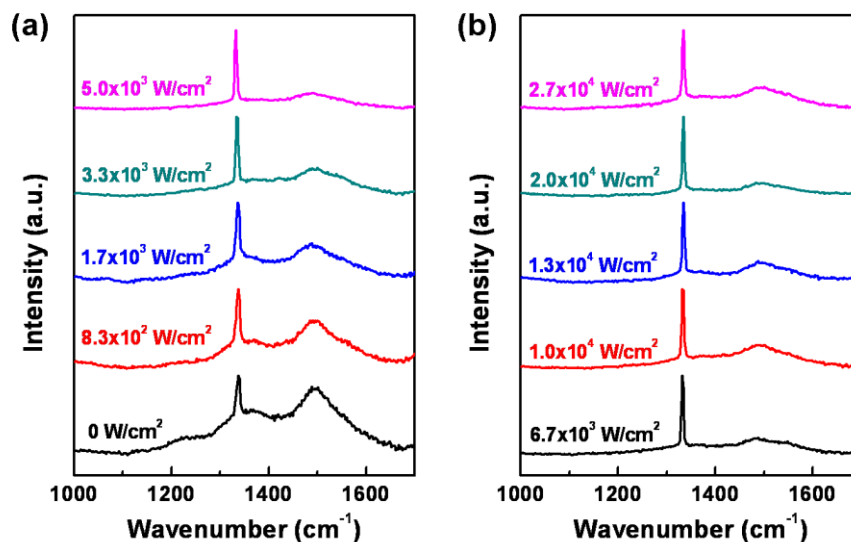
Figure 5.6 Raman spectra of diamond films deposited without laser excitation and with laser excitations at different laser power densities.

Figure 5.7 shows the corresponding Raman shifts (left, solid squares) and full width at half maximum (FWHM; right, solid triangles) values of the diamond peaks shown in Fig. 5.6. Diamond peak shifts are correlated to residual stresses in the diamond films, whereas FWHM values of the peaks represent diamond qualities. It is observed that the diamond peak shifted from ~1338 to ~1332 cm^{-1} and then slightly increased to ~1334 cm^{-1}. At laser power densities of 5.0×10^3 and 6.7×10^3 W/cm^2, the diamond peak position was closest to 1332 cm^{-1}, which is the peak position of natural diamond. The FWHM curve of the diamond peaks has similar shape to that of the Raman shift curve, as shown in Fig. 5.7 (right, solid triangles). The shift and broadening of Raman peaks for the samples deposited without laser excitation and with low-power-density $(8.3 \times 10^2 \sim 3.3 \times 10^3$ W/cm$^2)$ laser excitations were believed resulting from low diamond

qualities due to defects, impurities and non-diamond carbon contents. The diamond quality increased as the incident laser power increased. On the other hand, when the laser power density increased beyond 6.7×10^3 W/cm^2, another factor, residual stress, became dominant in determining the position of the diamond peak. The major contribution of the residual stress comes from the thermal stress developed during the cooling-down process from the growth temperature to room temperature, which is caused by the thermal expansion mismatch between the diamond films and the substrates [8-13]. For the diamond films deposited with high laser power density larger than 1.0×10^4 W/cm^2, diamond films were much thicker, which introduced higher lateral stress, and resulted in the shift and broadening of the diamond Raman peaks. Based on the Raman spectroscopy, it is believed that diamond crystals with best quality can be obtained when the incident power density is 5.0×10^3~6.7×10^3 W/cm^2.
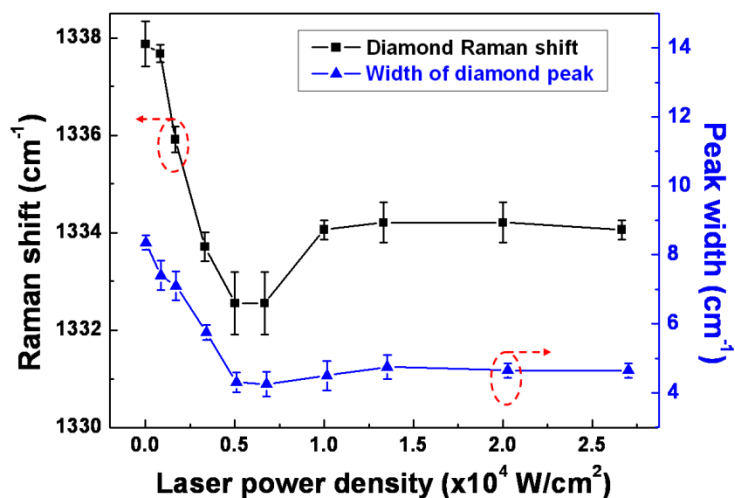
Figure 5.7 Raman shifts (left, solid squares) and full width at half maximum values (right, solid triangles) of diamond peaks as functions of laser power densities.

5.3 Conclusions

Resonant excitation of precursor molecules using different laser powers in laser-assisted growth of diamond crystals was studied to modify diamond surface morphology, obtain high diamond crystal quality, and high energy coupling efficiency. At a laser power density range of $5.0 \times 10^3 \sim 1.0 \times 10^4$ W/cm^2, {100}-oriented diamond crystals were grown in the center area of the deposited diamond films. According to the Raman spectroscopy of the diamond films deposited with laser excitations at different incident laser powers, best diamond qualities could be obtained when the incident power density was in a range of $5.0 \times 10^3 \sim 6.7 \times 10^3$ W/cm^2. The increment rates of diamond film thicknesses indicate that the highest efficiency of laser energy coupling could be achieved in a range of $5.0 \times 10^3 \sim 6.7 \times 10^3$ W/cm^2. Considering all the above factors, it is believed that the incident power density of 6.7×10^3 W/cm^2 is the optimal value under the growth condition used in this study. This study suggests a laser-assisted approach for modifications of surface orientations in crystal growth through laser excitations of precursor molecules.

References

[1]. Bagratashvili, V. N., Letokhov, V. S., Makarov, A. A., and Ryabov, E. A., "Multiple Photon IR Laser Photophysics and Photochemistry. III", Laser Chemistry **4,** 185 (1984).

[2]. Yao, L., Mebel, A. M., Lu, H. F., Neusser, H. J., and Lin S. H., "Anharmonic Effect on Unimolecular Reactions with Application to the Photodissociation of Ethylene", Journal of Physical Chemistry A, **111,** 6722 (2007).

[3]. Komaki, K., Yanagisawa, M., Yamamoto, I., and Hirose, Y. "Synthesis of Diamond in Combustion Flame under Low Pressures", Japanese Journal of Applied Physics **32,** 1814 (1993).

[4]. Miller, J. A. and Melius, C. F., "Kinetic and thermodynamic issues in the formation of aromatic compounds in flames of aliphatic fuels", Combustion and Flame **91,** 21 (1992).

[5]. Bauerle, D. in Laser Processing and Chemistry; Springer: Berlin, Heidelberg, Part I, pp 31 (2000).

[6]. Kim, J. G. and Yu, J., "Behavior of residual stress on CVD diamond films", Materials Science and Engineering B **57**, 24 (1998).

[7]. Bagratashvili, V. N., Letokhov, V. S., Makarov, A. A., and Ryabov, E. A., "Multiple-Photon Infrared Laser Photophysics and Photochemistry. II", Laser Chemistry **1,** 216 (1983).

[8]. Xu, Z. Q., Lev, L., Lukitsch, M., and Kumar, A., "Effects of surface pretreatments

on the deposition of adherent diamond coatings on cemented tungsten carbide substrates", Journal of Materials Research **22,** 1012 (2007).

[9]. Nakamura, Y., Sakagami, S., Amamoto, Y., and Watanabe, Y., "Measurement of internal stresses in CVD diamond films", Thin Solid Films **308,** 249 (1997).

[10]. Fan, Q. H., Fernandes, A., Pereira, E., and Gracio, J., "Evaluation of biaxial stress in diamond films", Diamond and Related Materials **8,** 645 (1999).

[11]. Fan, Q. H., Gracio, J., and Pereira, E., "Residual stresses in chemical vapour deposited diamond films", Diamond and Related Materials **9,** 1739 (2000).

[12]. Kuo, C. T., Lin, C. R., and Line, H. M., "Origins of the residual stress in CVD diamond films", Thin Solid Films **290,** 254 (1996).

[13]. Yalamanchi, R. S. and Harshavardhan, K. S. "Diamond growth in combustion flames". Journal of Applied Physics **68,** 5941 (1990).

CHAPTER 6

Growth of {100}-oriented Diamond Films and Crystals

6.1 Introduction

6.2 Experiments, results, and discussion

6.2.1 Excitation of ethylene through vibration-rotation transitions

6.2.2 Growth of {100}-oriented diamond films and crystals

6.2.3 Mechanism study using mass spectrometry

6.2.4 Theoretical simulations

6.3 Conclusions

6.1 Introduction

Crystallographic orientations determine the optical, electrical, mechanical, and thermal properties of crystals. Control of crystallographic orientations has been studied by changing the growth parameters, including temperature, pressure, proportion of precursors, and surface conditions. In chapter 5, we also described diamond film with {100}-oriented diamond facets with laser vibrational excitations of ethylene molecules at certain laser power densities. However, molecular dynamic mechanisms underlying these controls remain largely unknown. In this chapter, we achieved control of crystallographic orientations in diamond growth through a joint experimental and theoretical study of laser resonant vibrational excitation of precursor molecules. Resonant vibrational excitation of the ethylene molecules using a wavelength-tunable CO_2 laser steers the chemical reactions and promotes proportion of intermediate oxide species, which results in preferential growth of {100}-oriented diamond films and diamond single crystals in open air. Quantum molecular dynamic simulations and reaction-pathway calculations provide an in-depth understanding of molecular reaction mechanisms in the steering of chemical reactions and control of crystallographic orientations. This finding opens up a new avenue for controlled chemical vapor deposition of crystals through resonant vibrational excitations to steer surface chemistry.

Laser control of chemical reactions through resonant excitations has been extensively studied in bimolecular collisions, unimolecular decompositions, and gas-solid

reactions [1-5] However, the effects of laser control of reactions are usually too weak to be significant for material synthesis [6]. Control of chemical reactions via resonant vibrational excitation of precursor molecules is promising in that molecular vibrations are directly involved in the rearrangement of their bonds to become products [1, 5]. Lasers are ideal energy sources for vibrational excitations because their narrow bandwidth prepares a single vibrational eigenstate [5], which makes precise control of reaction pathways feasible. One approach to laser control is active intervention, in which the phases of reagent motions are controlled during the course of the reaction [6]. This active intervention may preferentially lead reagents to one of many different reaction routes. In this study, we introduced active intervention to material synthesis and achieved control of the chemical reaction and, hence, controlled crystallographic orientations through laser resonant vibrational excitations of precursor molecules in CVD of diamond.

Many properties of diamond, including thermal conductivity, optical behavior, and mechanical properties, depend on diamond crystallographic orientations [7, 8]. Preferential growth of {100}-textured diamond films has been pursued for years because of their superior properties over those of {111}- and {110}-textured diamonds [9-16]. Mechanically, {100}-textured diamond films have lower roughness and higher wear resistance as compared with other crystallographic directions [9]. Optical properties of {100}-textured films are superior to those of {111}-textured films in terms of refractive index and extinction coefficient [9]. Research efforts have been exerted to achieve orientation-controlled growth of diamond. Liu *et al.* have studied control of diamond

textures by varying the growth parameters, including substrate temperature, precursor concentration, and film thickness [7]. By applying bias-enhanced nucleation [11, 12] and introducing nitrogen into the growth precursors [13, 14], {100}-textured diamond films have also been successfully deposited. These methods are capable of producing {100}-textured diamond films with reproducibility. However, the molecular reaction mechanism remains elusive, and further investigation is needed to obtain an in-depth understanding of the control of crystallographic orientation. In our previous study, resonant excitations of precursor molecules have been applied in the synthesis of diamond films and crystals [15, 16]. Diamond growth rate and quality were significantly promoted. Diamond crystals with sizes up to 5 mm were successfully obtained in open air [16]. Insight into the laser control of chemical reactions and control of diamond crystallographic orientations were investigated in this research.

6.2 Experiments, results, and discussion

6.2.1 Excitation of ethylene through vibration-rotation transitions.

We introduced resonant excitations of precursor molecules using a wavelength-tunable CO_2 laser to steer the chemical reactions in diamond formation which led to the preferential growth of {100}-textured diamond of high phase purity. The diamond growth process was steered by resonantly exciting ethylene (C_2H_4) molecules to higher vibrational and rotational states. A schematic illustration of the experimental setup is shown in Fig. 6.1a. The detailed experimental method is similar with that in previous chapters. Tungsten carbide plates were used as substrates. The wavelength of the tunable CO_2 laser ranged from 9.2 to 10.9 µm. Figure 6.1b shows a representative absorption spectrum of the laser energy by the $C_2H_4/C_2H_2/O_2$ flame with respect to the laser wavelength. Several absorption peaks were observed at different wavelengths. The strongest peak at 10.532 µm corresponds to the Q branch ($\Delta J = 0$) of a fundamental vibration mode (v_7, CH_2-wagging) of the ethylene molecules [16]. Another absorption peak at 10.22 µm corresponds to the R branch ($\Delta J = 1$) of the CH_2-wagging mode [17, 18], which means that the molecules were excited to a higher level of vibrational state with a higher level of rotation energy, as schematically indicated in Fig. 6.1c.
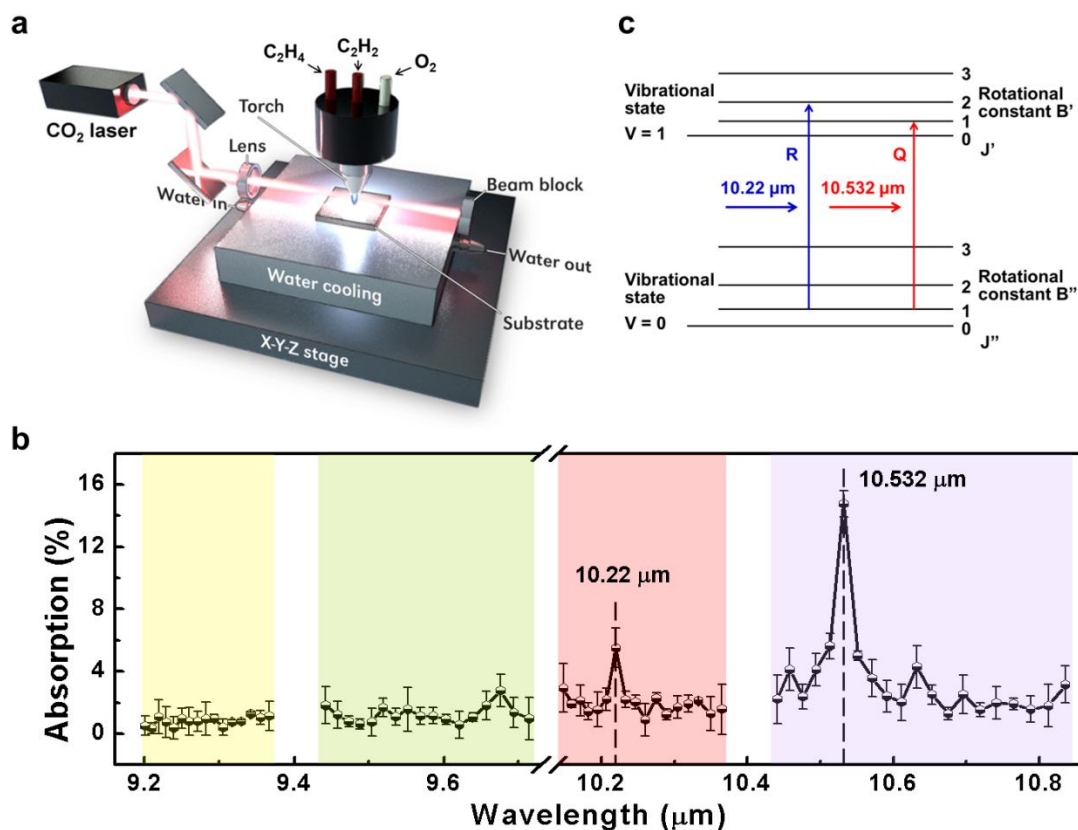
Figure 6. 1 Absorption of laser energy by the C_2H_4/C_2H_2/O_2 flame. (a) Schematic of the experimental setup. (b) Absorption of laser energy by the C_2H_4/C_2H_2/O_2 flame. The four colored regions indicate emission bands of the wavelength tunable CO_2 laser. The error bars indicate standard deviations. (c) Vibration-rotation transitions of an ethylene molecule with CO_2 laser excitations at different wavelengths.

6.2.2 Growth of {100}-oriented diamond films and crystals

We compared the excitations of ethylene molecules in the combustion flame by laser irradiation at 10.22, 10.333 (non-resonant wavelength), and 10.532 μm and deposited diamond films with all other parameters the same. Figure 6.2 shows representative SEM images of diamond films deposited for 15 (upper) and 60 min.

(lower), respectively. Diamond films deposited without laser excitation were also included for comparison. It was observed that diamond films deposited by the 10.22 μm laser excitation exhibited predominantly {100} surfaces, while those deposited under the other three conditions showed random orientations. This phenomenon does not change with deposition time, with similar film morphology at different deposition time (15 and 60 min.). It was demonstrated that vibrational excitation of ethylene molecules at 10.22 μm leads to a preferential growth of {100}-textured diamond films. Figure 6.3 shows the thicknesses of the four diamond films. Both the excitations at 10.22 and 10.532 μm increased the film thickness, while the excitation at 10.333 μm had weak impact on the film thickness. This is in good agreement with the energy absorption shown in Fig. 6.1b, where the absorption of laser energy by the $C_2H_4/C_2H_2/O_2$ flame is the highest at 10.532 μm, followed by that at 10.22 μm, while no obvious absorption is observed at 10.333 μm.
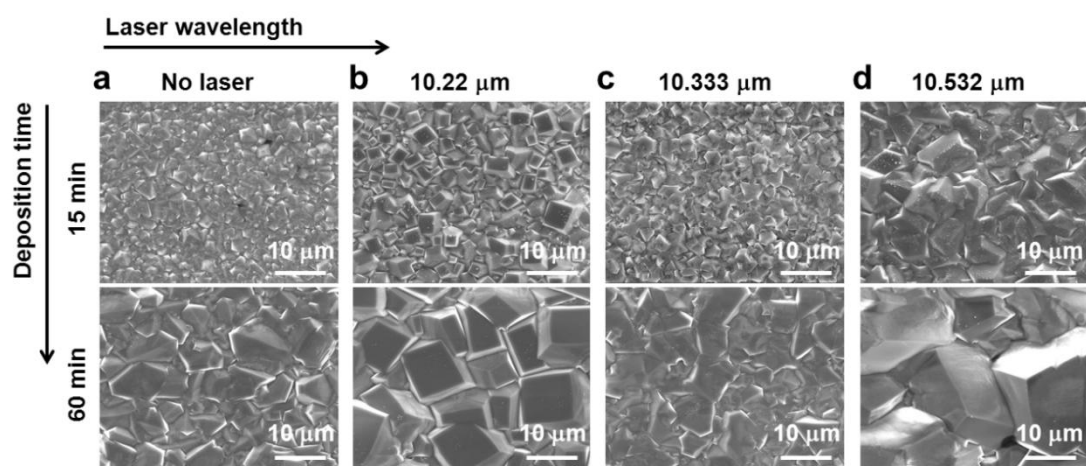
Figure 6.2 SEM images of the diamond films. Diamond films deposited without laser (a), with CO_2 laser irradiation at different wavelengths of 10.22 (b), 10.333 (c), and 10.532 μm (d). (upper: 15-min deposition, lower: 60-min deposition).
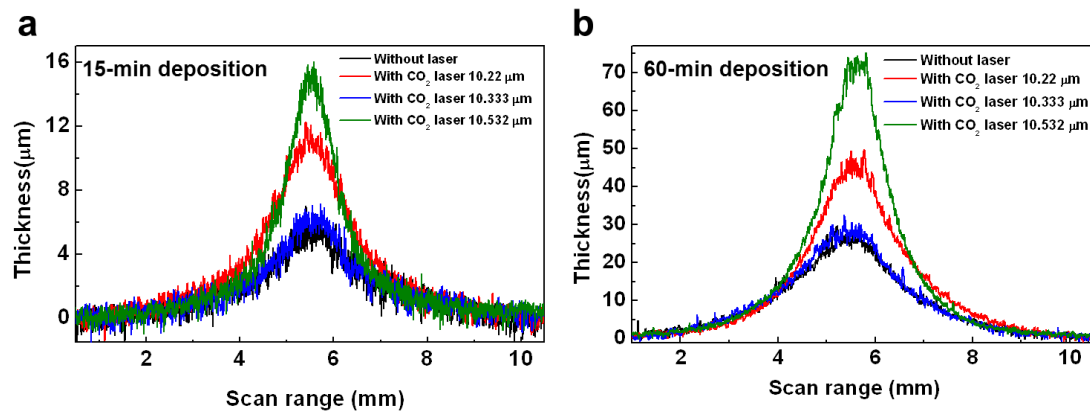
Figure 6. 3 Thicknesses of the diamond films deposited without laser excitation and with CO_2 laser excitations at 10.22, 10.333, and 10.532 μm for a) 15 and b) 60 min.

Under the resonant excitation at 10.22 μm, single crystal diamond with a size of 300 μm was grown in 5 hr. in open air, as shown in Fig. 6.4. Different from the diamond crystals deposited through vibrational excitation of ethylene at 10.532 μm [18], this diamond crystal exhibited high uniformity. A flat {100} surface, as shown in Fig. 6.4b, demonstrated the preferential growth of the {100} surface for long time deposition. No twinning was observable in the SEM images on the {100} surface. Twinnings abundantly exist on {111} surfaces, which is believed to be caused by the faster growth of {111} surfaces compared to that of {100} surfaces [15]. The crystal shape of diamond facets is determined by the growth rate of the {100} surface (V_{100}) and that of the {111} surface (V_{111}), as indicated by the diamond growth parameter, $\alpha = \sqrt{3}(V_{100}/V_{111})$ [7, 22]. The facets that show up at the final stage of crystal growth are those along which the growth velocity is the least. The growth velocity of the {111} surfaces should be greater than that of the {100} surfaces in order to obtain the predominantly {100} surfaces. It has been

widely accepted in diamond growth that a higher growth velocity in a certain sector will result in lower phase purity in that sector, which results in the twinnings on {111} surfaces [8, 21, 22]. A lower concentration of twinnings on the {100} surface indicates high quality {100}-oriented diamond crystals.
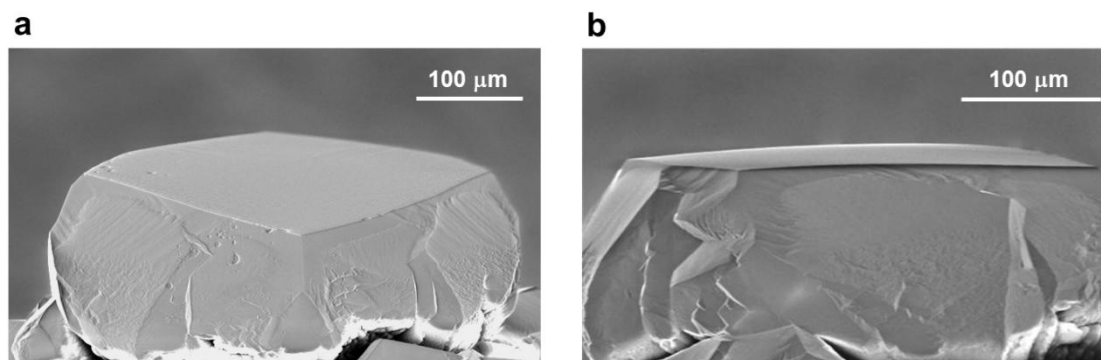
Figure 6.4 SEM images of a single-crystal diamond grown for 5 hr with CO_2 laser excitation at 10.22 μm. a) Tilted view and b) side view.

Raman spectroscopy was performed to determine the phase purity of the diamond films and crystals deposited. Figure 6.5a shows the Raman spectra of the diamond films deposited for 60 min under different excitation conditions. The shift of the diamond peak from 1332 (phase-pure natural diamond) to 1335 cm^{-1} was ascribed to the residual stresses in the diamond films caused by differences in the coefficients of thermal expansion (CTE) between the diamond films and the substrates. The D band is related to disordered carbon structures, and the G band corresponds to sp^2 graphite phases in diamond films. It is obvious that both the D- and G bands are suppressed in diamond films deposited with laser excitations at 10.22 and 10.532 μm, indicating an increased

purity of diamond sp^3 bonding. The spectrum of the diamond film deposited with laser excitations at 10.22 μm exhibited even lower D- and G- bands, indicating that the {100} surfaces have better phase purity than other surfaces. This is in agreement with the transmission electron microscopic (TEM) study of different diamond growth sectors, which revealed that the ‹100› sector has a low density of dislocations, while the ‹111› sectors are highly defective, containing a high density of dislocations and stacking faults [8]. Figure 6.5b shows the Raman spectra of diamond crystals, including those deposited with 10.22 (shown in Fig. 6.4a) and 10.532 μm excitations (reported in Ref. 18) as well as a type Ia natural diamond. The diamond peaks of these three crystals are all located at 1332 cm^{-1}. The D- and G-bands are invisible in all spectra, which indicate very high purity of the diamond sp^3 bonding. The full width at half maximum (FWHM) value of the {100}-oriented diamond is 3.3 cm^{-1}, which is similar to that of the natural diamond (3.1 cm^{-1}), much narrower than that of the diamond crystal deposited with the 10.532 μm excitation (4.5 cm^{-1}). Therefore, the {100}-oriented diamond crystal deposited with vibrational excitation of ethylene at 10.22 μm has high phase purity and high crystal quality.
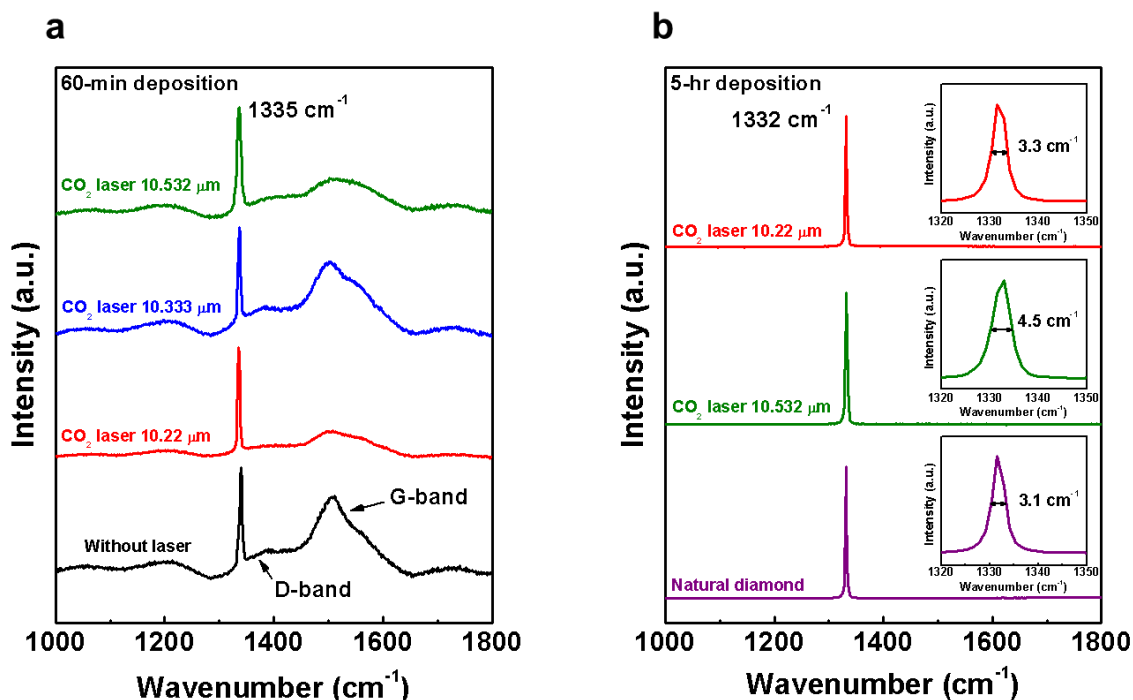
Figure 6.5 Raman spectra of the diamond films and crystals. a) Diamond films deposited for 60 min without laser excitation, with CO_2 laser excitation at 10.22, 10.333, and 10.532 μm, respectively. b) Diamond crystals grown for 5 hr with CO_2 laser excitation at 10.22 and 10.532 μm. A natural diamond crystal (type Ia) is also characterized as comparison. Insets in (b) show the FWHM of the diamond peak for each crystal.

6.2.3 Mechanism study using mass spectrometry

Mass spectroscopy (MS) of the $C_2H_4/C_2H_2/O_2$ combustion flames used for diamond growth was performed under different excitation conditions to investigate mechanisms of the preferential growth of {100}-textured diamond. The experimental setup for the MS detection is schematically shown in Fig. 6.6. Ionization of species occurs in the combustion flame, making the flame suitable for direct analysis using MS.

Positive ions in the $C_2H_4/C_2H_2/O_2$ flames were detected using a time-of-flight mass spectrometer (MS, AccuTOF^{TM}, JEOL USA, Inc.), as shown in Fig. 6.7. A stainless steel orifice with an inner diameter of 400 μm on the mass spectrometer collects ions in open air. The combustion torch was fixed on a motorized XYZ stage, and the relative position of the flame to the orifice was precisely adjusted so that the tip of the flame inner cone was right in front of the orifice under all excitation conditions. The MS data were analyzed using the TSSPro software (Shrader Analytical and Consulting Laboratories, Inc. Version 3.0) and the MS Tools software (JEOL USA, Inc.).
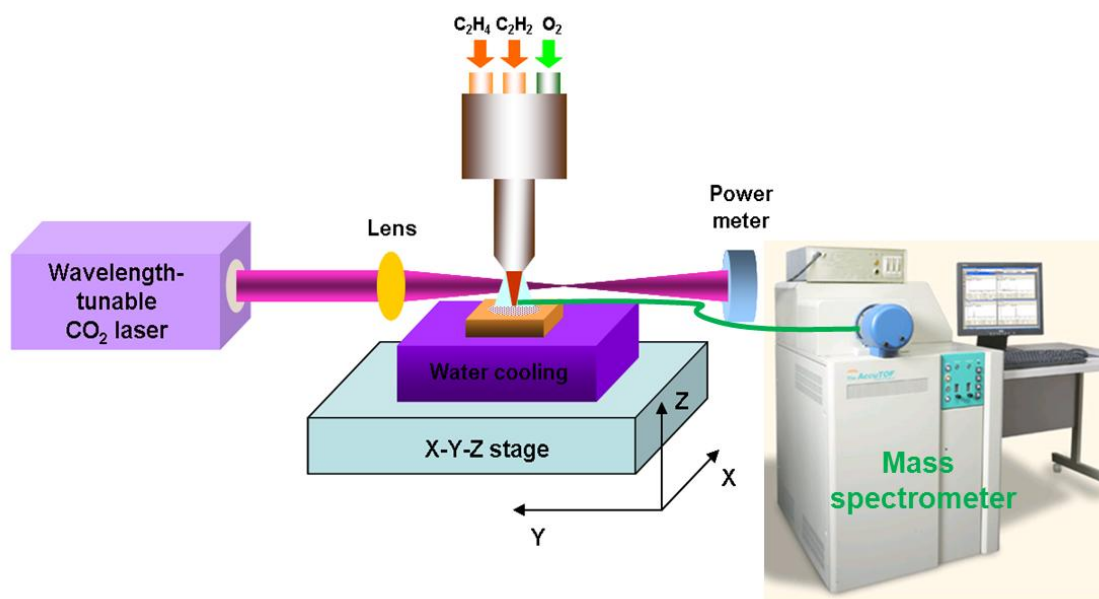
Figure 6.6 Schematic diagram of the experimental setup for mass spectrometry of the combustion flame.
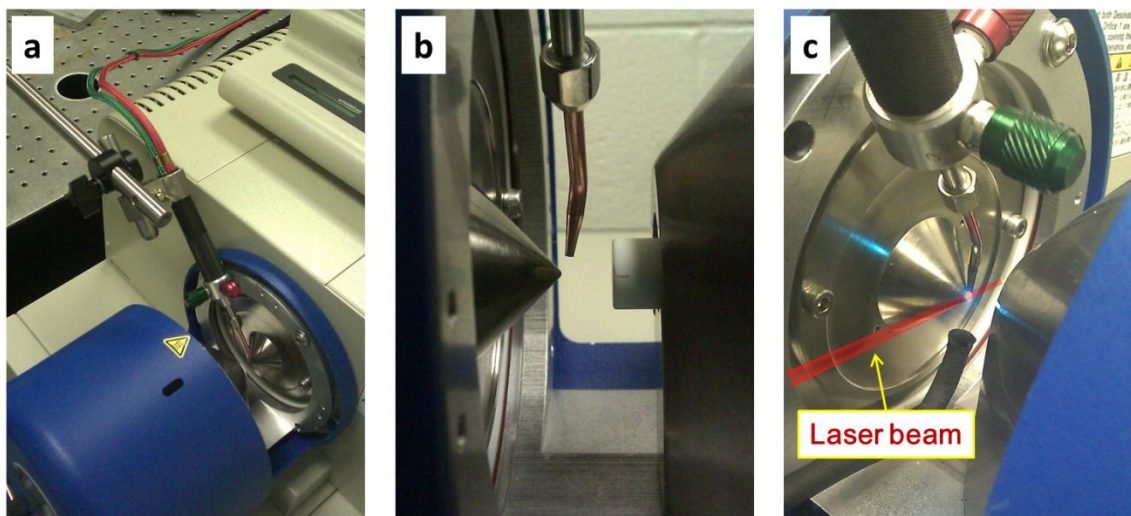
Figure 6.7 Pictures of the setup of flame mass spectrometry. (a) Picture of the mass spectrometer and the flame setup. (b) A close view of the relative position of the MS orifice and the flame nozzle. (c) Picture of flame analysis using the mass spectrometer.

Figure 6.8a shows a representative mass spectrum of the $C_2H_4/C_2H_2/O_2$ flame, in which positive ions with m/z values ranging from 12 to 47 are detected and assigned as CH_x^+ (x = 0~3), $C_2H_x^+$ (x = 0~5), $C_3H_x^+$ (x = 0~5), CH_xO^+ (x = 1~3) and $C_2H_xO^+$ (x = 2~5) ions. Considering differences in ionization potentials among different species, the height of each line does not necessarily represent the absolute concentration of each species. Nevertheless, MS analysis of the flame is valuable to determine the evolvement of species concentration under different excitation conditions, given that the variation of ions is proportional to that of related species. Figure 6.8b provides a chromatogram of the total ion current (TIC) of the $C_2H_4/C_2H_2/O_2$ flame under different excitation conditions, which provides the intensity of all detected ions in the flame. Figure 6.9 shows

chromatograms of CH_3^+, CH_3O^+, $C_2H_3^+$, and $C_2H_3O^+$ as examples. The chromatogram of

each ion has similar shape with that of the TIC. Intensity of each ion can be obtained by

calculating the average value of the corresponding scans. Average intensity of each

species when the flame was under laser excitation at 10.532 μm is marked by a red

dashed line. A comparison of the ion intensity between the flame under excitation at

10.22 and 10.532 μm indicate that intensities of the CH_3^+ and $C_2H_3^+$ ions were highest at

10.532 μm, whereas those of the CH_3O^+ and $C_2H_3O^+$ ions were highest at 10.22 μm.
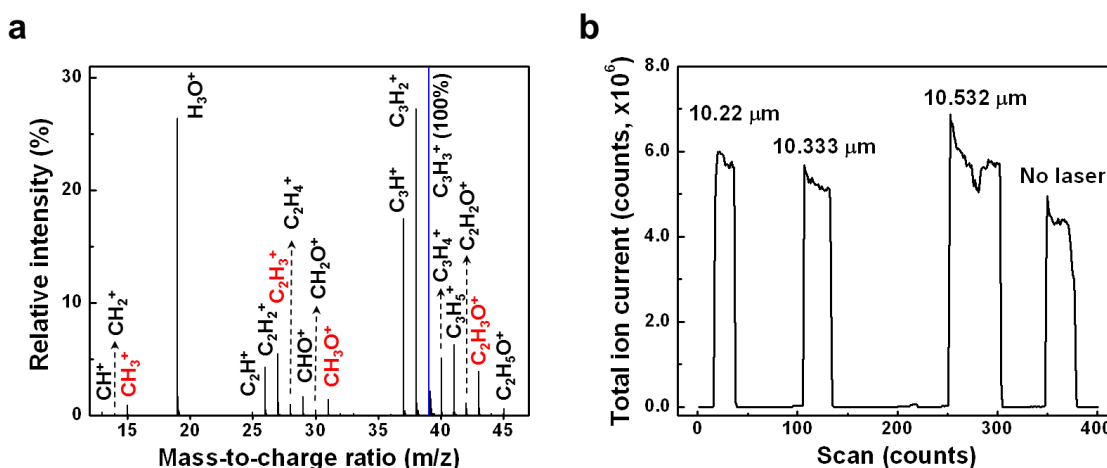
Figure 6.8 Mass spectrometry of the $C_2H_4/C_2H_2/O_2$ flame. a) Mass spectrum of the flame irradiated with CO_2 laser at 10.22 μm. b) Chromatogram of the flame under different excitation conditions.
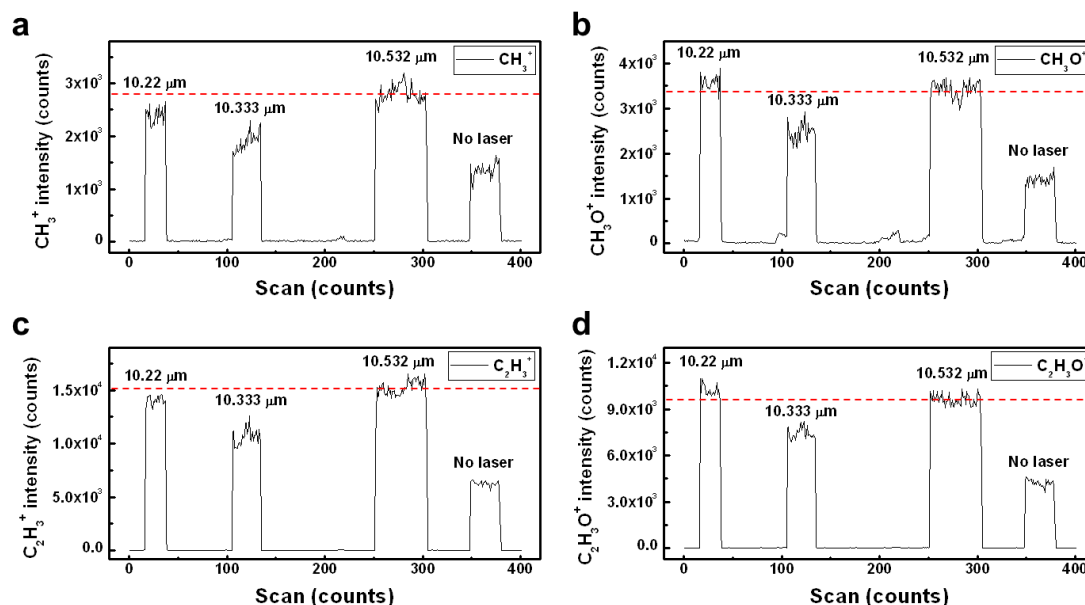
Figure 6.9 Chromatograms of a) CH_3^+, b) CH_3O^+, c) $C_2H_3^+$, and d) $C_2H_3O^+$ ions derived from the total ion current (TIC) of the $C_2H_4/C_2H_2/O_2$ flame without and with CO_2 laser irradiations at different wavelengths.

The intensity of each ion can be obtained by calculating the average value of the corresponding scans. The concentration of each ion was derived by dividing its intensity with the TIC value in order to eliminate the variation of its absolute value in different measurements. Because species containing one or two carbons are of interest to diamond growth [22], relative concentrations of CH_x^+ (x = 0~3), $C_2H_x^+$ (x = 0~5), CH_xO^+ (x = 1~3), and $C_2H_xO^+$ (x = 2~5) ions were calculated and summarized respectively, as shown in Fig. 6.10. In Fig. 6.10a, the concentrations of both CH_x and C_2H_x species were increased by laser excitations at 10.22 and 10.532 μm. The CH_xO and C_2H_xO species show similar trends in Fig. 6.10b. However, a detailed comparison between Figs. 6.10a

and 6.10b reveals a slight difference between the species intensities with laser excitations at 10.22 and 10.532 μm. Concentrations of the CH_x and C_2H_x species are the highest at 10.532 μm, whereas those of the CH_xO and C_2H_xO species are the highest at 10.22 μm. As discussed in the beginning of this section, the excitation of ethylene molecules by the CO_2 laser at 10.22 μm corresponds to the R branch (ΔJ=1) of the CH_2 wagging mode, which means that the molecules are excited to a higher level of vibrational state with a higher level of rotation energy. Because the energy transfer by the rotational-translational channel through binary molecular collision is much faster than that by the rotational-vibrational channel [23], higher rotational energy will result in higher translational energy, which is reflected by higher temperature. That means the excitation of ethylene molecules by the CO_2 laser at 10.22 μm resulted in higher flame temperature than the excitations at other wavelengths (with the same quantity of laser energy absorbed). The increased flame temperature consequently resulted in promoted oxidation of the carbon hydride species. In other words, concentration of the oxygen-containing species (CH_xO, C_2H_xO, etc.) was increased by higher flame temperature caused by the CO_2 laser excitation at 10.22 μm.
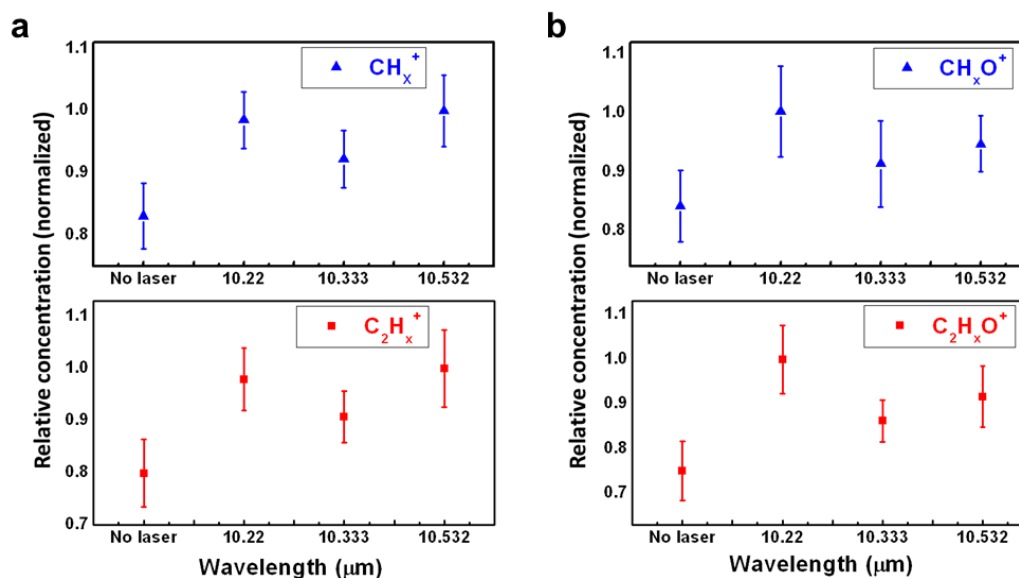
Figure 6.10 Relative concentrations of a) CH_x^+ (x = 0~3), and $C_2H_x^+$ (x = 0~5) ions and b) CH_xO^+ (x = 1~3), and $C_2H_xO^+$ (x = 2~5) ions with CO_2 laser excitations at different wavelengths.

6.2.4 Theoretical simulations

In order to obtain an in-depth understanding of the preferential growth of the {100}-oriented diamond surfaces, simulations were conducted by Drs. Yi Gao and Jaeil Bai from Professor Xiao Cheng Zeng's group from Department of Chemistry at University of Nebraska-Lincoln. Quantum molecular dynamics (QMD) simulations were performed for exploration of intermediate species in the $C_2H_4/C_2H_2/O_2$ flames. It is shown, in the simulation, that as the temperature of the flame is increased, the CH_xO (x = 1~3) and C_2H_xO (x = 2~5) species appear with larger population through the combustion process. The Cambridge sequential total energy package (CASTEP) software was employed for the QMD simulation. The plane-wave energy cutoff was set at 170 eV. A

0.2 eV finite smearing scheme was used for the self-consistent field (SCF) calculation. The supercell of the system t was a $14 \times 14 \times 14$ Å^3 cubic box. The simulation cell initially contained four C_2H_4, four C_2H_2, and eight O_2 molecules. The temperature of the system was controlled at 2800, 3000, and 3200 K, respectively, using a Nóse thermostat. The time step of the QMD simulation was 0.8 fs. Figure 6.11 shows the time evolution of the C_2H_4 molecules and intermediate CH_xO (x = 1~3) and C_2H_xO (x = 2~5) species in the flames, based on the QMD simulations. The vertical axis in the figures shows the averaged numbers of intermediate species observed per 20 fs during the simulations. The figures show that as the temperature of the flames is increased, the CH_xO (x= 1~3) and C_2H_xO (x= 2~5) species appear in the early stage and result in a larger population through the combustion process, which is consistent with the mass spectrometry data.
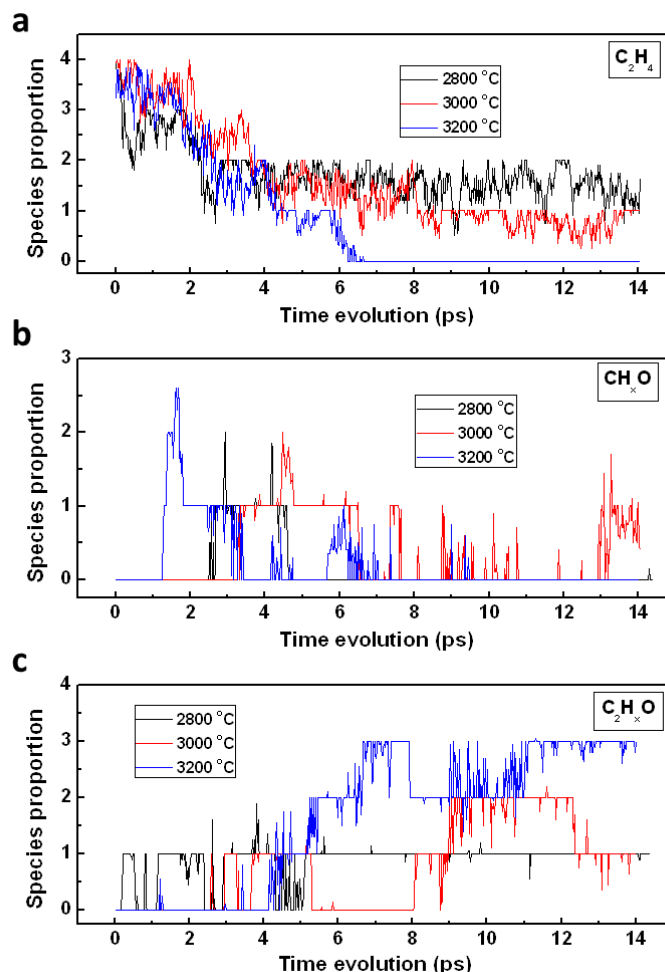
Figure 6.11 Time evolution of (a) C₂H₄, (b) CH$_x$O (x = 1~3) and (c) C₂H$_x$O (x = 2~5) species under different temperatures. The vertical axis in each figure shows the average numbers of the species observed per 20 fs during the QMD simulations.

To gain molecular insights into the relative abundance of produced species on different diamond surfaces, we computed the reaction pathways of two smaller hydrocarbon oxide species, CHO and CH$_2$CO, based on periodic density-functional theory (DFT) calculations. The reaction pathways of two smaller hydrocarbon oxide species, CHO and CH$_2$CO, were computed based on periodic density-functional theory

(DFT) calculations. The two slab systems considered were four-layer 4×4 diamond {111} and {100} surfaces. All of the atoms of the bottom two layers were fixed, while those of the top two layers were fully relaxed. The vacuum slab was set as 20 Å to avoid interactions between the slab and its periodic images. The DFT calculations were carried out with the Perdew-Burke-Ernzerhof (PBE) [24] functional and double numerical polarized basis sets (DND) [25, 26]. The energy convergence for the self-consistent field calculations was set as 10^{-5} Hartree, and the energy convergence for the geometrical optimization was set as 2×10^{-5} Hartree. The reaction pathways were computed using the nudged elastic band (NEB) algorithm [27]. All calculations were carried out by using DMol^3 software package [25, 26].

The computed reaction pathways for CH_2CO and CHO on diamond {100} and {111} surfaces are shown in Fig. 6.12. It can be seen that the reaction path on the {111} surface is downward for CH_2CO while that for CHO on the {111} surface is slightly upward and then downward. This difference indicates that the CH_2CO splitting is much easier than CHO splitting on the diamond {111} surfaces and that the longer hydrocarbon oxides tend to split more easily. Furthermore, the intermediate states and transition states are energetically more favorable on the diamond {111} than those on the diamond {100} surface for both CHO and CH_2CO, suggesting that the splitting reactions on the diamond {111} are much more facile than those on the diamond {100}. To achieve preferential growth of the {100} surface, predominant growth of the {111} surface is needed [7, 22].

As such, the diamond {111} surface grows faster than the {100} surface, hence the diamond {100} surfaces tend to be exposed on the crystallites.
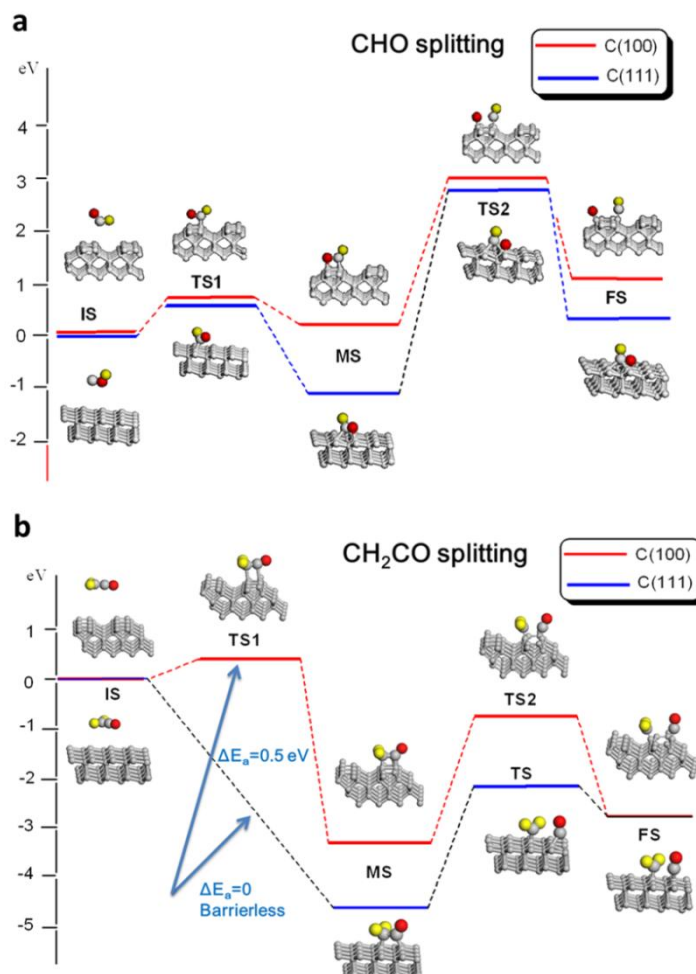
Figure 6.12 Simulated chemical reaction pathways. (a) Carbon-carbon bond breaking of CHO molecules on {111} (blue) and reconstructed {100} (red) diamond surfaces, respectively. (b) Carbon-carbon bond breaking of CH$_2$CO molecules on {111} (blue) and reconstructed {100} (red) diamond surfaces, respectively. Grey: carbon, red: oxygen, yellow: hydrogen; IS: Initial State, TS: Transition State, MS: Intermediate State, FS: Final State.

6.3 Conclusions

We demonstrated a laser-assisted combustion process to synthesize {100}-oriented diamond films and single crystals through resonant vibrational excitation of precursor molecules. The CO_2 laser beam at 10.22 μm excites the ethylene molecules to a higher vibrational state with higher rotational energy in the combustion flame, which increases the relative concentrations of the CH_xO and C_2H_xO species. Theoretical simulations of the reaction pathway indicates that these species react more easily with diamond {111} surfaces than with {100} surfaces, leading to a fast growth of the {111} surface of diamond and resulting in {100}-oriented diamond. This finding opens up a new avenue for controlled chemical vapor deposition of crystals through resonant vibrational excitation of precursor molecules.

References

[1]. Crim, F. F., "Making Energy Count", Science **317,** 1707 (2007).

[2]. Potter, E. D., Herek, J. L., Pedersen, S., Liu, Q., and Zewail, A. H. "Femtosecond laser control of a chemical reaction", Nature **355,** 66 (1992).

[3]. Bechtel, H. A., Kim, Z. H., Camden, J. P., and Zare, R. N. "Bond and mode selectivity in the reaction of atomic chlorine with vibrationally excited CH_2D_2", Journal of Chemical Physics **120,** 791 (2004).

[4]. Utz. A. L. "Mode selective chemistry at surfaces", Current Opinions in Solid State & Mater Science **13,** 4 (2009).

[5]. Killelea, D. R., Campbell, V. L., Shuman, N. S., and Utz, A. L. "Bond-Selective Control of a Heterogeneously Catalyzed Reaction", Science **319,** 790 (2008).

[6]. Zare, R. N., "Laser Control of Chemical Reactions", Science **279,** 1875 (1998).

[7]. Liu, T., Raabe, D., Mao, W., and Zaefferer, S. "Microtexture and Grain Boundaries in Freestanding CVD Diamond Films: Growth and Twinning Mechanisms", Advanced Functional Materials **19,** 3880 (2009).

[8]. Butler, J. E. and Oleynik, I. "A mechanism for crystal twinning in the growth of diamond by chemical vapour deposition", Philosophical Transactions of the Royal Society A **366,** 295 (2008).

[9]. Avigal, Y., Glozman, O., Etsion, I., Halperin, G., and Hoffman, A., "[100]-Textured diamond films for tribological applications", Diamond and Related Materials **6,** 381 (1997).

[10]. Su, Q. F. , Xia, Y. B., Wang, L. J. , Liu ,J. M., and Shi, W. M., "Influence of texture on optical and electrical properties of diamond films", Vacuum **81,** 644 (2007).

[11]. Schade, A., Rosiwal, S. M., and Singer, R. F., "Influence of surface topography of HF-CVD diamond films on self-mated planar sliding contacts in dry environments", Diamond and Related Materials **15,** 1682 (2006).

[12]. Fabisiak, K., Banaszak, A., Kaczmarski, M., and Kozanecki, M. "Paramagnetic defects in diamond films synthesized by the hot filament chemical vapour deposition", Crystal Research Technology **41,** 535 (2006).

[13]. Stoner, B. R., Sahaida, S. R., Bade, J. P., Southworth, P., and Ellis, P. J., "Highly oriented, textured diamond films on silicon via bias-enhanced nucleation and textured growth", Journal of Materials Research **8,** 1334 (1993).

[14]. Fox, B. A., Stoner, B. R., Malta, D. M., Ellis, P. J., Glass, R. C., and Sivazlian, F. R., "Epitaxial nucleation, growth and characterization of highly oriented, (100)-textured diamond films on silicon", Diamond and Related Materials **3,** 382 (1994).

[15]. Locher, R., Wild, C., Herres, N., Behr, D., and Koidl, P. "Nitrogen stabilized <100> texture in chemical vapor deposited diamond film", Applied Physics Letters **65,** 34 (1994).

[16]. Ayres, V. M., Bieler, T. R., Kanatzidis, M. G., Spano, J., Hagopian, S., Balhareth, H., Wright, B. F. Farhan, M., Abdul Majeed, J., Spach, D, Wright, B. L., and Asmussen, J., "The effect of nitrogen on competitive growth mechanisms of diamond thin films", Diamond and Related Materials **9,** 236 (2000).

[17]. Ling, H. Xie, Z. Q., Gao, Y., Gebre, T., Shen, X. K., and Lu, Y. F., "Enhanced chemical vapor deposition of diamond by wavelength-matched vibrational excitations of ethylene molecules using tunable CO_2 laser irradiation", Journal of

Applied Physics **105**, 064901 (2009).

[18]. Xie, Z. Q., Zhou, Y. S., He, X. N., Gao, Y., Park, J. B., Ling, H., and Lu, Y. F., "Fast Growth of Diamond Crystals in Open Air by Combustion Synthesis with Resonant Laser Energy Coupling", Crystal Growth & Design **10,** 1762 (2010).

[19]. Gallaway, W. S. and Barker, E. F. "The Infra-Red Absorption Spectra of Ethylene and Tetra-Deutero-Ethylene under High Resolution", Journal of Chemical Physics **10,** 88 (1942).

[20]. Xing, X., Baek S. J., Wang, P., and Ng, C. Y., "Rovibrationally selected and resolved state-to-state photoionization of ethylene using the infrared-vacuum ultraviolet pulsed field ionization-photoelectron method", Journal of Chemical Physics **125**, 133304 (2006).

[21]. Steeds, J. W., Gilmore, A., Wilson, J. A., and Butler, J. E., "On the nature of extended defects in CVD diamond and the origin of compressive stresses", Diamond Related Materials **7,** 1437 (1998).

[22]. Wolden, C. A., in Diamond Films Handbook, eds: Asmussen J, Reinhard DK, (Marcel Dekker, New York), pp 80 (2002).

[23]. B äuerle, D., Laser Processing and Chemistry (Springer-Verlag, Berlin Heidelberg), pp 22 (2000).

[24]. Perdew, J. P., Burke, K., and Ernzerhof, M., "Generalized gradient approximation made simple", Physical Review Letters **77,** 3865 (1996).

[25]. Delley, B., "An all-electron numerical method for solving the local density functional for polyatomic molecules", Journal of Chemical Physics **92,** 508 (1990).

[26]. Delley, B. "From molecules to solids with the DMol3 approach", Journal of

Chemical Physics **113,** 7756 (2000).

[27]. Henkelman, G. and J ónsson, H., "Improved tangent estimate in the nudged elastic band method for finding minimum energy paths and saddle points", Journal of Chemical Physics **113,** 9978 (2000).

CHAPTER 7

Mode-selective Reactions in Chemical Vapor Deposition of Diamond

7.1 Introduction

7.2 Experiments, results and discussion

7.2.1 Excitations of propylene through different vibrational modes

7.2.2 Mode-selective reactions for diamond deposition

7.2.3 Mechanism study using OES and MS

7.3 Conclusions

7.1 Introduction

One important objective of laser-induced MEP is to achieve control of chemical reactions through selective bond breaking. Reaction control has been avidly pursued in material synthesis to drive reactions to desired directions, to synthesize novel materials and structures, to reduce byproducts, or to achieve high energy efficiency. Laser control of chemical reactions through resonant excitations has been extensively studied in bimolecular collisions, unimolecular decompositions, and gas-solid reactions [1-5]. However, the effects of laser control of reactions are usually too weak to be significant for material synthesis [6]. Here we studied laser-induced mode-selective reactions in diamond growth through laser resonant vibrational excitations of precursor molecules, in which two critical issues in laser control of chemical reactions for material synthesis were addressed. Firstly, the frequency match between the laser and the molecular vibrational modes made laser resonant vibrational excitations strong enough to impact the entire reaction system. Secondly, selective excitations of different vibrational modes indicated different channels to couple laser energy for control of chemical reactions. Excitation of the mode towards the reaction coordinate (C-C stretching) significantly promoted the C-C bond breaking and suppressed diamond growth, while excitations of the "spectator" modes resulted in vibrationally excited reaction products (e.g. CH_3) and promoted diamond growth.

Chemical reactions hinge on energy distribution among internal and translational

energies of reagents. Knowing the roles of different kinds of energy (vibrational, rotational, or translational) in a reaction system allows better control over the outcomes of chemical reactions in material synthesis. Control of chemical reactions via mode-selective vibrational excitation of precursor molecules is promising in that molecular vibrations are directly related to the rearrangement of their bonds to become products [1, 5]. Lasers are ideal energy sources for vibrational excitations because their narrow bandwidth prepares a single vibrational eigenstate [5], which makes precise control of reaction pathways feasible.

Two approaches to reaction control through vibrational excitations have been reported. The first one is state preparation, in which one or more vibration modes of the reagent were selectively excited before collision [6]. In such procedures, intramolecular vibrational energy redistribution (IVR) requires careful attention because it competes with the reaction and can limit or prevent bond-selective control [5]. The second approach is active intervention, in which the phases of reagent motions are controlled during the course of the reaction [6]. This active intervention may preferentially lead reagents to one of many different reaction routes. The second approach is more promising in material synthesis because the energy deposited is less affected by the IVR, making mode-selective reactions more feasible at macro scales. However, the active intervention approach is less established [6]. In this study, we introduced active intervention to material synthesis, and achieved mode-selective reactions through laser resonant vibrational excitations of precursor molecules in chemical vapor deposition (CVD) of

diamond.

Diamond CVD has been well established in industry to produce diamond thin films and crystals [7]. All CVD methods, including plasma CVD, hot filament CVD, and combustion flame CVD, hinge on near-equilibrium thermal heating to induce reactions in the precursor gases required for diamond growth. Consequently, it is not possible to achieve selectivity among various competing chemical processes for diamond growth. In our previous studies, we applied vibrational excitations of precursor molecules in combustion flame deposition of diamond [8, 9]. Laser energy was coupled into the reactions through vibrational excitations of the CH_2 wagging mode of ethylene molecules. By introducing vibrational excitations, reaction rate in the combustion flame was promoted, concentration of chemical species was increased, and diamond growth was enhanced both in growth rate and phase purity. However, only one vibrational mode was available in these excitations, which provides limited information on mode selectivity. In order to obtain an in-depth understanding of vibrational excitations in diamond growth, selective excitations of different modes of larger molecules need to be studied.

7.2 Experiments, results and discussion

7.2.1 Excitations of propylene through different vibrational modes.

Propylene (C_3H_6) was used as the precursor. As discussed in Chapter 2, four out of the twenty-one IR active vibrational modes of propylene fall in the wavelength range of the CO_2 laser, including CH_3 rocking mode (out-of-plane wagging, ν_{17}, 1044.7 cm^{-1}, or 9.572 μm), a combination of C=C-C bending and C=CH$_2$ twisting modes (963 cm^{-1}, or 10.384 μm), CH_3 symmetric wagging mode (ν_{12}, 934.5 cm^{-1}, or 10.7 μm), and C-C stretching mode (ν_{13}, 919 cm^{-1}, or 10.881 μm) [10, 11]. The first mode has weaker IR activity as compared with the other three. The wavelength-tunable CO_2 laser can be tuned to 9.586, 10.365, 10.696, and 10.885 μm, respectively, to match these four vibrational modes. The experimental setup is schematically shown in Fig. 7.1. The laser power was adjusted for each wavelength so that the absorbed laser energy was kept the same for all of the four modes. Optical images of the flame irradiated by the CO_2 laser at different wavelengths as well as that without laser irradiation are shown in Figure 7.2. With laser irradiation, the flame became shorter and brighter, which indicates the promotion of chemical reactions and the increase in concentration of species. The excitation of the CH_3 rocking mode (at 9.586 μm) had less impact on the flame as compared with the other three excitations, which was caused by its weaker IR activity.
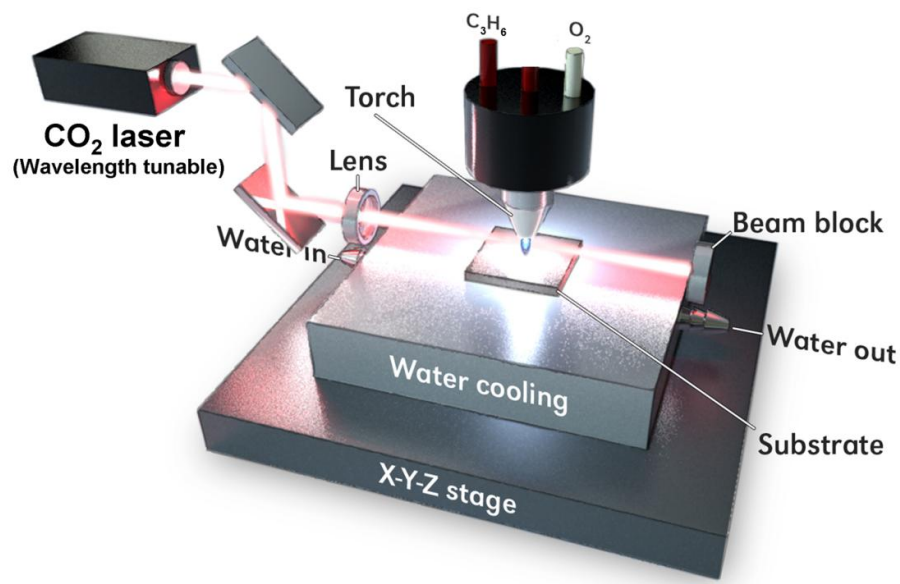
Figure 7.1 Schematic experimental setup for mode-selective excitations of propylene molecules in diamond deposition.
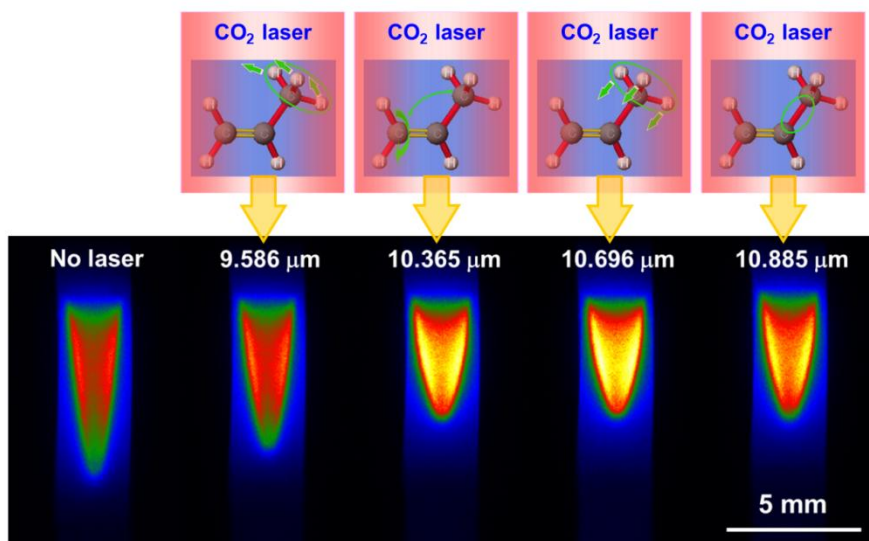
Figure 7.2 Optical images of the C_3H_6/O_2 flame without laser irradiation and with laser irradiations at four different wavelengths respectively related with excitations of CH_3 rocking mode (9.586 µm), a combination of C=C-C bending and C=CH₂ twisting modes (10.365 µm), CH_3 wagging mode (10.696 µm), and C-C stretching mode (10.885 µm). The related mode is shown above each flame.

7.2.2 Mode-selective reactions in diamond deposition

Diamond films were deposited with excitations of the four different vibrational modes, as well as without laser excitation. Experimental details are similar to those in Chapter 3. Besides the differences in laser wavelengths and incident laser powers, all other growth parameters, including substrate temperature, flame-to-nozzle distance, and deposition time, were all the same. Typical SEM micrographs of the diamond films are shown in Fig. 7.3. It is obviously observed that diamond growth is promoted by exciting the CH_3 rocking, the combination of C=C-C bending and $C=CH_2$ twisting, and the CH_3 wagging modes as indicated by increased diamond grain sizes. Astonishingly, excitation of the C-C stretching mode suppressed the diamond growth as manifested by smaller diamond grain sizes, shown in Fig. 7.3e. The differences are more obvious when comparing film thicknesses, as shown in Fig. 7.3f. Excitation of the C-C stretching mode suppressed the diamond film thickness to as small as 1~2 μm, while the excitations of all of the other three modes increased the thickness compared to the one deposited without laser excitation.
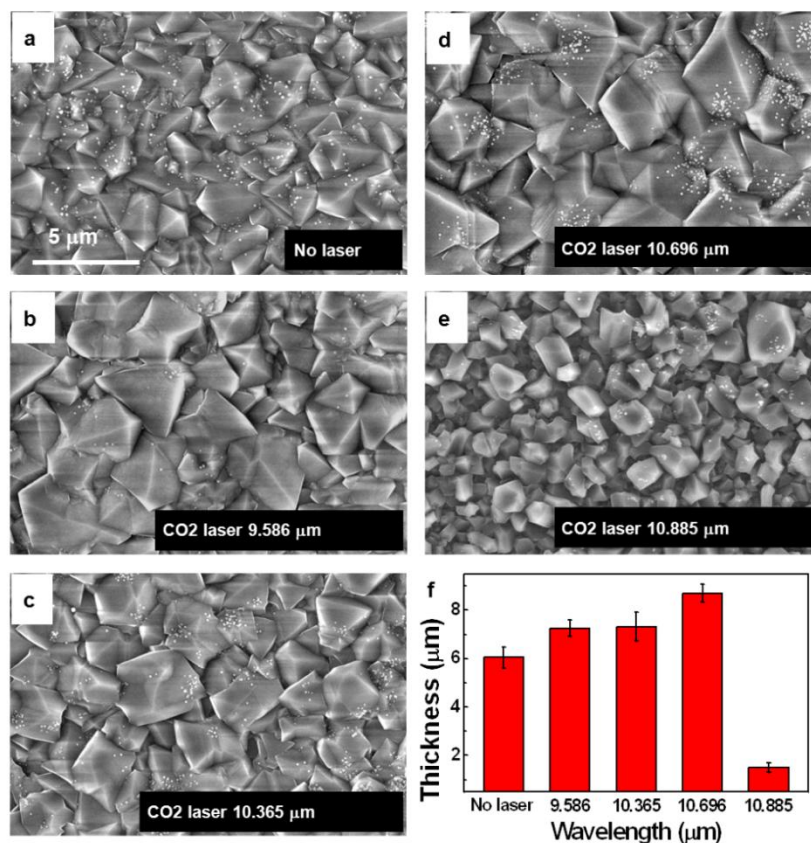
Figure 7.3 SEM images (a-e) and thicknesses (f) of diamond films deposited (a), without laser and with laser excitations of (b), CH$_3$ rocking mode (9.586 µm), (c), a combination of C=C-C bending and C=CH$_2$ twisting modes (10.365 µm), (d), CH$_3$ wagging mode (10.696 µm), and (e), C-C stretching mode (10.885 µm).

Raman spectra of the diamond films shown in Fig. 7.4 indicate differences in diamond phase purity. The diamond peak at 1338 cm^{-1} is higher and sharper for the films deposited with excitations of the CH$_3$ rocking, the combination of C=C-C bending and C=CH$_2$ twisting, and the CH$_3$ wagging modes. The non-diamond bands, including the D-band (around 1350 cm^{-1}), which is related to disordered carbon structures, and G-band (around 1530 cm^{-1}), which is related to the sp^2 graphite phase, are both suppressed, indicating higher purity of diamond phase in the films deposited under those three

conditions. However, the diamond film deposited with excitation of the C-C stretching mode shows poor phase purity, as indicated by its low diamond peak and relatively high D- and G-bands. The stronger background continuum indicates high photoluminescence of the diamond film, which means that there are more defects in the film deposited with excitation of the C-C stretching mode. The experimental results clearly demonstrate that mode-selective reactions through laser resonant excitations of different vibrational modes of the precursor molecules have a distinct impact on diamond growth.
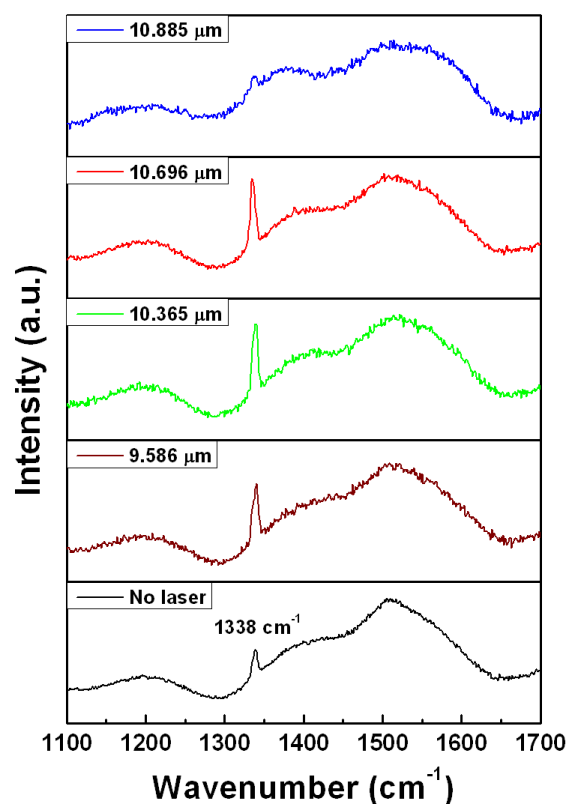
Figure 7.4 Raman spectra of diamond films deposited without laser and with laser excitations of CH$_3$ rocking mode (9.586 µm), a combination of C=C-C bending and C=CH$_2$ twisting modes (10.365 µm), CH$_3$ wagging mode (10.696 µm), and C-C stretching mode (10.885 µm).

7.2.3 Mechanism study using OES and MS

In order to understand the mechanisms, optical emission spectroscopy (OES) and mass spectrometry (MS) were performed to investigate the combustion flame under different excitation conditions. Experimental details are similar with those in previous chapters.

Figure 7.5 shows the OES spectra of the C_3H_6/O_2 flame without laser excitation and with laser excitations at different wavelengths, in which the emission peaks of C_2, CH, and OH radicals were detected. Intensities of each radical obtained under each of the five conditions were calculated by integrating related signals. The intensities of these three radicals in the flames irradiated by the CO_2 laser were compared with those in the flame without laser irradiation. The ratios are shown in Fig. 7.5b. Under all of the four laser-involved conditions, the concentrations of the C_2, CH, and OH radicals were increased. However, in the C-C stretching excitation, the increase in the C_2 and CH concentrations is much lower than those in the other three excitations. On the other hand, concentration of the OH concentration is higher in the C-C stretching excitation than in the other three excitations. This is in agreement with the fact that OH plays an important etching role in the combustion flame deposition of diamond [12, 13]. Diamond growth is a balance between attaching carbon-containing species on the diamond growth surface and etching of non-carbon atoms or structures. Over-populated etching species, such as OH, results in over-etching of the growth surface, leading to suppressed diamond growth.

Besides C_2, CH, and OH, there are many more species in the combustion flame. Mass spectrometry was applied to explore more details of the reactions. Combustion flame itself is an ionization source in which most of the species have a portion of ions [14]. This makes MS a suitable approach for real-time analysis of the combustion flame.
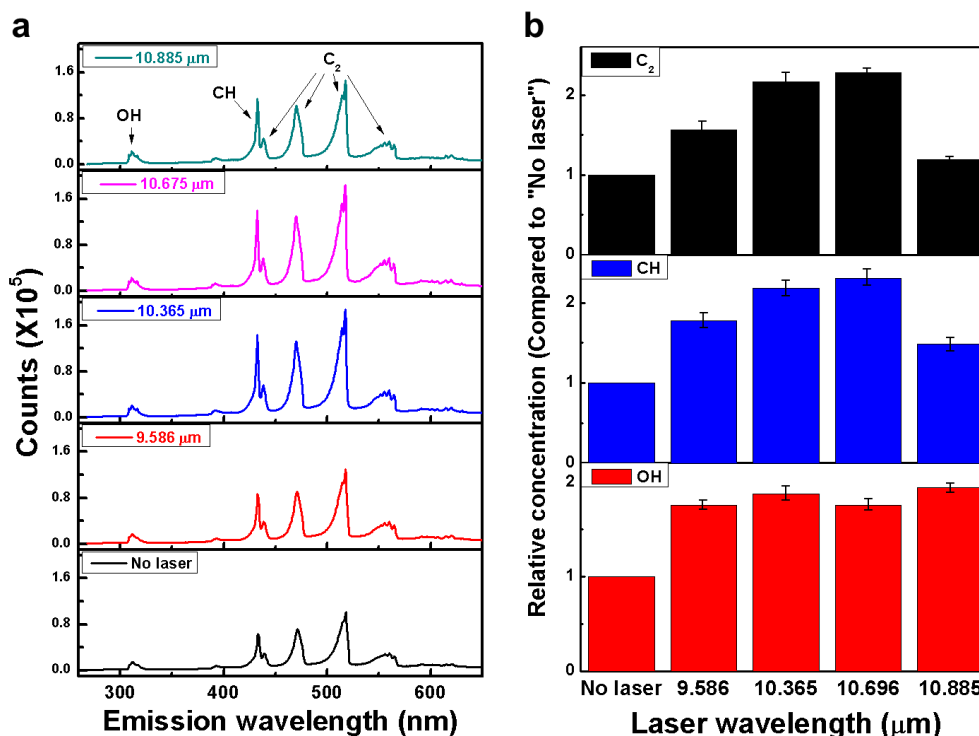
Figure 7.5 Optical emission spectroscopy of the C_3H_6/O_2 flame. (a), Optical emission spectra of the flame without laser irradiation and with laser irradiations at 9.586, 10.365, 10.696 and 10.885 µm. The peaks in each spectrum are respectively assigned to OH, CH and C_2 radicals; (b), Relative concentrations of OH, CH, and C_2 radicals in each flame. The value of each column is the ratio of the radical concentration in the laser irradiated conditions over that in the no-laser condition.

Figure 7.6 shows a chromatograph of the C_3H_6/O_2 flame without laser irradiation and with laser irradiations at the four wavelengths. Examples of the positive mass spectra with and without laser excitation at 10.696 μm are given in Fig. 7.7. $C_xH_yO_z$ (x = 0~12, y = 0~12, z = 0~3) ions with m/z values ranging from 12 to 150 were detected. Considering differences in ionization potential among different species, the height of each line does not necessarily represent the exact concentration of each species. Nevertheless, MS analysis of the flame is valuable in determining the evolvement of species concentration under different excitation conditions, given that the variation of ions is proportional to the variation of related species.
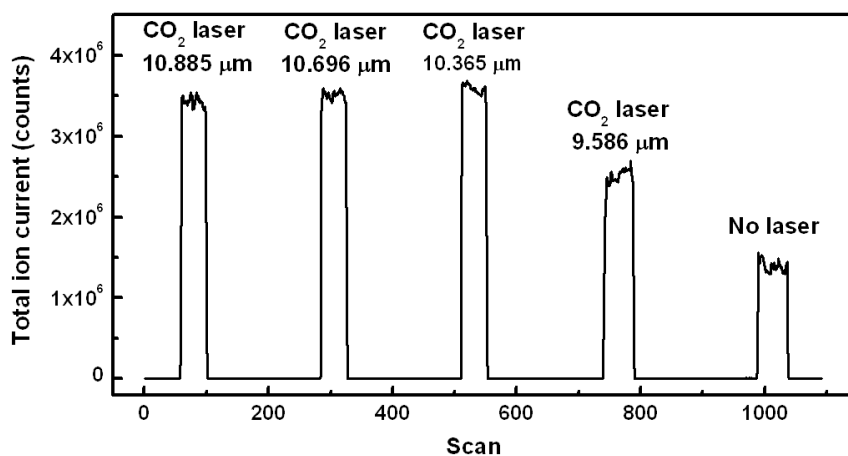
Figure 7.6 Chromatograph of the flame when irradiated by the CO_2 laser at 10.885, 10.696, 10.365, and 9.586 μm, and without laser irradiation.
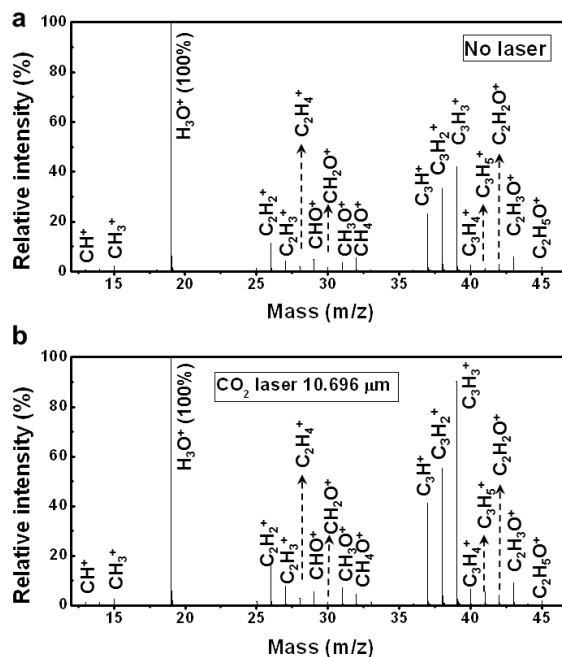
Figure 7.7 Mass spectrum of the flame (a), without laser irradiation and (b), with laser irradiation at 10.696 μm.

The C_3H_6/O_2 combustion flame is a complicated chemical reaction involving a number of bond cleavages and rearrangements, among which the C-C single bond cleavage is a favorable reaction coordinate [15]. Directly depositing energy on the C-C stretching mode is more efficient in exciting the molecules to their transition states and in driving the chemical reactions. Consumption of oxygen will, therefore, be less. The promoted C-C bond breaking and decreased oxygen consumption are both confirmed by comparing the evolvement of concentrations of the CH_3^+, $C_2H_3^+$ (direct product of the C-C single bond breaking), and O_2^- ions, as shown in Fig. 7.8. The increase of CH_3 and C_2H_3 concentrations by excitation of the C-C stretching mode, as shown in Fig. 7.8a, is much higher than that by excitation of all of the other three modes, indicating a high

efficiency when directly coupling laser energy to the bond that relates to the reaction coordinate. The lower consumption of O_2 in the excitation of the C-C stretching mode results in higher concentration of O_2 molecules, as indicated by a higher concentration of O_2^- ions in Fig. 7.8b. More O_2^- ions result in more O^- and OH^- ions, as shown in Fig. 7.8c. All three species play roles in etching [16], resulting in over-etching of the diamond growth surface, and leading to the suppressed diamond growth. It should be pointed out that the normalized concentration of each species in Fig. 7.8 is the "ratio" of that species in each spectrum, which does not reflect the exact concentration of the species in the flame. This is different from that of the OES spectrum, in which the emission intensity is determined by the "amount" of each species. This explains why the evolvement of the OH species under different excitation conditions looks different in the OES and MS analyses.

When the CH_3 wagging (v_{12}) mode was excited, little energy was channeled to the C-C breaking coordinate. Most of the energy deposited on this mode is conserved in the CH_3 radicals, resulting in vibrationally excited CH_3 products [5, 17]. The vibrationally excited CH_3 radicals have lower energy potential for further reactions, making them easier to react with other species. The concentration of the CH_3 species is, hence, lowered in the flame with excitation of the CH_3 wagging mode, as demonstrated in Fig. 7.8d. This phenomenon is in good agreement with the study by Killelea *et al.* [5] and Yan *et al.* [17]. It has been demonstrated in both reports that excitation localized in the reactive bond (reaction coordinate) promotes transition state access and bond cleavage, whereas

excitation in the vibrations of nonreactive (spectator) bonds correlates with excitation of reaction products. The excitation of the combination of C=C-C bending and C=CH$_2$ twisting modes (at 10.365 μm) involves too many bonds and motions; the CH$_3$ rocking mode (at 9.586 μm) is less IR active. Both excitation conditions lead to more complicated results which need further investigation.
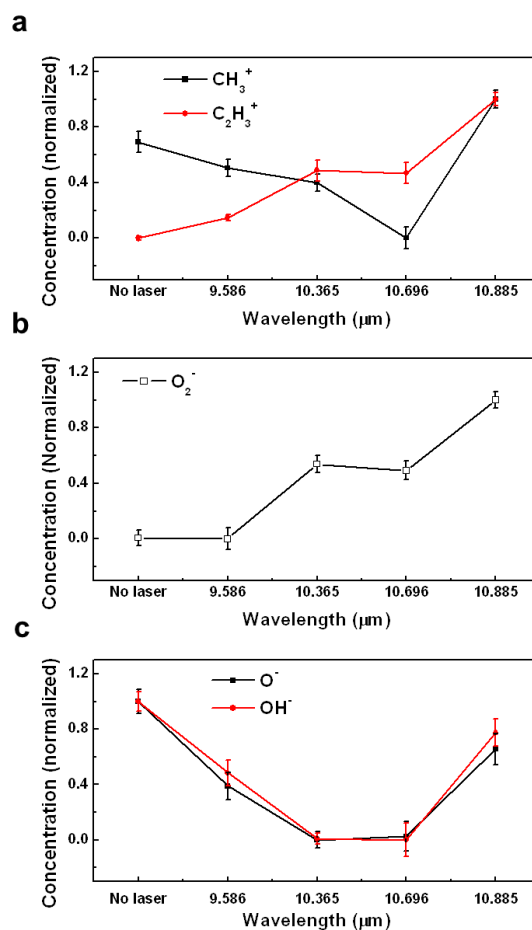
Figure 7.8 Concentration of (a) CH$_3^+$, C$_2$H$_3^+$, (b) O$_2^+$, and (c) O$^-$ and OH$^-$ ions in the flame and their evolvement under different laser irradiation conditions. The concentrations were all normalized. Error bars indicate standard deviations of each ion concentration.

7.3 Conclusions

We studied mode-selective reactions in diamond growth through laser resonant vibrational excitations of precursor molecules using a wavelength-tunable CO_2 laser. It was proved that excitation of the vibrational mode toward the reaction coordinate promotes transition state access and bond cleavage, but this also results in over-populated etching species which suppressed the diamond growth. Excitations of the modes not directly related to the reaction coordinate result in vibrationally excited reaction products, leading to formation of beneficial species for diamond growth. This research is helpful in establishing the active intervention in control of chemical reactions, which opens up a new avenue for mode-selective reactions in material synthesis through laser resonant vibrational excitations.

References

[1]. Crim, F. F., "Making Energy Count", Science **317,** 1707 (2007).

[2]. Potter, E. D., Herek, J. L., Pedersen, S., Liu, Q., and Zewail, A. H., "Femtosecond laser control of a chemical reaction", Nature **355,** 66 (1992).

[3]. Bechtel, H. A., Kim, Z. H., Camden, J. P., and Zare, R. N., "Bond and mode selectivity in the reaction of atomic chlorine with vibrationally excited CH_2D_2", Journal of Chemical Physics **120,** 791 (2004).

[4]. Zhang, W. Q., Kawamata, H., and Liu, K. P., "CH stretching excitation in the early barrier F + CHD_3 reaction inhibits CH bond cleavage", Science 325, 303 (2009).

[5]. Killelea, D. R., Campbell, V. L. Shuman, N. S. and Utz, A. L., "Bond-Selective Control of a Heterogeneously Catalyzed Reaction", Science **319,** 790 (2008).

[6]. Zare, R. N., "Laser Control of Chemical Reactions", Science **279,** 1875 (1998).

[7]. Butler, J. E. and Oleynik, I. "A mechanism for crystal twinning in the growth of diamond by chemical vapour deposition", Philosophical Transactions of the Royal Society A **366,** 295 (2008).

[8]. Xie, Z. Q., Zhou, Y. S., He, X. N., Gao, Y., Park, J. B., Ling, H., and Lu, Y. F., "Fast Growth of Diamond Crystals in Open Air by Combustion Synthesis with Resonant Laser Energy Coupling", Crystal Growth & Design **10,** 1762 (2010).

[9]. Xie, Z. Q., He, X. N., Hu, W., Guillemet, T., Park, J. B., Zhou, Y. S., Bai, J., Gao, Y., Zeng, X. C., Jiang, L., and Lu, Y. F., "Excitations of precursor molecules by different laser powers in laser-assisted growth of diamond films", Crystal Growth & Design **10,** 4928 (2010).

[10]. Chao, J. and Zwolinski, B. J., ""Ideal gas thermodynamic properties of ethylene and

propylene", Journal of Physical Chemistry Ref. Data **4,** 251 (1975).

[11]. Lord, R. C. and Venkateswarlu, P., "The Infrared Spectra of Propylene and Propylene-d_6",
Journal of Optical Society of America **43,** 1079 (1953).

[12]. Komaki, K., Yanagisawa, M., Yamamoto, I., and Hirose, Y., "Synthesis of Diamond
in Combustion Flame under Low Pressures", Japanese Journal of Applied Physics
32, 1814 (1993).

[13]. Miller, J. A. and Melius, C. F., "Kinetic and thermodynamic issues in the formation
of aromatic compounds in flames of aliphatic fuels", Combustion and Flame **91,** 21
(1992).

[14]. Gaydon, A. G. and Wolfhard, H. G., Flames: Their Structure, Radiation and
Temperature (Fourth edition) Ch. 13, Chapman and Hall, London (1979).

[15]. DeBoer, G. D. and Dodd, J. A., "Ab Initio Energies and Product Branching Ratios
for the O + C_3H_6 Reaction", Journal of Physical Chemistry A 111, 12977 (2007).

[16]. Asmussen, J. and Reinhard, D. K., Diamond Films Handbook Ch. 4 (Marcel
Dekker, New York, NY (2002).

[17]. Yan, S., Wu, Y. T., Zhang, B., Yue, X. F., and Liu, K. "Do vibrational excitations
of CHD_3 preferentially promote reactivity toward the chlorine atom?", Science 316,
1723 (2007).

CHAPTER 8

Summary of Current Work and Suggested Future Directions

8.1 Summary of current work

8.2 Suggested future directions: synthesis of gallium nitride through resonant excitation of ammonia (NH$_3$)

   8.2.1 Similarities between NH$_3$ and C$_2$H$_4$ molecules in laser-induced vibrational resonant excitations

   8.2.2 Resonant excitation of ammonia molecules for synthesis of GaN

8.1 Summary of current work

Laser-induced multi-energy processing (MEP) introduces resonant vibrational excitations of precursor molecules to conventional chemical vapor deposition for material synthesis. In this study, efforts were extended to explore the capability of resonant vibrational excitations for promotion of energy efficiency in chemical reactions, for enhancement of diamond deposition, and for control of chemical reactions through mode-selective vibrational excitations. A novel synthetic process was developed to grow diamond films and crystals in open air using laser-assisted MEP through laser resonant vibrational excitations and defy the traditional difficulties in diamond growth. The research project mainly focused on resonant vibrational excitations of ethylene (C_2H_4) and propylene (C_3H_6) precursor molecules using lasers in combustion flame deposition of diamond, which led to: 1) promotion of efficiency of chemical reactions; 2) enhancement of diamond growth with higher growth rate and better crystallization; 3) steering of chemical reactions which lead to preferential growth of {100}-oriented diamond films and crystals; and 4) mode-selective control of chemical reactions through selective excitations of different vibrational modes.

Vibrational resonant excitation of the C_2H_4 precursor molecules was achieved using a wavelength-tunable CO_2 laser in combustion flame CVD of diamond films. The CVD processes were accelerated due to the stronger laser energy coupling with the C_2H_4 molecules. Compared with the common CO_2 laser at 10.591 μm, the laser wavelength of

10.532 μm is much more effective to excite the C_2H_4 molecules through the CH_2 wagging vibration mode. Diamond films deposited with the tunable laser excitation have larger grain size, better crystallinity, and faster growth rate than those without laser excitation. Under the laser irradiation of 800 W at the wavelength of 10.532 μm, the diamond grain size and film thickness increased by 200~300% and 160%, respectively. Besides the increases in grain size and film thickness, the crystallization of diamond structure was also enhanced in the film.

Fast growth of diamond crystals on Si substrates was achieved in open air through laser-assisted MEP by resonantly exciting ethylene molecules. High-quality diamond crystals up to 5 mm in length and 1 mm in diameter were obtained. A high diamond growth rate up to 139 μm/hr was achieved on a silicon substrate. Optical emission spectra of the flame with and without laser irradiation indicate that the laser-induced vibrational excitation enhances the reaction and increases the active radicals in the flame, which result in the fast growth of high-quality diamond crystals.

Resonant excitation of precursor molecules using different laser power densities in laser-assisted growth of diamond was studied to modify diamond surface morphology, obtain high diamond crystal quality, and high energy coupling efficiency. At a laser power density range of $5.0 \times 10^3 \sim 1.0 \times 10^4$ W/cm^2, {100}-oriented diamond crystals were grown in the deposited diamond films. According to the Raman spectroscopy of the diamond films deposited with laser excitations at different incident laser powers, best diamond qualities could be obtained when the incident power density was in a range of

$5.0 \times 10^3 \sim 6.7 \times 10^3$ W/cm^2. The increment rates of diamond film thicknesses indicate that the highest efficiency of laser energy coupling could be achieved in a range of $5.0 \times 10^3 \sim 6.7 \times 10^3$ W/cm^2. This study provides understanding of the laser-assisted MEP in certain details, and suggests further investigation directions in mechanisms of vibrational excitations and preferential growth of {100}-oriented diamond.

Efforts were extended to grow {100}-oriented diamond films and single crystals through resonant vibrational excitation of precursor molecules, and to understand the mechanisms for the preferential growth of the {100}-oriented diamond. The CO_2 laser which was tuned to 10.22 μm excited the ethylene molecules to a higher vibrational state with higher rotational energy in the combustion flame, which increased the relative concentrations of the oxides of carbon hydride species (CH_xO and C_2H_xO species in special). Theoretical simulations of the reaction pathway indicates that these species react more easily with diamond {111} surfaces than with {100} surfaces, leading to a fast growth of the {111} surface of diamond and resulting in {100}-oriented diamond. This finding opens up a new avenue for controlled chemical vapor deposition of crystals through resonant vibrational excitation of precursor molecules.

Mode-selective reactions in diamond growth through laser resonant vibrational excitations of propylene (C_3H_6) molecules were studied using a wavelength-tunable CO_2 laser. It was proved that excitation of the vibrational mode toward the reaction coordinate promotes transition state access and bond cleavage, but this also results in over-populated

etching species which suppressed the diamond growth. Excitations of the modes not directly related to the reaction coordinate result in vibrationally excited reaction products, leading to formation of beneficial species for diamond growth. This research is helpful in establishing the active intervention in control of chemical reactions, which suggests a new paradigm for mode-selective reaction control in material synthesis through laser resonant vibrational excitations.

8.2 Suggested future directions: synthesis of gallium nitride through resonant excitation of ammonia (NH_3)

8.2.1 Similarities between NH_3 and C_2H_4 molecules in laser-induced resonant vibrational excitations.

Similar to C_2H_4, NH_3 is another molecule that has high absorption coefficient of CO_2 laser energy through vibrational resonant excitations. The umbrella mode (v_2, symmetric N-H bending) of NH_3 has split energy levels at 932.51 cm^{-1} (10.724 μm) and 968.32 cm^{-1} (10.324 μm) [1]. Both frequencies match well with the CO_2 laser wavelengths of 10.719 μm and 10.333 μm. The absorption coefficients of NH_3 [2] and C_2H_4 gases at the CO_2 laser emission band 00^o1-01^o0 are shown in Fig. 8.1. The two absorption peaks for NH_3 at around 10.724 and 10.324 μm are very obvious, similar to that for C_2H_4 at 10.532 μm (v_2, CH_2 wagging). It is believed that by tuning the laser to both matching wavelengths and irradiating the reacting NH_3 gas in the chemical reactions, NH_3 molecules would be resonantly excited and the reactions would be promoted. This has a potential significance in materials synthesis because ammonia is a major nitrogen source for synthesis of nitride materials, such as gallium nitride (GaN).
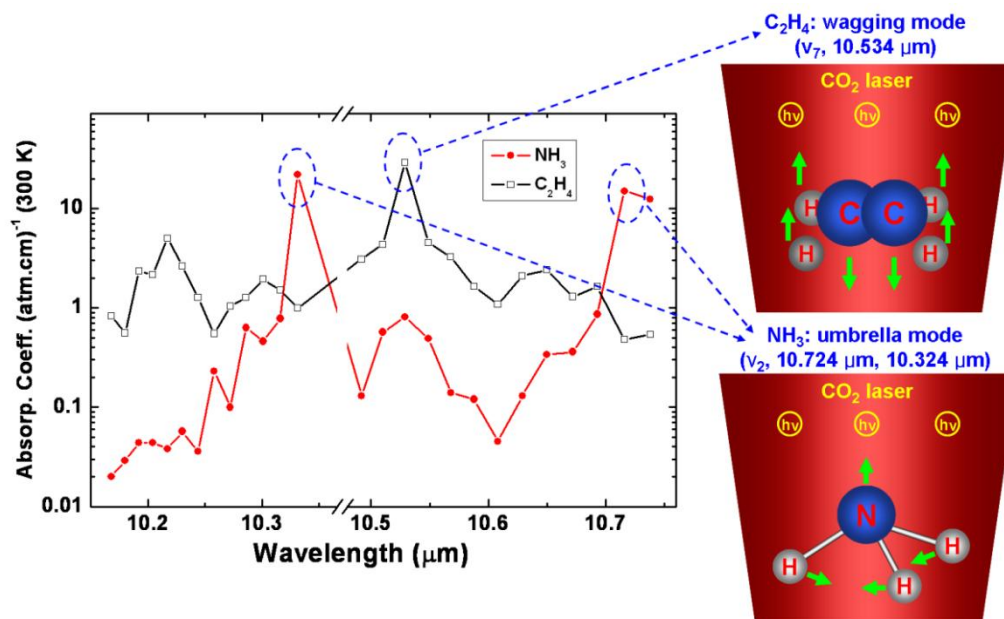
Figure 8.1 Absorption coefficients of NH_3 and C_2H_4 gases at the CO_2 laser 00^o1-10^o0 emission band and their corresponding vibrational modes.

8.2.2 Resonant excitation of ammonia molecules for synthesis of GaN.

Gallium nitride (GaN) is a promising semiconductor material, especially in areas where conventional semiconductors cannot be used. The unique properties of GaN have found widespread applications. First, its wide, direct band gap (3.4 eV) enables short-wavelength light emission, which makes full-color display, high-density digital storage and energy-efficient lighting feasible [3-5]. Second, the strong bond strength of GaN makes it very competitive in high-power/high-temperature applications, such as advanced power distribution, electric vehicles, and avionics [6-8]. Since GaN cannot be grown from its stoichiometric melt by the Czochralski or Bridgman methods commonly used for typical semiconductors, numerous efforts have been made to create low-pressure

epitaxy of GaN. Metalorganic vapor phase epitaxy (MOVPE) [9-11], hydride vapor phase epitaxy (HVPE) [12-14], and molecular beam epitaxy (MBE) [15-17] have been successful in synthesizing GaN epilayers.

A common difficulty in synthesis of GaN is the low decomposition efficiency of ammonia (NH_3), which is the predominant nitrogen source for all of the synthesis methods. Hence, a high temperature substrate is needed for pyrolysis of NH_3 [16, 18], which in turn results in a large density of defects in GaN epilayers as well as substrate warp caused by differences of thermal expansion coefficients between GaN epilayers and substrates [19]. The high substrate temperature also obstructs GaN from being incorporated in low-temperature applications, such as organic optoelectronics [4, 5]. To address this critical issue, laser-assisted metalorganic vapor phase epitaxy (L-MOVPE) is suggested to promote the dissociation of NH_3 molecules using the wavelength-tunable CO_2 laser, as shown in Fig. 8.2. It is anticipated that with the suggested technique, one vibrational mode of the NH_3 molecule can be resonantly excited. Dissociation of N-H bonds will, therefore, be promoted; and related chemical reactions will be enhanced, enabling us to grow GaN epilayers with much lower substrate temperatures.
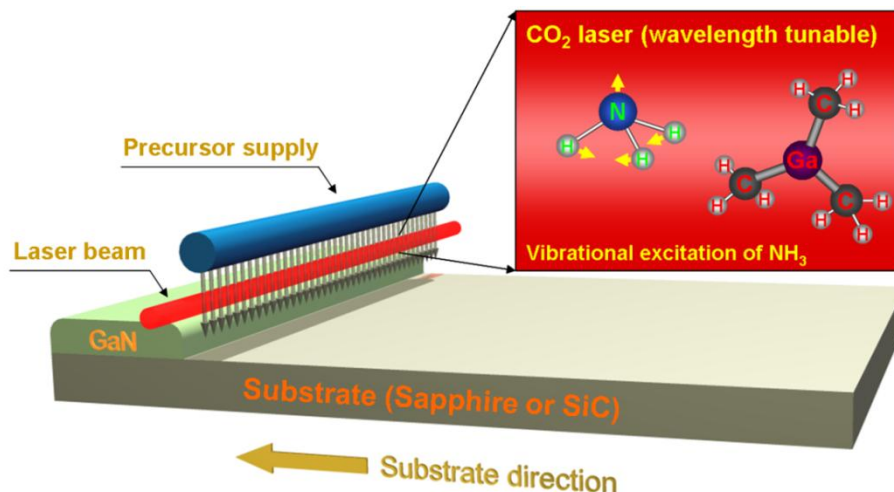
Figure 8.2 Resonant excitation of NH_3 molecules and lateral epitaxy of GaN film.

Laser energy is absorbed by NH_3 molecules through resonant excitation of the umbrella mode (v_2, symmetric N-H bending) of NH_3 [20], as shown in Fig. 8.1. By tuning the CO_2 laser emission wavelength, highly efficient coupling of laser energy and excitation of the NH_3 molecules will be achieved. The CO_2 laser emission wavelength will be tuned to either 10.333 or 10.719 μm to efficiently excite the NH_3 molecules. With this wavelength tunability to achieve high-efficiency excitation of NH_3 molecules, dissociation of the N-H bonds will be significantly promoted. Different from traditional MOVPE processes which rely on substrate heating for the dissociation of N-H bonds, this method requires much less energy from the substrate; and, hence, the substrate temperature will be maintained at much lower levels. Like the enhancement of diamond growth with resonant excitation of C_2H_4 molecules, resonant excitation of NH_3 molecules is expected to promote the epitaxy of GaN. It should also be pointed out that both the TMGa precursor and the main byproduct of the reaction, CH_4, have no resonant

wavelength within the tunable range of the CO_2 laser. As a result, the laser irradiation will have no significant effect on these two molecules, and hence no extra byproduct will be introduced by the laser irradiation.
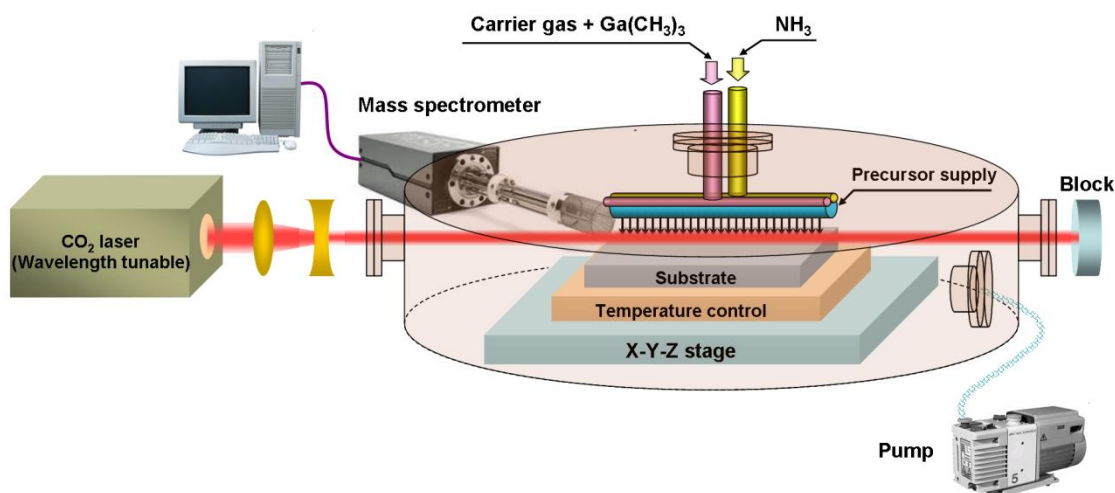
Figure 8.3 Schematic diagram of the experimental setup for L-MOVPE of GaN epilayers.

The wavelength-tunable CO_2 laser plays important roles in promoting chemical reactions through resonant excitation of NH_3 molecules. As a first step, resonant vibrational excitation of NH_3 will be investigated through experimental efforts. A schematic diagram of the experimental setup is shown in Fig. 8.3. A wavelength-tunable kilowatt CO_2 laser will be used to resonantly excite NH_3 molecules. Two parameters of the laser, including beam diameter and laser power, will be adjusted in order to vary laser energy density for optimal conditions of excitation. Shape and diameter of the laser beam will be adjusted by a series of antireflective-coated zinc selenide (ZnSe) lenses.

Precursors of NH_3 and $Ga(CH_3)_3$ (TMGa) carried by nitrogen (N_2) gas will be introduced into a vacuum chamber after evacuation. The gas flow rate will be controlled by mass-flow controllers. The pressure in the chamber will be controlled by pressure controllers. The vacuum chamber has a ZnSe window to introduce the CO_2 laser beam into the gas flow, and another ZnSe window will allow extra laser energy to be dissipated outside of the chamber. Both windows will be cooled and purged with N_2 gas to avoid thermal damage, fogging, or residual deposition due to the high power of the CO_2 laser.

References

[1] McBride, J. O. P. and Nicholls, R. W., "The vibration-rotation spectrum of ammonia gas. I", Journal of Physics B **5,** 408 (1972).

[2] Patty, R. R., Russwurm, G. M., McClenny, W. A., and Morgan, D. R., "Carbon dioxide laser absorption coefficients for determining ambient levels of O_3, NH_3, and C_2H_4", Applied Optics **13**, 285 (1974).

[3] Landwehr, G., Waag, A., Fischer, F., Lugauer, H. J., and Schüll, K., "Blue emitting heterostructure laser diodes", Physica E **3,** 158 (1998).

[4] Kim, H., Dang, C., Song, Y. K., Zhang, Q., Patterson, W., Nurmikko, A. V., Kim, K. K., Song, S. Y., and Han, J., "Nitride-organic semiconductor hybrid heterostructures for optoelectronic devices", Physica Status Solidi (S) **4,** 2411 (2007).

[5] Wu, M., Gong, Z., Kuehne, A. J. C., Kanibolotsky, A. L., Chen, Y. J., Perepichka, I. F., Mackintosh, A. R., Gu, E., Skabara, P. J., Pethrick, R. A., and Dawson, M. D., "Hybrid GaN-organic microstructured light-emitting devices via ink-jet printing", Optical Express **17,** 16436 (2009).

[6] Asif Khan, M., Kuznia, J. N., Olson, D. T., Schaff, W. J., Burm, J. W., and Shur, M. S., "Microwave performance of a 0.25 pm gate AIGaN/GaN heterostructure field effect transistor", Applied Physics Letters **65,** 1121 (1994).

[7] Jain, S. C., Willander, M., Narayan, J., and Van Overstraeten, R., "III–nitrides: Growth, characterization, and properties", Journal of Applied Physics **87,** 965 (2000).

[8] Pearton, S. J., Abernathy, C. R., and Ren, F., Gallium nitride processing for electronics, sensors and spintronics, Springer London (2006).

[9] Nakamura, S., Harada, Y., and Seno, M., "Novel metalorganic chemical vapor

deposition system for GaN growth", Applied Physics Letters **58,** 2021 (1991).

[10] Paszkiewicz, R., Paszkiewicz, B., Korbutowicz, R., Kozlowski, J., Tlaczala, M., Bryja, L., Kudrawuec, R., and Misiewicz, J., "MOVPE GaN grown on alternative substrates", Crystal Research and Crystal Technology, **36,** 971 (2001).

[11] Ravash, R., Bläsing, J., Hempel, T., Noltemeyer, M., Dadgar, A., Christen, J., and Krost, A., "Metal organic vapor phase epitaxy growth of single crystalline GaN on planar Si(211) substrates", Applied Physics Letters **95,** 242101 (2009).

[12] Usui, A., Sunakawa, H., Sakai, A., and Yamaguchi, A. A., "Thick GaN epitaxial growth with low dislocation density by hydride vapor phase epitaxy", Japanese Journal of Applied Physics **36,** L899 (1997).

[13] Larsson, H., Gogova1, D., Kasic1, A., Yakimova, R., Monemarl, B., Miskys, C. R., and Stutzmann, M., "Free-standing HVPE-GaN layers", Physica Status Solidi (C) **7,** 1985 (2003).

[14] Kwon, H. Y., Moon, J. Y., Choi, Y. J., Shin, M. J., Ahn, H. S., Yang, M., Chang, J. H., Yi, S. N., and Ha, D. H., "Initial growth behaviors of GaN layers overgrown by HVPE on one-dimensional nanostructures", Materials Science and Engineering B **166,** 28 (2010).

[15] Kim, W., Aktas, O., Botchkarev, A.E., Salvador, A., Mohammad, S. N., and Morkoc, H., "Reactive molecular beam epitaxy of wurtzite GaN-Materials characteristics and growth kinetic", Journal of Applied Physics **79,** 7657 (1996).

[16] Mesrine, M., Grandjean, N., and Massies, J., "Efficiency of NH_3 as nitrogen source for GaN molecular beam epitaxy", Applied Physics Letters **72,** 350 (1998).

[17] Santhakumar, K., Kim, D. W., Song, H., Jang, E. S., Lee, S. H., and Lee, C. R.,

"Growth and characterization of GaN nano-columns grown on gallium-coated Si (111) by using molecular beam epitaxy", Journal of Korean Physical Society **54,** 190 (2009).

[18] Krukowski, S., Kempisty, P., and Strąk, P., "Review: GaN growth by ammonia based methods - density functional theory study", Crystal Research and Crystal Technology **44,** 1038 (2009).

[19] Feng, Z. C., III-nitride semiconductor materials, Imperial College Press, London (2006).

[20] Gatti, F., Iung, C., Leforestier, C., and Chapuisat, X., "Fully coupled 6D calculations of the ammonia vibration-inversion-tunneling states with a split Hamiltonian pseudospectral approach", Journal of Chemical Physics **111**, 7236 (1999).

LIST OF PUBLICATIONS

Journal papers

1. **Z.Q. Xie,** J. Bai, Y.S. Zhou, Y. Gao, J.B. Park, T. Guillemet, L. Jiang, X.C. Zeng, and Y.F. Lu. "Control of crystallographic orientation in diamond synthesis through laser resonant vibrational excitation of precursor molecules". (submitted)

2. **Z.Q. Xie,** Y.S. Zhou, X.N. He, Y.Gao, T.Guillemet, J.B. Park, M.M. Wang, L. Jiang, and Y.F. Lu "Mode-selective reactions in chemical vapor deposition of diamond through laser vibrational excitations". (in preparation)

3. **Z.Q. Xie,** X.N. He, W. Hu, T. Guillemet, J.B. Park, Y.S. Zhou, J. Bai, Y. Gao, X.C. Zeng, L. Jiang, and Y.F. Lu. "Excitations of precursor molecules by different laser powers in laser-assisted growth of diamond films". *Crystal Growth & Design* 10, 4928–4933 (2010).

4. **Z.Q. Xie,** Y.S. Zhou, X.N. He, Y. Gao, J.B. Park, H. Ling, L. Jiang, and Y.F. Lu. "Fast growth of diamond crystals in open air by combustion synthesis with resonant laser energy coupling". *Crystal Growth & Design* 10, 1762-1766 (2010).

5. X.N. He, **Z.Q. Xie**, Y. Gao, W. Hu, L.B. Guo, L. Jiang, and Y.F. Lu, "Mass spectrometry of solid samples in open air using combined laser ionization and ambient metastable ionization", Spectrochimica. Acta Part B: Atomic Spectroscopy 67, 64-73 (2012).

145

6. M. Mahjouri-Samani, Y. S. Zhou, W. Xiong, **Z. Q. Xie,** L. Jiang, and Y. F. Lu. "Alternating-diameter carbon nanotubes grown by periodic variation of temperature in laser-assisted chemical vapor deposition". (submitted)

7. J.B. Park, W. Xiong, **Z.Q. Xie,** Y. Gao, M. Qian, M. Mitchell, M. Mahjouri-Samani, Y.S. Zhou, L. Jiang, and Y.F. Lu, "Transparent interconnections formed by rapid single-step fabrication of graphene patterns", *Applied Physics Letters* 99, 053103 (2011).

8. T. Guillemet, **Z.Q. Xie,** Y.S. Zhou, J.B. Park, A. Veillere, W. Xiong, J.M. Heintz, J.F. Silvain, N. Chandra, and Y.F. Lu. "Stress and Phase Purity Analyses of Diamond Films Deposited through Laser-Assisted Combustion Synthesis". *Applied Materials and Interfaces* 3, 4120-4125 (2011).

9. A. Veillère, T. Guillemet, **Z.Q. Xie,** C.A. Zuhlke, D.R. Alexander, J.F. Silvain, J.M. Heintz, N. Chandra, and Y.F. Lu. "Influence of WC-Co substrate pretreatment on diamond film deposition by laser-assisted combustion synthesis". *Applied Materials and Interfaces* 3, 1134-1139 (2011).

10. Y. Gao, Y.S. Zhou, M. Qian, **Z.Q. Xie,** H.F. Luo, L. Jiang, and Y.F. Lu. "Fast Growth of Branched Nickel Monosilicide Nanowires by Laser-Assisted Chemical Vapor Deposition". *Nanotechnology* 22, 235602 (2011).

11. J.B. Park, W. Xiong, Y. Gao, M. Qian, **Z.Q. Xie,** M. Mitchell, Y.S. Zhou, L. Jiang, and Y.F. Lu. "Fast growth of graphene patterns by laser direct writing". *Applied*

Physics Letters 98, 123109 (2011).

12. T. McKindra, M. J. O'Keefe**, Z.Q. Xie,** and Y.F. Lu. "Characterization of diamond thin films deposited by a CO_2 laser-assisted combustion-flame method". *Materials Characterization* 61, 661-667 (2010).

13. X.N. He, X.K. Shen, T. Gebre, **Z.Q. Xie,** L. Jiang, and Y.F. Lu. "Spectroscopic determination of rotational temperature in $C_2H_4/C_2H_2/O_2$ flames for diamond growth with and without tunable CO_2 laser excitation". *Applied Optics* 49, 1555-1562 (2010).

14. H. Ling, **Z.Q. Xie,** Y. Gao, T. Gebre, X.K. Shen, and Y.F. Lu. "Enhanced chemical vapor deposition of diamond by wavelength-matched vibrational excitations of ethylene molecules using tunable CO_2 laser". J*ournal of Applied Physics* 105, 064901 (2009).

15. X.K. Shen, H. Wang, **Z.Q. Xie,** Y. Gao, H. Ling, and Y.F. Lu. "Detection of trace phosphorus in steel using laser-induced breakdown spectroscopy combined with laser-induced fluorescence". *Applied Optics* 48, 2551-2558 (2009).

16. H. Ling, J. Sun, Y.X. Han, T. Gebre, **Z.Q. Xie,** M. Zhao, and Y.F. Lu. "Laser-induced resonant excitation of ethylene molecules in $C_2H_4/C_2H_2/O_2$ reactions to enhance diamond deposition". *Journal of Applied Physics* 105, 014901 (2009).

Conference papers

1. **Z.Q. Xie,** X.N. He, W. Hu, Y. Gao, T. Guillemet, J.B. Park, Y.S. Zhou, and Y.F. Lu. "Laser-Power-Resolved Excitations of Ethylene Molecules in Laser-Assisted Synthesis of Diamond Films". *Proceedings of ICALEO* N205 (2011).

2. **Z.Q. Xie,** Y.S. Zhou, X.N. He, Y. Gao, J. B. Park, T. Guillemet, and Y.F. Lu. "Laser-assisted synthesis of diamond crystals in open air through vibrational excitation of precursor molecules". *Proceedings of Photonics West* 7921-8 (2011).

3. **Z.Q. Xie,** X.N. He, Y. Gao, Y.S. Zhou, J.B. Park, T. Guillemet, and Y.F. Lu. "Laser-induced resonant vibrational excitation of precursor molecules in multi-energy processing for diamond synthesis". *Proceedings of ICALEO* P154 (2010).

4. **Z.Q. Xie,** J.B. Park, X.N. He, Y. Gao, Y.S. Zhou, and Y.F. Lu. "Resonant excitation of ethylene molecules in the combustion flame CVD of diamond using a wavelength tunable CO_2 laser". *Proceedings of Photonics West* 7585-8 (2010).

5. **Z.Q. Xie,** J.B. Park, X.N. He, Y. Gao, T. Guillemet, Y.S. Zhou, and Y.F. Lu. "Laser Resonant Vibrational Excitations of Precursor Molecules in Multi-Energy Processing for Diamond Synthesis". 47th Annual Technical Meeting of Society of Engineering Science (2010).

6. **Z.Q. Xie,** H. Ling, Y.X. Han, X.K. Shen, T. Gebre, and Y.F. Lu. "CO_2 laser resonant excitation of precursor molecules in diamond deposition using combustion-flame method". *Proceedings of ICALEO* M704 (2008).

7. X. N. He, L. B. Guo, **Z. Q. Xie**, X. Huang, W. Hu, X. Y. Zeng and Y. F. Lu, "Laser-induced breakdown spectroscopy with improved spectral resolutions through the generation of high-temperature and low-density plasmas", Proc. SPIE 8244, 82440H (2012)

8. X.N. He, **Z.Q. Xie,** Y.S. Zhou, L.B. Guo, W. Hu, and Y.F. Lu. "Spectral resolution improvement in laser-induced breakdown spectroscopy through the generation of high-temperature and low density plasmas". *Proceedings of ICALEO* P147 (2011).

9. L.S. Fan, **Z.Q. Xie,** J.B. Park, X.N. He, Y.S. Zhou, and Y.F. Lu. "Synthesis of nitrogen-doped diamond films by vibrational excitation of precursor molecules using CO_2 laser in a combustion flame process". *Proceedings of ICALEO* N206 (2011).

10. X.N. He, **Z.Q. Xie,** T. Gebre, and Y.F. Lu. "Spectroscopic determination of rotational temperature in $C_2H_4/C_2H_2/O_2$ flames for diamond growth with and without tunable CO_2 laser excitation". 47th Annual Technical Meeting of Society of Engineering Science (2010).

11. Y. Gao, J.B. Park, Y.S. Zhou, X.N. He, **Z.Q. Xie,** and Y.F. Lu. "Growth of Carbon Nano-onions in the Open Air by Laser Resonant Excitation of Ethylene Precursor". *Proceedings of ICALEO* N305 (2010).

12. X.N. He, T. Gebre, X.K. Shen, **Z.Q. Xie,** Y.S. Zhou, and Y.F. Lu. "Optical emission spectroscopy study of premixed C_2H_4/O_2 and $C_2H_4/C_2H_2/O_2$ flames for diamond growth with and without CO_2 laser excitation". *Proceedings of Photonics West* 7585, 75850A-10 (2010).

LIST OF AWARDS

1. Student Paper Award (1st place), International Congress on Applications of Lasers & Electro-Optics (ICALEO) 2011, Laser Institute of America (2011).

2. The Bill Holm Award (1st place), Department of Electrical Engineering, University of Nebraska-Lincoln (2011).

3. Outstanding Graduate Research Assistant Award, Honorable Mention, University of Nebraska-Lincoln (2011).

4. Poster Presentation Award (2nd place), International Congress on Applications of Lasers & Electro-Optics (ICALEO) 2010, Laser Institute of America (2010).

5. Dean's Fellowship, University of Nebraska-Lincoln (2010).